COMPLEX STABILITY BEHAVIOR IN NOVEL PROTEIN CONSTRUCTS: AGGREGATION OF FC- AND HSA- BASED FUSION PROTEINS

by

AMANDA ANN CORDES

B.S., Oregon State University, 2006

M.S., University of Colorado Boulder, 2009

A dissertation submitted to the

Faculty of the Graduate School of the

University of Colorado in partial fulfillment

Of the requirement for the degree of

Doctor of Philosophy

Department of Chemical and Biological Engineering

2011

This thesis for the degree of Doctor of Philosophy entitled:
Complex Stability Behavior in Novel Protein Constructs:
Aggregation of Fc- and HSA- Based Fusion Proteins
written by Amanda Ann Cordes
has been approved for the Department of Chemical and Biological Engineering

Dr. Theodore W. Randolph

Dr. John F. Carpenter

Date _____

The final copy of this thesis has been examined by the signatories, and we
Find that both the content and the form meet acceptable presentation standards
Of scholarly work in the above mentioned discipline.

ABSTRACT

Cordes, Amanda Ann (Ph.D., Chemical and Biological Engineering)

Complex Stability Behavior in Novel Protein Constructs: Aggregation of Fc- and HSA- Based Fusion Proteins

Thesis directed by Professor Theodore W. Randolph

The development of protein based biopharmaceuticals has resulted in the ability to treat many serious conditions, including endogenous protein deficiencies, cancer and autoimmune disorders. However, in order to be successful drug candidates, these more complex molecules require stable formulations that can last from manufacturing through transportation to patient administration. Fusion proteins, which are constructed from unrelated proteins or protein domains, present additional formulation challenges. In these proteins, domains did not co-evolve for stability and thus conditions favoring the stability of one domain may destabilize the other.

Our current hypotheses are that the least stable protein will also be the least stable domain in the fusion and that selective stabilization of this least stable domain can be used to reduce overall aggregation of the fusion protein, with preferential binding of cosolutes to the native state being one method of achieving selective domain stabilization.

Abatacept, an Fc-CTLA4 fusion protein, is used as a model to investigate the stability behavior of Fc fusion proteins. Fc-CTLA4 exhibits markedly different aggregation rates with only a small shift in pH. Changing from pH 7.5 to pH 6 causes a two order of magnitude increase in rate of monomer loss during incubation at 40 °C. The aggregation behavior during accelerated stability studies at elevated temperature was found to be controlled by conformational instability of the protein. Conditions which destabilized the CTLA4 domain and the C_H2 portion of the Fc domain lead to a decreased activation energy for aggregation and an increased aggregation rate.

Fc-CTLA 4 was also studied to examine how conditions which increase conformational stability impact the progression of aggregation due to other physical stresses (e.g., exposure to air/water and water/ice interfaces and freeze concentration during freezing). No changes were detected in the amount of monomer lost or number of particles formed between solution conditions at pH 6.0 and pH 7.5, despite large differences in conformational stability under these solution conditions.

Two HSA fusion proteins (HSA-hGH and HSA-GCSF) were studied to investigate small molecule ligand binding as a selective stabilization strategy, with octanoic acid used as the ligand. Addition of octanoic acid resulted in increased conformational stability for HSA, HSA-hGH and HSA-GCSF. Repulsive protein-protein interactions were only increased for HSA and HSA-hGH; HSA-GCSF protein-protein interactions remained unchanged. Reductions in aggregation were seen in the case of HSA-hGH. Thus it appears that specific binding to a domain of a fusion protein can reduce aggregation in more than one way (i.e. increasing both colloidal and conformational stability). No changes in HSA-GCSF aggregation were observed with the addition of octanoic acid, despite the increases in conformational stability, indicating the ligand binding stabilization approach does not appear to be applicable to all HSA fusions.

DEDICATION

To Trevor, per usual and as always,

and in memory of Randall Saito

ACKNOWLEDGEMENTS

This thesis would not exist without the help and support of many individuals. First, thank you to my advisor Ted Randolph, for all of the support and guidance these past five years, as well as for allowing me to pursue opportunities outside of lab. The internship experience was invaluable and I appreciate having that chance. Thank you to John Carpenter for all of your help and for sharing your lab in Denver. It was always a pleasure working with the students there. And a big thank you to the rest of my thesis committee: Rich Noble, Stephanie Bryant and Joel Kaar. Serving on committees may be a requirement of professors, but it wasn't a requirement to serve on mine in particular, and I appreciate greatly the time you took to do so.

To all of my labmates, past and current, it wouldn't have been the same (or possible) without you. I was lucky to have the opportunity to work with you and learned something from you all. In particular, thanks are due to Jonas Fast and Matt Hoehne.

Thank you to Paul Handke and Meghana Rangan for your friendship. Not that I would ever complain about grad school, but I appreciate your understanding and commiseration if I did.

And finally, thank you to my family. Especially Trevor, who had confidence in me even when I had none. To list all the ways in which you supported me throughout this would require an entire chapter; I can only hope that I was able to return the favor. I am beyond lucky to have you in my life.

TABLE OF CONTENTS

LIST OF TABLES

LIST OF FIGURES

CHAPTER 1

INTRODUCTION

1.1 General Background

Therapeutic proteins currently provide a means of treatment for many serious diseases, including autoimmune disorders, endogenous protein deficiencies and cancer [1]. These proteins are complex molecules that require not only the correct amino acid sequence, but also the correct folded three dimensional structures and higher order assembly state in order to function. Due to these requirements for a therapeutic protein, protein stability is an important area of research.

The primary structure of a protein consists of the polypeptide chain of amino acids linked by peptide bonds. Each amino acid contains a central carbon atom with an amino group, a carboxyl group, a hydrogen atom and a unique side chain. Hydrogen bonding between the N-H and C=O bonds in the protein backbone lead to secondary structure motifs including alpha helices, beta sheets and random coils [2]. Side chain interactions then determine how the protein folds into its tertiary structure. Some of this is driven by the ordering of hydrophobic groups on the interior of the protein and hydrophilic groups at the surface, but van der Waals forces, salt bridges and covalent disulfide bonds all contribute to tertiary structure. Quaternary structure is the arrangement of non-covalent subunits to create the active form of the protein. The simplest quaternary structure is a dimer, consisting of two folded monomer subunits. Aggregation is typically defined as non-native association and thus proteins exhibiting native quaternary structure would not be considered aggregates.

The stability of proteins is a complex, multifaceted topic, but it can be roughly divided into two areas: chemical stability and physical stability [3]. The chemical stability relates to

reactions that can change the composition of the protein, such as deamidation, oxidation, beta elimination and glycation [3]. Fragmentation of the polypeptide chain as well as disulfide bond cleavage or shuffling are other pathways of chemical degradation. In a deamidation reaction, an asparagine or glutamine amino acid is converted to aspartic or glutamic acid, respectively. Glycation involves the reaction of a reducing sugar with a basic amino acid to form a Schiff base. Oxidation can damage the side chains of many amino acids including histidine, methionine, cysteine, tryptophan and tyrosine. Formulation conditions can be chosen to minimize the above chemical instabilities [3]. For example, both deamidation and oxidation can be influenced by changing the solution pH. Glycation can be reduced by the choice of appropriate excipients, which in this case would be non-reducing sugars such as sucrose or trehalose rather than reducing sugars such as glucose, fructose or maltose [3.]

For a protein to be considered physically stable, it must maintain the proper three-dimensional folded structure as well as the correct higher order assembly state, which is typically monomer for therapeutic proteins. The conformational stability, or the stability of the folded protein structure, is quantified by the free energy of unfolding, ΔG_{unf} [3], and is determined by *intra*molecular interactions. It can be measured using thermally-induced protein unfolding (monitored with differential scanning calorimetry or circular dichroism) or chaotrope-induced unfolding with urea and guanidine hydrochloride (monitored with fluorescence spectroscopy or circular dichroism). Colloidal stability is determined by *inter*molecular interactions. In colloidally-stable systems, repulsive intermolecular interactions inhibit aggregation [4.] These interactions are reflected in protein osmotic second virial coefficients for the buffer systems (B_{22}); repulsive intermolecular interactions result in positive values of B_{22}. During formulation development, the colloidal and conformational stability of proteins in potential formulations is

assessed to determine the most stable solution conditions for a given protein [5]. Accelerated stability studies expose the protein formulations of interest to a variety of stresses, such as elevated temperature or agitation, to obtain the aggregation results more rapidly than is possible for solutions under normal protein storage conditions [6]. Formulation conditions for single domain proteins are aimed at maximizing both B_{22} and ΔG_{unf}.

The first two steps of the protein aggregation pathway are depicted in the Lumry-Eyring framework as a conformational change from a native-like conformation to an aggregation competent conformation and then association of these aggregation competent species into an initial aggregate [7, 8, 9], as shown in Figure 1-1. It is important to note that complete unfolding of the protein is not required to produce an aggregation competent species and that the initial aggregates formed during the association step may be reversible. When these steps are depicted on a reaction energy diagram (Figure 1-2), there is an associated activation energy barrier for each step in the aggregation pathway. Increasing the energy of the intermediate aggregation competent state, reflected by an increased free energy of unfolding (ΔG_{unf}), increases the activation energy barrier for step one. The protein-protein interactions are related to the height of the second barrier, with more repulsive protein-protein interactions raising the activation energy for association.

For the initial steps in a given protein aggregation pathway, either conformational or colloidal stability can be rate limiting [8, 9]. In cases where the aggregation appears to be first order, a unimolecular event (i.e. unfolding) likely governs the aggregation and increasing conformational stability can reduce said aggregation. If the association step is rate limiting, the reaction may appear to be second order or higher, depending on the size of the initial aggregate. Modulating protein-protein interactions to make them more repulsive can reduce the reaction

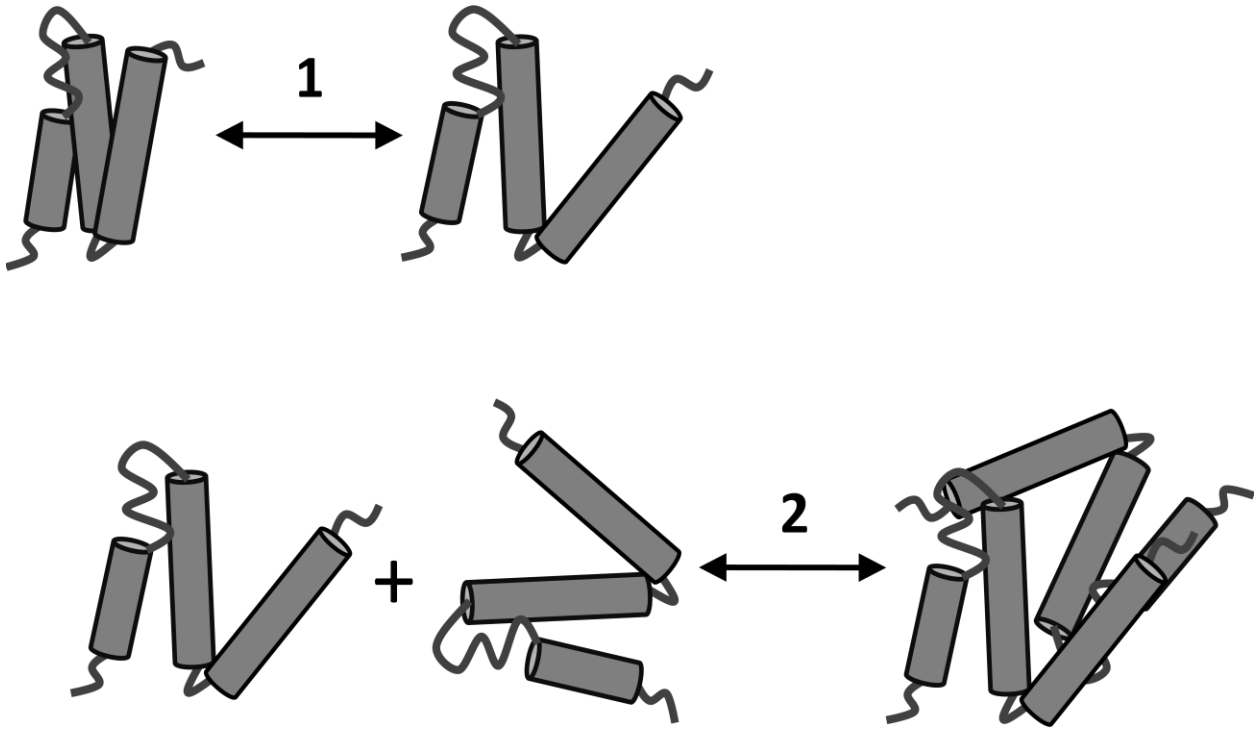

Figure 1-1: The initial steps in the protein aggregation pathway. Step one is a conformational change to an aggregation competent conformation and step two is the reversible association of two aggregation competent species to form an initial aggregate.

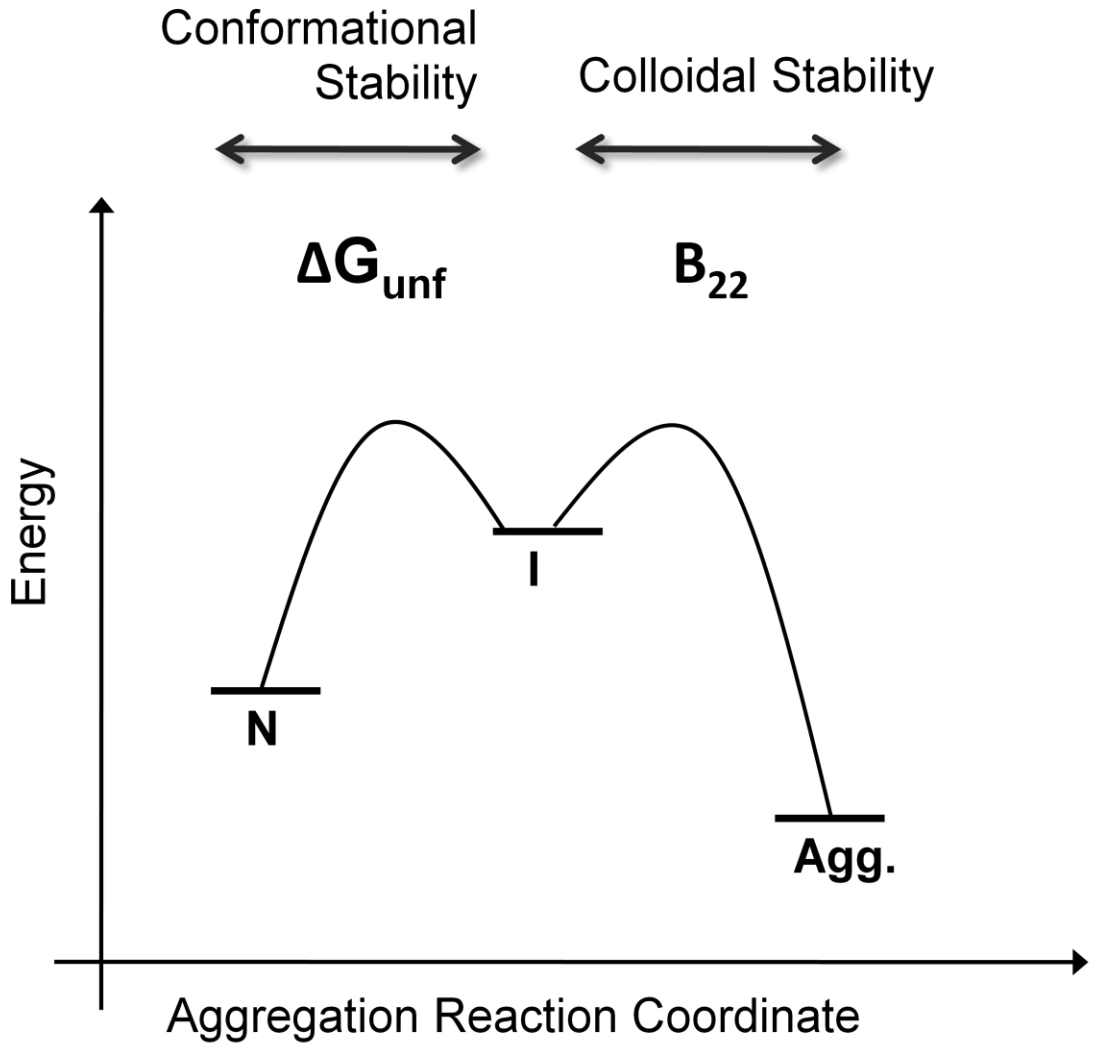

Figure 1-2: Reaction energy diagram of the first two steps in the protein aggregation pathway. In this figure, N represents the native conformation of the therapeutic protein and I is an aggregation competent conformation different from that of the native state. Agg represents the initial aggregate typically, although not always, composed of two I monomers.

rates in these cases [8, 9]. The apparent reaction order may also be concentration dependent, switching from an apparent first order to an apparent second order reaction with changes in concentration [10].

The changes to chemical stability can have an impact of physical stability and vice versa. An example of this interdependence is illustrated in the situation of proteins that aggregate physically then undergo reactions to become covalently linked by disulfide bonds. Oxidation has also been shown to reduce the conformational stability of proteins [11]. In some cases it can be difficult to balance the requirements between physical and chemical stability. For example, the deamidation rate is typically at a minimum between pH 3 and pH 6 [3], but depending on the pI of the protein, it may not be possible to formulate there due to solubility concerns.

Since aggregation is taken to mean any non-native protein association, protein aggregates encompass a wide range of sizes and possible morphologies as the aggregation proceeds beyond the initial steps. After the initial conformational perturbation and association steps, the following steps involve a conformational rearrangement of the protein to create an irreversible aggregate and the growth to larger aggregate sizes [9]. During aggregation, steps may be occurring in parallel, and not every step will necessarily be involved in the aggregation pathway for a given protein [9]. The smallest possible protein aggregate is a dimer, composed of two monomeric protein units. Smaller oligomers, including dimers up to aggregates of 0.1 um, are generally considered to be soluble aggregates. Here the term "soluble" indicates the aggregates are detectable by size exclusion chromatography (SEC) and are not large enough to be filtered out by the resin of the guard column or pelleted during centrifugation prior to SEC analysis [12]. Aggregates not detectable by traditional SEC methods are considered "insoluble". This includes

protein particles in the visible and sub visible ranges. Depending on the aggregation pathway, protein aggregates may be amorphous or may form more ordered fibril structures [9].

Because therapeutic proteins require the proper folded structure and assembly state to be active, developing a stable formulation for these products is important. By selecting the optimal buffer conditions and excipients, it is possible to create products with the appropriate shelf life and the ability to withstand potential sources of damage so that the drug can be safely administered to the patient. Salt concentrations and pH conditions might be chosen to optimize colloidal stability by changing protein-protein interactions. Examples of this include using salts to provide charge shielding for attractive protein-protein interactions or formulating at a pH value some distance from the pI, where the protein will have a greater net charge and presumable more repulsive protein-protein interactions. Preferentially excluded excipients, such as sucrose, are included in formulations due to the increased conformational stability they provide [13]. Non-ionic surfactants such as polysorbate 20 are also added to protect protein products from damage due to agitation [14].

In addition to the physical and chemical stability considerations involved when developing a formulation, there are also commercial factors at play. Liquid formulations are preferred over lyophilized formulations and there has recently been a push towards products in pre-filled syringes that can be administered at home [15]. These different requirements necessitate an understanding of the unique protein degradation pathways so each formulation can be designed to reduce protein degradation.

Therapeutic protein products are exposed to conditions which can compromise their stability and potentially induce aggregation during all stages of the product life cycle [16, 17, 18]. During manufacture, interaction with surfaces such as membranes during a filtration step can

cause aggregation [19]. Pumps may shed microparticles to which proteins then adsorb. Pumps can also cause cavitation and the air/water interface created during this cavitation can damage proteins [17]. Agitation during shipping can also damage protein, most likely through the increased amount of air-water interface turnover caused by the shaking. During storage, the proteins can interact with container materials, such as silicon oil in pre-filled syringes or vial stoppers, and these materials, or leachates from these materials, can interact unfavorably with the proteins [17]. Finally, proteins may be exposed to changes in temperature during storage, including the possibility of undergoing freeze-thaw cycles when stored for use at home [20]. Thus it is important to develop a robust formulation to help protect proteins from these stresses which may alter the protein conformation or assembly state in such a way that reduces product quality or performance. Consequences of this instability include loss of product and the resulting loss of profit from being unable to sell this product.

More seriously, there are concerns for patient welfare if the aggregated product is injected into a patient. The drug efficacy may not be at the desired levels if the active sites of the molecule are compromised when the protein forms an aggregate [21]. Previous research also suggests that the repetition of ordered epitopes (such as those present in aggregates) facilitates an immune response [22]. If the therapeutic protein is being delivered as a replacement for endogenous protein, the immune response can generate neutralizing antibodies which may not only render the drug ineffective but also have the potential to cross-react with the native protein. Neutralizing antibodies have been implicated in the case of patients treated with recombinant epoetin alpha who experienced pure red cell aplasia, where their levels of endogenous erythropoetin were essentially reduced to zero [23, 24]. Repetitive blood transfusions were then required to treat the

patients. The treatment of hemophilia by administration of factor VIII is also affected by the presence of anti-drug antibodies induced by the drug product [25].

Recently the presence of particles in formulations has been linked to the creation of an adverse immune response [22, 26], particularly particles in the 1-10 μm range which are hypothesized to be especially effective at triggering this immune response. The current guidance on the acceptable level of particles in the final product comes from the United States Pharmacopeia (USP) and was based on traditional small molecule drugs. The guidelines were primarily focused the risk patients faced from capillary occlusion caused by the particles, and not on the potential for immunogenicity [27]. In addition, the specifications are for the number of particles larger than 10 μm and larger than 25 μm, which may not be the size range of concern for product immunogenicity.

There are many sources of non protein particles from the manufacturing process, including cellulose from filters, metal particles shed from pumps, and in the case of pre-filled syringes, silicone oil droplets from the syringes and tungsten from the needle attachment [28, 29]. Protein can adsorb onto these particles, presenting ordered, spaced epitopes of the therapeutic protein for detection by the immune system. The particles may also be formed from aggregated protein product alone. Protein formulations can be designed to stabilize the proteins against interactions with the foreign particles and to reduce the formation of larger protein particles.

Further complicating the study of particles is the difficulty in detecting and analyzing these particles in solution, due to their size and potentially low levels. The current USP method for detection of particles is based on light obscuration. While this method can indicate the size of the particles, it provides no information on the particle composition, making it less useful for root cause analysis and determination of the source of particles [27]. There is support developing

for micro flow imaging techniques as an orthogonal method to light obscuration. This technique allows one to determine not only the size but also the morphology and optical properties of the particles in solution [30]. Micro flow imaging can detect and characterize particles in the 1-10 um size range and help to determine the composition of the particles [27], which then allows one to take a more directed strategy to prevent the formation of these particles.

For all of the above mentioned reasons involving patient safety, cost, time and profitability, it is important to understand and control protein aggregation. Robust formulations which stabilize the protein against a variety of stresses help ensure a safe product for the patient. Additional understanding of the driving forces of aggregation can help improve future formulations.

1.2 Fusion Protein Background

For the scope of this thesis, a fusion protein is defined as an artificial construct combining unrelated proteins or domains from those proteins (Figure 1-3). The domains are not covalently bound together; rather, the DNA coding each protein/domain is expressed together as a single polypeptide. Fusion proteins are a growing class of therapeutic molecules, with several FDA approved products and many more in late stage development [31]. The fusion protein notation used here is in the form of X-Y, where X and Y are the proteins or protein domains combined to create the fusion and X-Y is the resulting fusion protein product.

There are many potential fusion protein partners, including the Fc or Fab antibody domains [31, 32], human serum albumin (HSA), transferrrin, C-terminal peptide of hCG, and heparin [33], although all of the FDA approved fusion protein products currently on the market fall into the Fc fusion class. HSA fusion constructs including human serum albumin-human growth hormone as

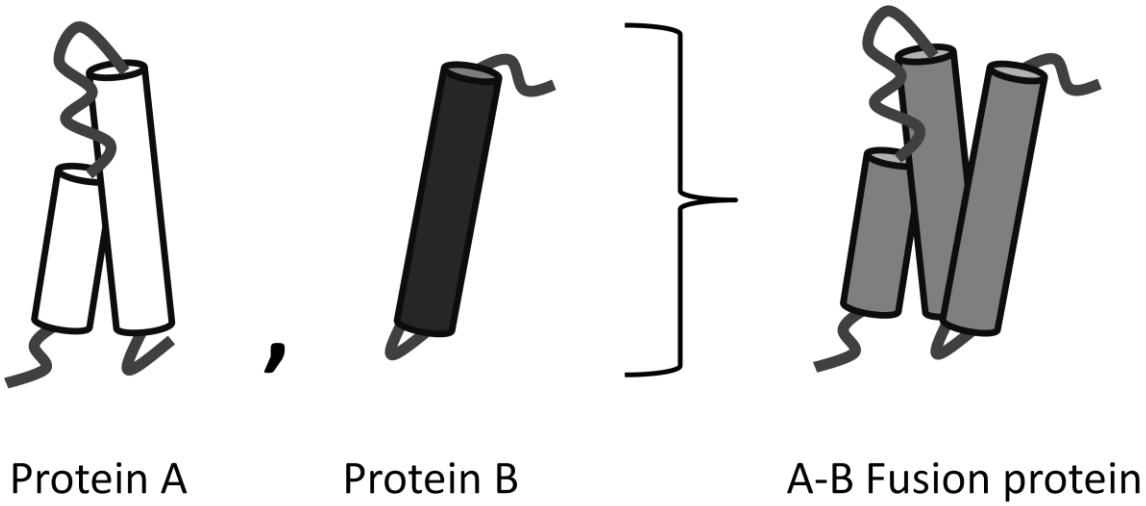

Figure 1-3: Schematic of a generic fusion protein. In this figure, Protein A and Protein B are unrelated proteins, or domains from unrelated proteins. The A-B fusion protein is the resulting product when Protein A and Protein B are expressed together in a single polypeptide chain.

well as human serum albumin-granulocyte colony stimulating factor have been investigated in clinical trials, although neither was approved by the FDA.

The Fc fusion class is based on human antibodies. Antibodies are composed of two heavy chains and two light chains, depicted in Figure 1-4, with the heavy chain being approximately twice the molecular weight of the light chain [2]. The heavy chains are connected by disulfide bonds in the hinge region between the Fc and Fab domains. Each light chain has a variable region and a constant region, while the heavy chain has a variable region and three constant regions (C_H1, C_H2 and C_H3). The Fab (fragment antigen binding) domain is composed of the light chain as well as the heavy chain variable region and constant region [2]. The Fc (fragment crystallizable) domain consists of the C_H2 and C_H3 regions of the two heavy chains and has a molecular weight of approximately 50 kDa. It is the Fc domain which is the current partner in all of the approved fusion proteins.

Human serum albumin (HSA) is another fusion partner of interest. HSA is a primarily alpha helical (approximately 67% by x-ray diffraction) protein [34]. It is composed of 585 amino acids and has a molecular weight of 67 kDa. In the body, HSA binds a wide variety of compounds including small molecule drugs, fatty acids, steroids and metal cations including copper (II), calcium, magnesium and zinc [34]. The entirety of the HSA protein is used a fusion partner, unlike Fc based fusions which use only a portion of the antibody.

Fusion proteins are of interest commercially because there can be additional benefits from combining the therapeutic protein of interest with HSA or with the Fc domain compared to the therapeutic protein alone. Both Fc and HSA fusions increase the circulation half life of the partnered domain [32, 35, 36, 37], reducing the required frequency of drug administration which is beneficial from a patient compliance perspective [38, 39]. An Fc fusion can also have additional

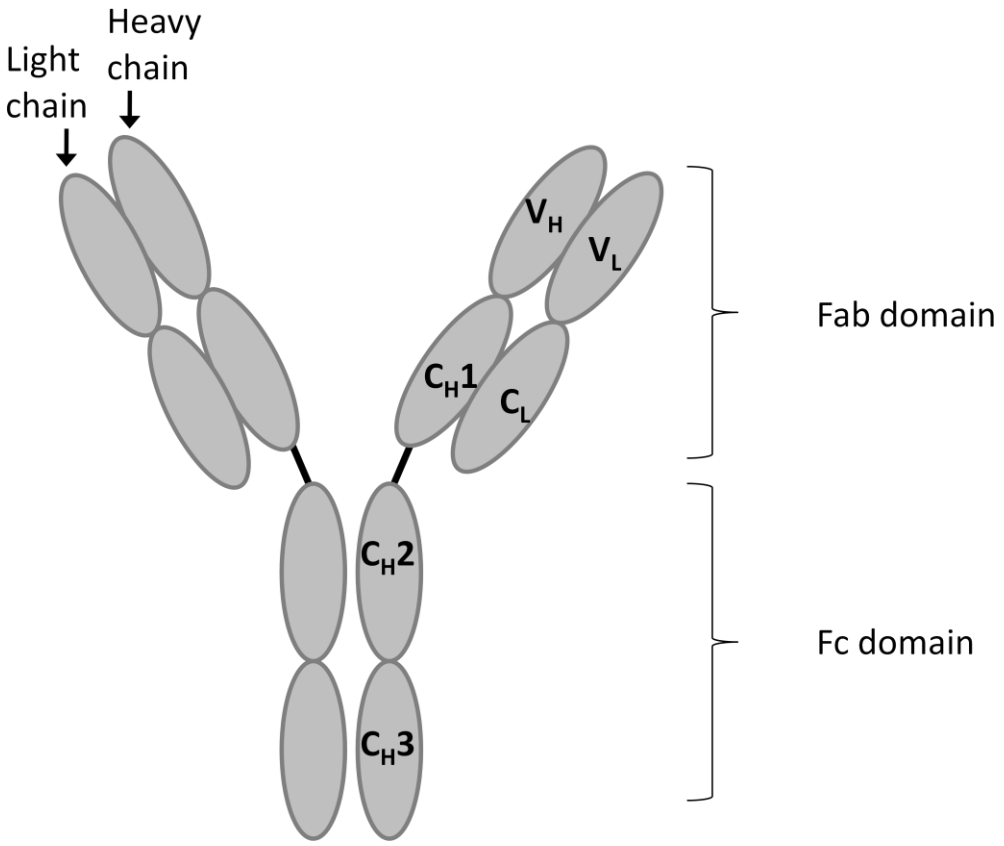

Figure 1-4: Antibody structure. Antibody molecules are composed of two heavy chains and two light chains. The Fab domain is composed of the light chains and a portion of the heavy chains. The Fc domain consists of the C_H2 and C_H3 regions of the heavy chains.

functionality related to the activity of the Fc domain including inducing antibody dependent cell mediated cytotoxicity or triggering the release of inflammatory cytokines [32]. If this additional functionality is not desired, the Fc domain can be mutated in order to remove its biological activity [40]. In such cases, the benefit of the increased circulation half life would still remain.

1.3 Challenges specific to fusion proteins

Formulation strategies may become more complicated with fusion proteins. Unlike natively occurring proteins, the domains in fusion proteins have not co-evolved. Thus, they may lack stabilizing intra-domain interactions. Furthermore, conditions which lead to repulsive interactions between molecules (increased colloidal stability, more negative B_{22}) may also cause repulsive intramolecular interactions between the domains resulting in reduced conformational stability (lower ΔG_{unf}).

Another challenge is predicting the aggregation/stability behavior of the new fusion protein construct from that of the two original domains. Each individual domain has its own level of conformational stability, reflected in the ΔG_{unf}, and colloidal stability as determined by the protein-protein interactions. Since the unfolding of a domain within a protein may proceed independently of another domain [41, 42, 43] and since there may not necessarily be stabilizing intradomain interactions between the unrelated fusion domains, domain conformational instability has the potential to be a major driving force for fusion protein aggregation. If no significant intradomain interactions occur when the fusion is created, the domain conformational stability of the original proteins may remain unchanged in the fusion, allowing a priori determination of the least stable domain.

However, colloidal stability of the individual domains is not expected to be predictive of the colloidal stability of the overall fusion protein. The colloidal stability is a function of two body interactions, which can give rise to non-ideal solution behaviors. The B_{22} (or second osmotic virial coefficient) is a measure of these non-ideal behaviors and can indicate whether protein-protein interactions are attractive (negative B_{22}) or repulsive (positive B_{22}) [44]. It can be derived from statistical mechanics for spherically symmetric forces [45] as seen in the following equation:

$$B_{22} = \frac{2\pi}{M^2}\int_0^\infty r^2(1 - e^{-u(r)/\kappa T})dr$$

M= protein molecular weight

R= intermolecular separation distance

u(r) = interaction potential

K = Boltzmann constant

T = absolute temperature

Hard sphere, electrostatic, van der Waals and other short range forces are all included in the interaction potential, u(r).

In addition to including the hard sphere, electrostatic and van der Waals forces, B_{22} values are impacted by charge distribution and protein geometry [46]. Thus the B_{22} values for a fusion protein are not expected to be additive based on the B_{22} values of the domains since both charge distribution and geometry could differ between the original domains and the new fusion. Furthermore, B_{22} values are determined for the entire protein; there is no measure of colloidal stability for a domain in a protein. As mentioned previously, it is possible for the unfolding of

domains within a protein to be independent, illustrating the qualitative difference in the parameters.

B_{22} behavior of the original domains and the fusion protein might correlate, but there is no basis to assume the B_{22} values of the original domains are predictive. For example, consider the case of creating a fusion from two domains, one with a +10 net charge and one with a -10 net charge. The electrostatic contribution to the B_{22} is described by the following equation [47]:

$$B_{22-electrostatic} = \frac{Z^2}{4M^2\rho_s m_{ions}}$$

where Z is the effective charge, M is the molecular weight, ρ_s is the solvent density and m_{ions} is the ion molal concentration. For both proteins, the electrostatic contribution to the B_{22} is positive. However, when the domains are combined in the fusion protein, the +10 net charge and the -10 net charge would not only reduce the electrostatic contribution with a new apparent charge of 0, but also could create a dipole on the overall molecule, increasing the likelihood of attractive protein-protein interactions. This would not have been apparent from the B_{22} values for the parent domains.

1.4 Objectives

Due to the increasing number of therapeutic fusion proteins, it is desirable to have an increased understanding of domain contributions to overall fusion protein behavior, in order to approach formulation of these molecules in a rational manner. To this end, we have developed two hypotheses. First, we hypothesize that the overall stability and aggregation of multi-domain proteins can be controlled by choosing formulation conditions that favor the stability of the least

conformationally stable subunit. Second, we hypothesize selective stabilization of this domain will reduce overall aggregation of fusion construct.

In this work, we use a model Fc-fusion and a model HSA-fusion to test the hypotheses and determine the impact of subunit stability on overall protein stability. The primary goal of the Fc-fusion study was to characterize the aggregation of this fusion and determine the driving forces. The goal of the HSA fusion studies was to not only examine the ways in which subunit stability influences the overall stability but also to determine if a formulation stabilization strategy could be developed that works across the HSA fusion protein class. To accomplish this, both conformational and colloidal stability studies of the complete fusion were performed, as well as stability studies of the HSA and hGH proteins alone, when possible. During these studies, cosolute binding was investigated as a way to achieve selective HSA domain conformational stabilization through the preferential binding of the cosolutes to the native state [8.]

This small molecule ligand binding as a selective domain stabilization strategy is based on the Wyman linkage function:

$$\left(\frac{\partial lnK}{\partial lna_x}\right)_{m_p} = v_x^{prod} - v_x^{react} = \Delta v_x$$

In this equation, K is the equilibrium constant, a_x is the activity of the ligand, v_x^{prod} and v_x^{react} are the numbers of ligand bound to the product and the reactant respectively and Δv_x is the difference in number of bound ligand [48, 13]. The gradient of the equilibrium constant with respect to ligand activity is related to the change in ligand binding between product and reactant; ligand binding will shift the equilibrium to the state with the greatest ligand binding. Since it is presumed that the protein will need a more native structure in order to bind the ligand, ligand binding should

drive the equilibrium towards a more native and less aggregation competent conformation. During the experiments, the stability of HSA and the HSA-fusion protein were compared in the presence and absence of the ligand. Octanoic acid was chosen as the primary stabilizing ligand. It is a known ligand of HSA, binding to subdomain IIIA and was used historically to prevent precipitation during the elevated temperature viral inactivation step during the purification of HSA from human sources [34, 49, 50].

In the case of the more pharmaceutically relevant Fc-fusion, once the driving forces for aggregation were determined, formulations that reduced monomer loss during elevated temperature studies were investigated for their ability to reduce aggregation under other conditions. Agitation and freeze/thawing were selected as additional stresses for the Fc-fusion since these stresses are also encountered over the life-cycle of a protein therapeutic [17]. Particle formation under the different conditions was also examined.

Overall conclusions about stability and recommendations for the HSA class are included.

1.5 References

1. Leader, B. Protein therapeutics: a summary and pharmacological classification. *Nature Reviews Drug Discovery* **2008,** *7* (1), 21-39.

2. Berg, J. M.; Tymoczko, J. L.; Stryer, L. Protein Structure and Function. In *Biochemistry*, 5th ed.; W.H. Freeman and Company: New York, 2002; pp 41-73.

3. Manning, M.; Patel, K.; Borchardt, R. Stability of Protein Pharmaceuticals. *Pharmaceutical Research* **1989,** *6* (11), 903-918.

4. Chi, E. Y.; Krishman, S.; Kendrick, B.; Chang, B.; Carpenter, J.; Randolph, T. Roles of Conformational Stability and Colloidal Stability in the Aggregation of Recombinant Human Granulocyte Colony Stimulating Factor. *Protein Science* **2003,** *12,* 903-913.

5. Chang, B.; Hershenson, S. Practical Approaches to Protein Formulation Development. In *Rational Design of Stable Protein Formulations;* Manning, C. a., Ed.; Plenum Publishers: New York, 2002; pp 1-25.

6. Randolph, T. Engineering Challenges of Protein Formulations. *AIChE Journal* **2007,** *53* (8), 1902-1907.

7. Lumry, R.; Eyring, H. Conformation changes of proteins. *J Phys Chem* **1954,** *58,* 110-120.

8. Chi, E. Physical Stability of Proteins in Aqueous Solution: Mechanism and Driving Forces in Nonnative Protein aggregation. *Pharmaceutical Research* **2003,** *20* (9), 1325-1336.

9. Roberts, C. Non-Native Protein Aggregation Kinetics. *Biotechnology and Bioengineering* **2007,** *98* (5), 927-937.

10. Raso, S. W.; Abel, J.; Barnes, J. M.; Maloney, K. M.; Pipes, G.; Treuheit, M. J.; King, J.; Brems, D. N. Aggregation of granulocyte-colony stimulating factor in vitro involves a conformationally altered monomeric state. *Protein Science* **2005,** *14,* 2246-2257.

11. Kim, Y.; Berry, A.; Spencer, D.; Stites, W. Comparing the effect on protein stability of methionine oxidation versus mutagenesis: steps toward engineering oxidative resistance in proteins. *Protein Engineering* **2001,** *14* (5), 343-347.

12. Philo, J. S. A Critical Review of Methods for Size Characterizatio of Non-Particulate Protein Aggregates. *Current Pharmaceutical Biotechnology* **2009,** *10,* 359-372.

13. Timasheff, S. N. Protein-solvent preferential interactions, protein hydration, and the modulation of biochemical reactions by solvent components. *PNAS* **2002,** *99* (15), 9721-9726.

14. Chou, D. K.; Krishnamurthy, R.; Randolph, T. W.; Carpenter, J. F.; Manning, M. C. Effects of Tween 20 and Tween 80 on the stability of Albutropin during agitation. *Journal of Pharmaceutical Sciences* **2005,** 1368-1381.

15. Wertheimer, A.; Santella, T. M.; Finestone, A.; Levy, R. Drug delivery systems improve pharmaceutical profile and facilitate medication adherence. *Advances in Therapy* **2005,** *22* (6), 559-577.

16. Cromwell, M.; Hilario, E.; Jacobson, F. Protein Aggregation and Bioprocessing. *The AAPS Journal* **2006,** *8* (3), 572-579.

17. Rathore, N.; Rajan, R. S. Current Perspectives on Stability of Protein Drug Products during Formulation, Fill and Finish Operations. *Biotechnol. Prob.* **2008,** *24* (3), 504-514.

18. Bee, J.; Randolph, T. W.; Carpenter, J.; Bishop, S.; Dimitrova, M. Effects of Surfaces and Leachables on the Stability of Biopharmaceuticals. *J Pharm Sci* **2011**.

19. Maa, Y.-F.; Hsu, C. C. Investigation on foulding mechanisms for recombinant human growth hormone sterile filtration. *Journal of Pharmaceutical Sciences* **1998,** *87* (7), 808-812.

20. Eugene, J.; McNally, C. The imporance of a thorough preformulation study.. In *Protein Formulation and Delivery*, 1st ed.; McNally, E., Ed.; Marcel Dekker: New York, 1999; pp 111-138.

21. Tooze, B. C. Introductio to protein structure. Garland Scicne: New York, 1998; p 410.

22. Rosenberg, A. Effects of Protein Aggregates: An Immunologic Perspective. *The AAPS Journal* **2006,** *8* (3), 501-507.

23. Bunn, H. Drug-Induced Autoimmune Red-Cell Aplasia. *New England Journal of Medicine* **2002,** *346* (7), 522-523.

24. Stravitz, R.; Chung, H.; Sterling, R.; Luketic, V.; Sanyal, A.; Price, A.; Purrington, A.; Shiffman, M. Antibody-Mediated Pure Red Cell Aplasia Due to Epoetin Alfa During Antiviral Therapy of Chronic Hepatitis C. *The American Journal of Gastroenterology* **2005,** *100* (6), 1415-1419.

25. Tamilvanan, S.; Raja, N.; Sa, B.; Basu, S. Clinical concerns of immunogenicity produced at cellular levels by biopharmaceuticals following their parenteral administration into human body. *Journal of Drug Targeting* **2010,** *18* (7), 489-498.

26. Carpenter, J. F.; Randolph, T. W.; Jiskoot, W.; Crommelin, D. J.; Middaugh, C. R.; Winter, G.; Fan, Y.-X.; Kirshner, S.; Verthelyi, D.; Kozlowski, S.; Clouse, K. A.; Swann, P. G.; Rosenberg, A.; Cherny, B. Overlooking Subvisible Particles in Therapeutic Protein Products:

Gaps That May Compromise Product Quality. *Journal of Pharmaceutical Sciences* **2009,** *98* (4), 1201-1205.

27. Narhi, L. O.; Jiang, Y.; Cao, S.; Benedek, K.; Shnek, D. A Critical Review of Analytical Methods for Subvisible and Visible Particles. *Current Pharmaceutical Biotechnology* **2009,** *10,* 373-381.

28. Ludwig, D.; Carpenter, J. F.; Hamel, J. B.; Randolph, T. W. Protein adsorption and excipient effects on kinetic stability of silicone oil emulsions. *J Pharm Sci* **2010,** *99* (4), 1721-1733.

29. Liu, W.; Swift, R.; Torraca, G.; Nashed-Samuel, Y.; Wen, Z. Q.; Jiang, Y.; Vance, A.; Mire-Sluis, A.; Freund, E.; Davis, J.; Narhi, L. Root Cause Analysis of Tungsten-Induced Protein Aggregation in Pre-filled Syringes. *PDA Journal of Pharmaceutical Science and Technology* **2010,** *64* (1), 11-19.

30. Barnard, J. G.; Singh, S.; Randolph, T. W.; Carpenter, J. F. Subvisible Particle Counting Provides a Sensitive Method of Detecting and Quantifying Aggregation of Monoclonal Antibody Caused by Freeze-Thawing: Insigns Into the Roles of Particles in the Protein Aggregation Pathway. *Journal of Pharmaceutical Scinces* **2011,** *100* (2), 492-503.

31. Jazayeri, J.; Carroll, G. Fc-based cytokines: prospects for engineering superior therapeutics. *BioDrugs* **2008,** *22* (1), 11-26.

32. In *Antibody Fusion Proteins,* 1st ed.; Chamow, S., Ashkenazi, A., Eds.; Wiley-Liss Inc: New York, 1999.

33. Schmidt, S. R. Current Status of Fusion Protein Applications Including the Use of the Zera Peptide. *AAPS National Biotechnology Conference*, San Francisco, 2011.

34. Peters, T. *All About Albumin;* Academic Press Inc: San Diego, 1996.

35. Muller, N.; Schneider, B.; Pfizenmajer, K.; Wajant, H. Superior serum half life of albumin tagged TNF ligands. *Biochem Biophys Res Commun* **2010,** *396* (4), 793-799.

36. Syed, S.; Schuyler, P.; Kulczycky, M.; Scheffield, W. Potent antithrombin activity and delayed clearance from the circulation characterize recombinant hirudin genetically fused to albumin. *Blood* **1997,** *89* (9), 3243-3252.

37. Yu, Z.; Fu, Y. Recombinant human albumin fusion proteins with long lasting biological effects. 7,244,833, July 17, 2007.

38. Ingersoll, K. The impact of medication regiment factors on adherence to chronic treatment: a review of literature. *J Behav Med* **2008,** *31* (3), 213-224.

39. Reginster, J.; Rabenda, V.; Neuprez, A. Adherence, patient preference and dosing frequency: understanding the relationship. *Bone* **2006,** *38* (4), S2-S6.

40. Davis, P.; Abraham, R.; Xu, L.; Nadler, S. G.; Suchard, S. J. Abatacept binds to the Fc receptor CD64 but does not mendiate complement-dependent cytotoxicity or antibody-dependent cellular cytotoxicity. *J Rheumatol* **2007,** *34*, 2204-2210.

41. Azuaga, A.; Dobson, C.; Mateo, P.; Conejero-Lara, F. Unfolding and aggregation during the thermal denaturation of streptokinase. *European Journal of Biochemistry* **2002,** *269* (16), 4121-4133.

42. Laptenok, S.; Visser, N.; Engel, R.; Wstphal, A.; van Hoek, A.; van Mierlo, C.; van Stokkum, I.; van Amerongen, H.; Visser, A. A general approach for detecting folding intermediates from steady-state and time-resolved fluorescence of single-tryptophan containing proteins. *Biochemistry* **2011,** *50* (17), 3441-3450.

43. Lee, A.; Clark, R.; Youn, H.; Ponter, S.; Burstyn, J. Guanidine hydrochloride-induced unfolding of the three heme coordination states of the CO-sensing transcription factor, CooA. *Biochemistry* **2009,** *48* (28), 6585-6597.

44. George, A.; Wilson, W. Predicting protein crystallization from a dilute solution property. *Acta Crystallogr D Biol Crystallogr* **1994,** *50* (4), 361-365.

45. McQuarrie, D. *Statisticam mechanics, p. 641;* Harper & Row: New York, 1976.

46. Neal, B.; Asthagiri, A.; Lenhoff, A. M. Molecular origins of osmotic second virial coefficients. *Biophysical Journal* **1998,** *75*, 2469-2477.

47. Asthagiri, D.; Paliwal, A.; Abras, D.; Lenhoff, A.; Paulaitis, M. A consistent experimental and modeling appraoch to light-scattering studies of protein-protein interactions in solution. *Biophysical Journal* **2005,** *88* (5), 3300-3309.

48. Tanford, C. Extension of the theory of linked functions to incorporate the effects of protein hydration. *Journal of Molecular Biology* **1969,** *39* (3), 539-544.

49. Aki, H.; Yamamoto, M. Biothermodynamic characterization of monocarboxylic and dicarboxylic aliphatic acids binding to human serum albumin: A flow microcalorimetric study. *Biophysical Chemistry* **1993,** *46*, 91-99.

50. Anraku, M.; Tsurusaki, Y.; Watanabe, H.; Maruyama, T.; Kragh-Hansen, U.; Otagiri, M. Stabilizing mechanisms in commercial albumin preparations: octanoate and N-acetyl-L-tryptophanate protect human serum albumin against heat and oxidative stress. *Biochimica et Biophysica Acta* **2004,** 9-17.

CHAPTER 2

FACTORS CONTRIBUTING TO THE AGGREGATION OF A THERAPEUTIC FC-CTLA4 FUSION PROTEIN

(A portion of this work has been published in the journal Biochemistry and appears as Jonas L. Fast, Amanda A. Cordes, John F. Carpenter, Theodore W. Randolph. Physical Instability of a Therapeutic Fc Fusion Protein: Domain Contributions to Conformational and Colloidal Stability. *Biochemistry* **2009,** *48,* 11724-11736.)

2.1 Introduction

Although there are multiple different fusion platforms in development, all of the currently approved fusion proteins are Fc fusions [1]. These are proteins in which the "fragment crystallizable" of an antibody is used as one half of the therapeutic fusion. Enbrel®, NPlate®, Orencia® and Arcalyst® are all examples of current Fc fusion products, and there are others in late stage clinical trials [2]. Fc fusions are an attractive platform for several reasons. First, the addition of the Fc domain to a protein of interest increases the molecular weight of the therapeutic product compared to the original protein [3]. This in turn can increase the circulation half-life of the drug. Second, the addition of the Fc domain can confer additional functionalities on the overall fusion product, since the antibody Fc domain is biologically active [3, 4]. Increased understanding of the stability behavior of Fc fusion proteins is thus desirable due to the potential growth of this therapeutic class and its platform nature, where the Fc domain may be conserved as a partner in multiple fusions [5].

For this work, Orencia® (abatacept) was chosen as a model fusion protein. Orencia® is composed of a human IgG1 Fc domain fused with the extracellular domain of CTLA4 (human cytotoxic T-lymphocyte associated factor) [6]. There are two amino acid chains connected by a disulfide bond in the hinge region, with each chain having an Fc portion and a CTLA4 portion [7]. Mutations in the C_H2 region of the Fc domain were used to remove the biological activity of the

Fc domain [4]. A model of the Fc-CTLA4 structure is shown in Figure 2-1. This therapeutic is approved for the treatment of rheumatoid arthritis and is formulated as a lyophilized powder.

The overall pI of Fc-CTLA4 is between 4.5-5.5, due to the variations in glycosylation. However, the theoretical pI values for each domain are very different. The theoretical pI for the CTLA4 domain is approximately 4.39 and the theoretical pI for the Fc domain is 7.16, based on SwisProt predictions from the amino acid sequence [8, 9]. The therapeutic protein is formulated at pH 7.2, which fits with the traditional formulation approach, based on the overall pI of the molecule. At this pH, the CTLA4 domain would be expected to have a fairly high net charge, leading to possible repulsive interactions between CTLA4 domains. The Fc domain likely has very little charge at the formulation pH, and thus the protein-protein interactions would not be as strongly repulsive between these domains. If the pH was shifted from the formulation pH to pH 6, which is between the two theoretical pI values for the individual domains, the domains would then have opposite charges. This could potentially create an overall dipole on the molecule and lead to increased attractive protein-protein interactions.

To investigate the driving forces for fusion protein aggregation, the aggregation of the Fc-CTLA4 fusion protein was studied and then compared with domain conformational stability and overall colloidal stability at the two pH conditions discussed above. Enzymatic digests were attempted to obtain the individual parent domains. Biopanning experiments were also conducted to identify peptide ligands for the Fc-CTLA4 fusion protein for potential use in selective domain stabilization.

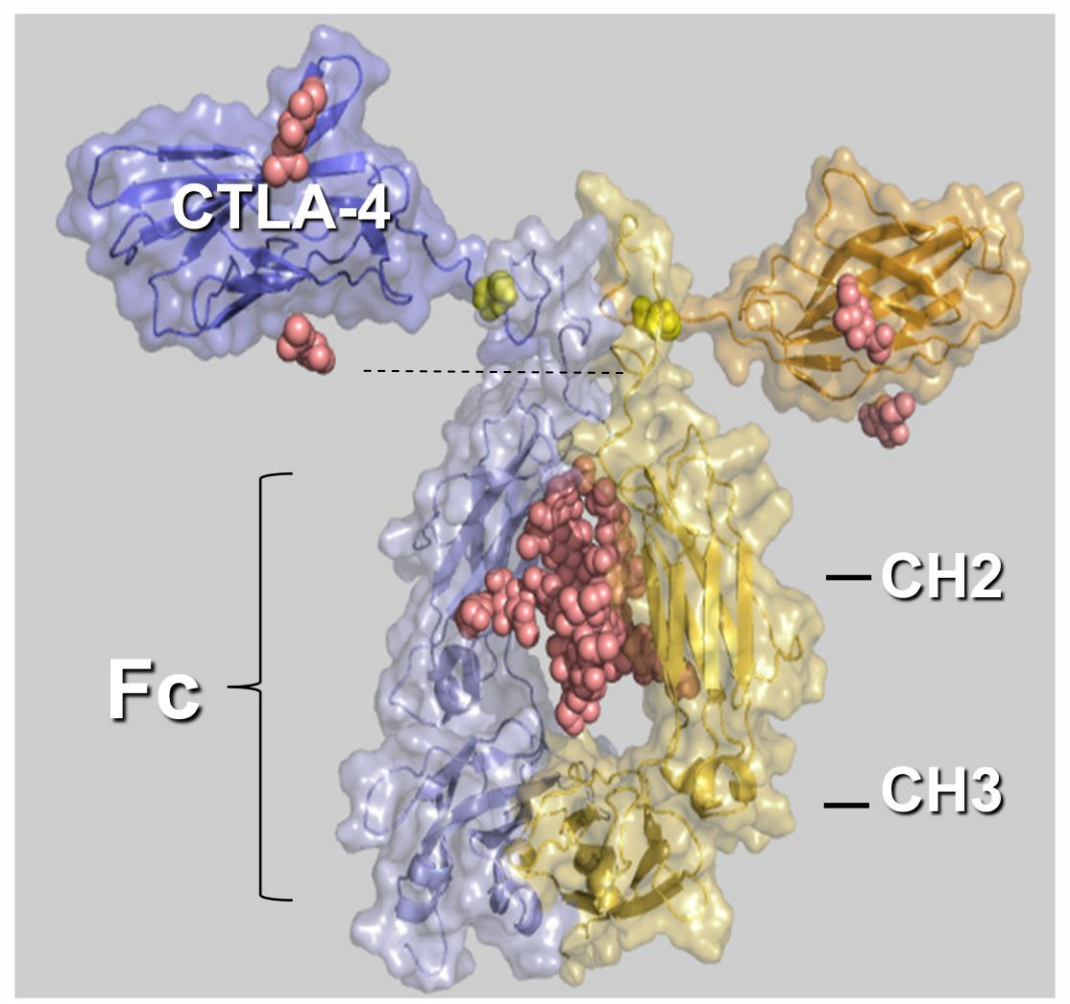

Figure 2-1: Model of Fc-CTLA4 fusion, courtesy of Jonas Fast and Ingemar Andre. Fc-CTLA4 is a homodimer composed of two polypeptide chains, represented here in blue and yellow. Each chain has an Fc portion and a CTLA4 portion. The two chains are connected by a disulfide bond in the hinge region.

2.2 Materials and Methods

2.2.1 Stock protein preparation:

Fc-CTLA4 was obtained as a white, lyophilized powder with 250 mg/vial. Upon reconstitution with 10 mL sterile water per packaging instructions, Fc-CTLA4 is present at 25 mg/mL in a buffer containing 50 mg/mL maltose, 1.72 mg/mL monobasic sodium phosphate and 1.46 mg/mL sodium chloride[2]. Sodium azide at 0.01% (w/v) was added to inhibit bacterial growth. Following reconstitution, Fc-CTLA4 was dialyzed at 4°C into the desired experimental buffer using Pierce 10,000 molecular weight cut off dialysis cassettes. The experimental buffers include 10 mM sodium phosphate, 25 mM sodium chloride at pH 7.5 and pH 6.0, 10 mM sodium phosphate, 200 mM sodium chloride at pH 6.0 as well as 50 mM Tris, 25 mM MES, 25 mM acetic acid, 25 mM sodium chloride at pH 6.0. The two primary buffers for experimentation are 10 mM sodium phosphate, 25 mM sodium chloride at pH 7.5 and pH 6.0, unless otherwise noted.

2.2.2 Accelerated stability studies:

Fc-CTLA4 at a concentration of 5 mg/mL in the desired buffer (10 mM sodium phosphate, 25 mM sodium chloride, 0.1 g/L sodium azide, pH 6 or pH 7.5) was aliqouoted by 100 μL into microcentrifuge tubes. Samples were then incubated at 40°C, 30°C or room temperature (approximately 22°C) in order to identify conditions at which aggregation occurred over a reasonable time frame. Three samples per condition were removed at each time point, centrifuged to remove insoluble aggregates and analyzed by HPLC size exclusion chromatography (SEC), using a Beckman System Gold with a Waterhouse autosampler and a 3000 SWXL Tosoh Biosciences SEC column with guard column. Unless otherwise noted, the

sample injection volume was 40 μL. The HPLC run time was 40 minutes at a flow rate of 0.6 mL/min, with a 100 mM sodium phosphate, 300 mM sodium chloride mobile phase at pH 7.0. Data was analyzed using Bomem/GRAMS AI software. The mass of each eluting peak was determined using the following equation:

$$Mass = \frac{(Peak\ area)(V_f)}{(\varepsilon_{280})10^6}$$

where V_f is the flowrate in mL/s and ε_{280} is the extinction coefficient in cm^2/mg.

2.2.3 Reaction order:

Samples with varying initial concentrations were prepared and analyzed as described in the accelerated stability section. The pH 7.5 samples were incubated at 40°C and the pH 6 samples were incubated at 30°C. At pH 7.5, the initial concentrations were 2.5 mg/mL, 5 mg/mL, 7.5 mg/mL, 10 mg/mL, 11.8 mg/mL and 13.6 mg/mL and at pH 6 the initial concentrations were 1 mg/mL, 5 mg/mL and 10 mg/mL. Initial concentrations are noted in the results.

2.2.4 Fluorescence monitored unfolding:

Fc-CTLA4 in solution at pH 6 and pH 7.5 was mixed with concentrated guanidine hydrochloride or urea (as indicated) to obtain increasing concentrations of denaturant. Final protein concentration was 0.1 mg/mL, with denaturant concentration ranging from 0-9.75 M for urea and 0-6 M guanidine hydrochloride. The fluorescence of the protein was measured from 300-400 nm using an excitation wavelength of 293 nm. The scans at each concentration were

used to obtain the unfolding curve by plotting the center of spectral mass vs. denaturant concentration. This data was also used to calculate the free energy of unfolding for each protein/condition combination as described previously [10, 11].

2.2.5 Thermal denaturation

The thermal denaturation of Fc-CTLA4 was measured by both circular dichroism (CD) and differential scanning calorimetry (DSC). For measurement of the T_m of the CTLA4 domain alone, CD was used to conserve limited materials. For the DSC experiments, samples with concentrations from 0.5-11 mg/mL were scanned from 5-105 °C at 1.5 atm overpressure. Scan rates were varied from 15-90 °C/hr. Activation energies were calculated from T_m values at different scan rates using the following equation [12]:

$$\ln\left(\frac{v}{T_m^2}\right) = \frac{AR}{E_a} - \frac{E_a}{RT_m}$$

In the above equation, *v* is the scan rate, R is the gas constant, T_m is the midpoint transition temperature, A is a pre-exponential factor, and E_a is the activation energy.

Far UV CD spectra was collected at 217 nm (β sheet signal) for protein samples as they were heated from 10 °C to 90 °C at a scan rate of 1 °C/min. Data is reported as molar ellipticity.

2.2.6 Thrombin digest-

A commercial thrombin digest kit (Thrombin Cleavage Capture Kit, Novagen, Rockland, MA) was used for the Fc-CTLA4 cleavage experiments. Experiments were carried out according to the enclosed instructions. Thrombin was provided at a stock concentration of 1 U/μL, and

diluted as noted. A 1:25 dilution (per kit instructions) was incubated at room temperature with Fc-CTLA4 for 5, 24 and 89 hours. A 1:200 thrombin dilution was incubated with Fc-CTLA4 at room temperature for 5 and 24 hours. The 1:25 thrombin dilution was also investigated for its activity at 30°C and 40°C during 12 hour incubations as well as in the presence of 25 mM EDTA, 1 M guanidine hydrochloride, and 25 mM EDTA/1M guanidine hydrochloride at room temperature. Increased thrombin concentration, above the suggested value, was also investigated, per Linsley et. al 1995. A final thrombin concentration of 100 U/mL was incubated with Fc-CTLA4 under the following conditions: room temperature/96 hours, 30°C/21 hours and 40°C/21 hours. Digestions were analyzed via SDS-PAGE.

2.2.7 E. coli phage display biopanning-

Biotinylated Fc-CTLA4 was prepared using the EZ-Link Sulfo-NHS-LC-Biotinylation kit (Fisher Scientific, Waltham, MA). The full OmpX *E. coli* phage display library was cultured to an OD600 of 1 in 50 mL of LB media containing 34 μg/mL chloramphenicol. 80 mL of cell culture were then centrifuged for 15 minutes at 3000g, supernatant removed and cells screened for streptavidin binding peptides. $1.25x10^9$ streptavidin coated magnetic beads (Dynabeads MyOne Streptavidin T1, Invitrogen, Carlsbad, CA) in PBS were added to the E. coli cells in the 15 mL falcon tube. The cells were then incubated with the beads on an orbital shaker at 4 C for 45 minutes, a magnet applied to the side of the tube to remove the beads and streptavidin bound E. coli, and the supernatant transferred to a new tube for positive section. For the positive selection step, the biotinylated Fc-CTLA4 was added at a concentration of 50 nM to the E. coli cells. The biotinylated protein and cells were then incubated on an orbital shaker for 45 minutes, then centrifuged and resuspended in PBS following the removal of the supernatant. $2.5x10^9$

beads were then added to the cell suspension and the incubation step repeated. Following incubation, the beads were washed three times by applying the magnet for 5 minutes, removing the supernatant and resuspending in cold PBS. After the third wash step, 1 μM biotin was added to remove the cells from the beads and cultured overnight in 25 mL LB media with 34 μg/mL chloramphenicol and 0.2% glucose. Five rounds of the magnetic cell selection were repeated to select for the strongest binding peptides to Fc-CTLA4. Post cell selection, cells were plated and individual colonies isolated for culture. Plasmids were extracted from each culture using a QIAGEN Plasmid Mini Prep Kit (Valencia, CA) and sequenced by Macrogen USA (Rockville, MD).

2.3 Results

2.3.1 Accelerated stability studies

During accelerated stability studies, the Fc fusion, Fc-CTLA4, exhibited markedly different aggregation rates with only a small shift in pH. An increase of two orders of magnitude in the aggregation rate was observed when changing the solution pH from pH 7.5 to pH 6. At pH 7.5 and 40 °C, the rate of monomer loss was 6 $\mu g*mL^{-1}*h^{-1}$, which corresponds to an apparent first order reaction rate constant of $0.0012 \pm 0.0002\ h^{-1}$. At pH 6 the observed aggregation rate/apparent first order rate constant increased to 800 $\mu g*mL^{-1}$*h-1 and $0.16 \pm 0.012\ h^{-1}$, respectively. With these differences in reaction rates, it took 15 days of incubation at pH 7.5 to see the same amount of monomer loss that was observed after 5 hours at pH 6 (Figure 2-2). There were further differences in the type of aggregate species present as well. All of the aggregates at pH 6.0 appeared to be soluble, with no detectable monomer loss by SEC. There

were insoluble aggregates present at pH 7.5 as a pellet was visible after centrifugation of the sample and SEC peak area was not conserved.

Increasing the concentration of sodium chloride to 200 mM at pH 6 resulted in only a slight decrease in aggregation, with the apparent first order reaction rate constant being reduced to $0.1 \pm 0.03\ h^{-1}$. Aggregation studies in the Tris/MES/acetic acid buffer system at pH 6 exhibited similar aggregation compared to the other buffers at that pH with an apparent first order rate constant of $0.08 \pm 0.01\ h^{-1}$.

The change in pH also lead to differences in reaction order, indicating a different mechanism controls aggregation at the two pH values. At pH 6 the apparent reaction order is between 1^{st} and 2^{nd} order and at pH 7.5 it is higher than 2^{nd} order with a possible concentration dependence.

2.3.2 Conformational stability

Chemical denaturation of Fc-CTLA4 by urea shows the presence of two unfolding transitions in Figure 2-3. The first unfolding transition is shifted to lower concentrations of denaturant at pH 6 as compared to pH 7.5, indicating that the change in pH is reducing the conformational stability of this domain. This is supported by the change in the free energy of unfolding for the transitions. The free energy of unfolding for the first transition was 14.5 ± 1.3 kJ/mol at pH 7.5 and 6.8 ± 1.3 kJ/mol at pH 6 in phosphate buffer. The second unfolding transition is not affected by the change in pH.

The buffer species has no impact on the unfolding transitions at pH 6, demonstrated by the overlapping curves in Figure 2-3 and the fact that the ΔG_{unf} for the first transition in the Tris/MES/acetic acid buffer was 6.0 kJ/mol, which is very close to the ΔG_{unf} in the phosphate

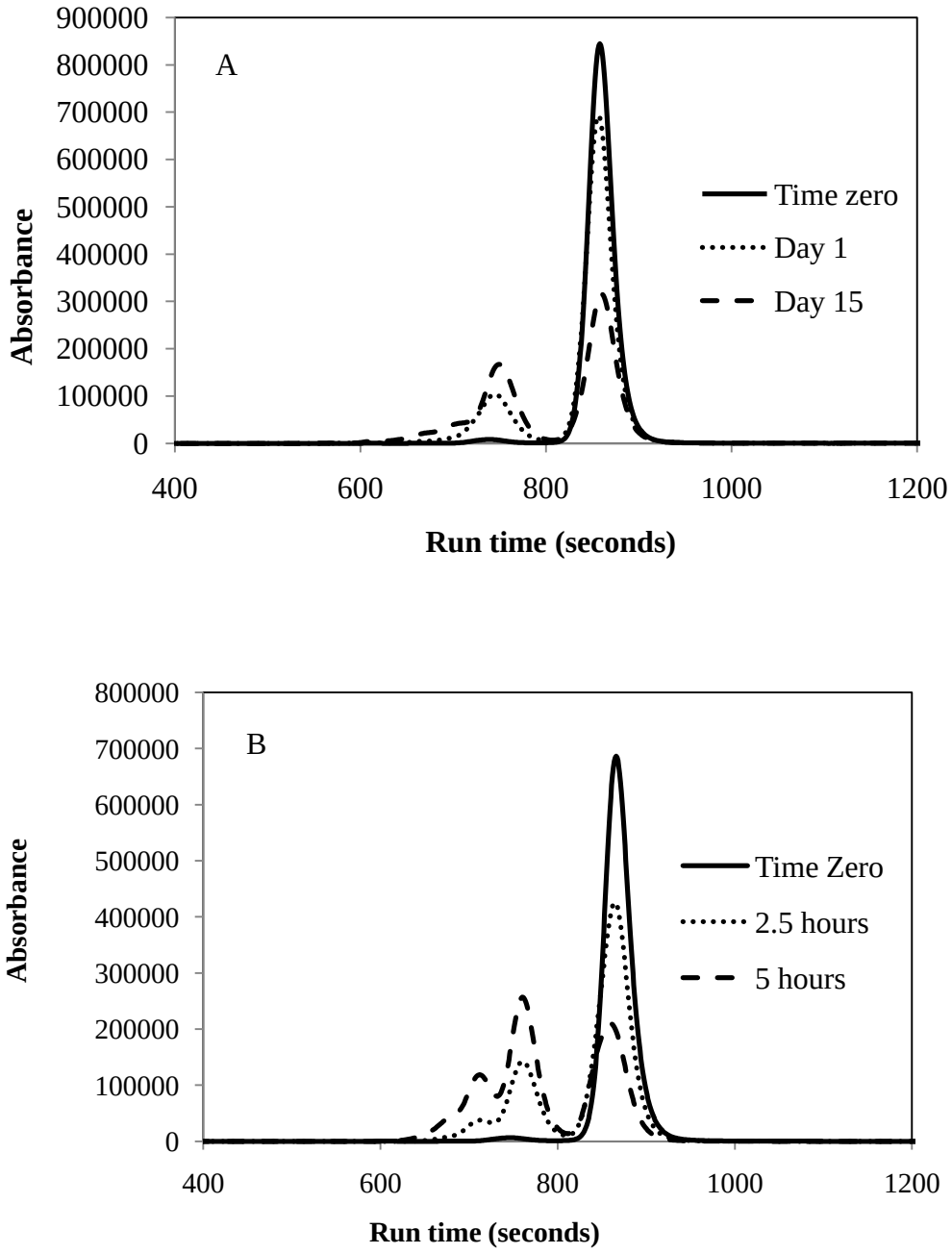

Figure 2-2: Size exclusion chromatograms of 40 C incubated samples at pH 7.5 (Panel A) and pH 6.0 (Panel B). Samples incubated one day (dotted) and 15 days (dashed) are compared to the stock protein (solid line) at pH 7.5 in Panel A and samples incubated 2.5 hours (dotted) and 5 hours (dashed) are compared to the stock protein (solid line) at pH 6.0 in Panel B.

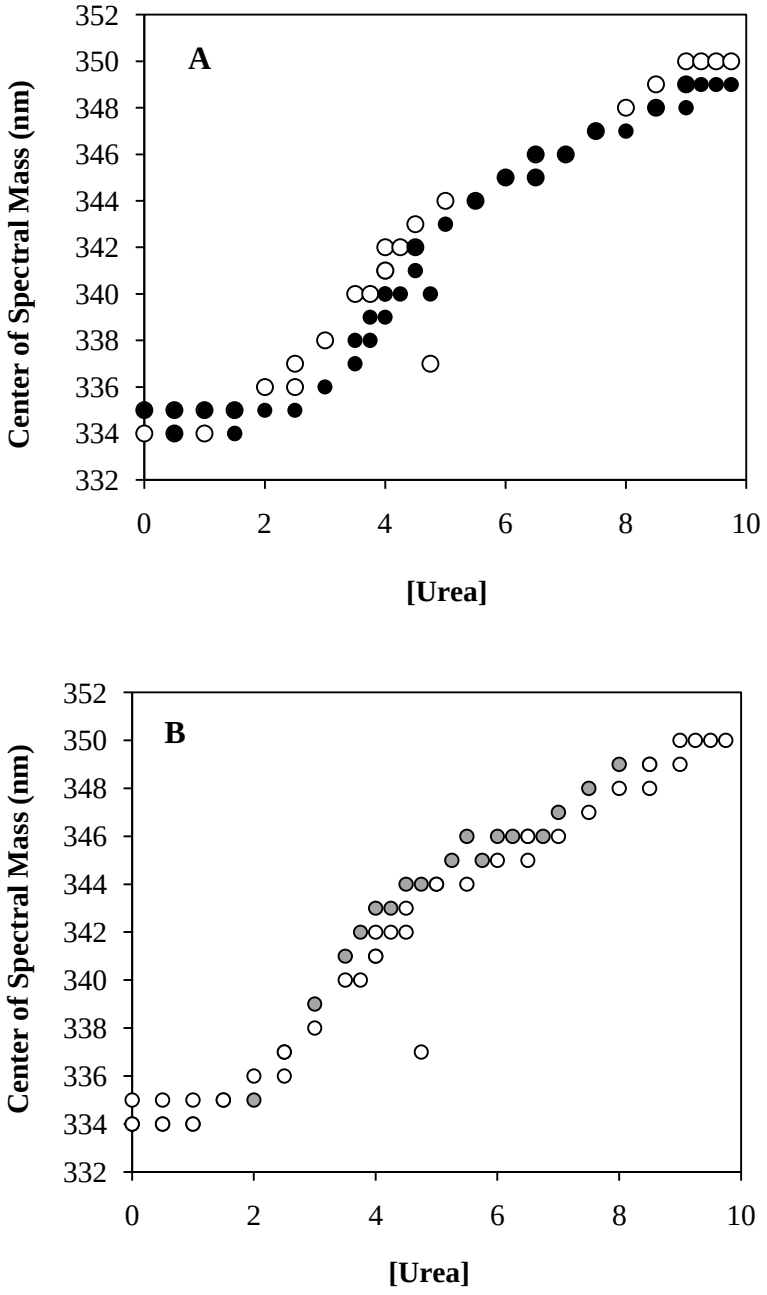

Figure 2-3: A) Fc-CTLA4 chemical denaturation at pH 6 (○) and pH 7.5 (●) in 10 mM sodium phosphate, 10 mM NaCl buffer. B) Fc-CTLA 4 chemical denaturation at pH 6 in either 10 mM sodium phosphate, 25 mM NaCl (○) or 50 mM Tris, 25 mM MES, 25 mM acetic acid, 25 mM NaCl (●). Note that the first transition has an earlier onset at pH 6 versus pH 7.5. No difference is observed at pH 6 as a function of buffer species.

buffer system.

Thermal denaturation of the Fc-CTLA4 fusion protein as measured by far UV CD exhibits two unfolding transitions. The CTLA4 domain alone undergoes one unfolding transition which overlaps with the first transition of the intact fusion (Figure 2-4). When measured by DSC, the fusion also exhibits two distinct unfolding transitions separated by 30 °C. The activation energy for the first transition was calculated to be 297 ± 13 kJ/mol at pH 6 and 361 ± 19 kJ/mol at pH 7.5. The activation energy for the second transition was not affected by the shift in pH (391 ± 14 kJ/mol at pH 6 and 391 ± 20 kJ/mol at pH 7.5).

2.3.3 Colloidal Stability

The second osmotic virial coefficients (B_{22}) were calculated from static light scattering data and can be seen in Table 2-1. As mentioned previously, the B_{22} is a measure of protein-protein interactions in solution. In the sodium phosphate buffer, at both pH 7.5 and pH 6, the net interaction is attractive. Switching to a Tris/MES/acetic acid buffer system at pH 6 results in repulsive protein-protein interactions. Table 2-1 also includes the relative aggregation rate for each buffer condition. The aggregation rate at pH 7.5 is low, compared to the aggregation in both pH 6 buffers which is relatively high.

2.3.4 Enzymatic digests

In order to compare the stability of the domains with the overall protein stability, enzymatic digestion of Fc-CTLA 4 was attempted as a way to separate the domains. The presumed sequence of Fc-CTLA 4 includes a thrombin digest site in the hinge region [8, 13]. One 50

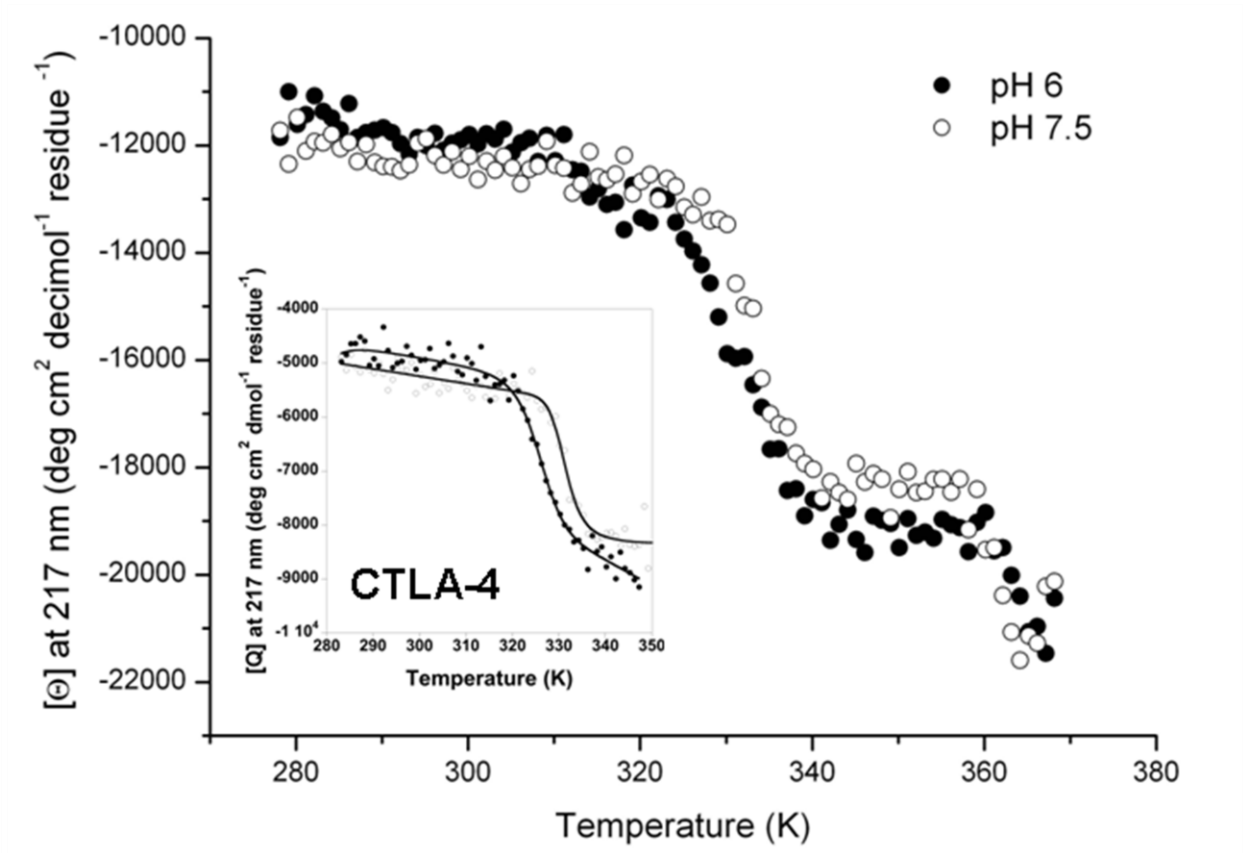

Figure 2-4: A Far UV CD thermal melt followed at 217 nm (β sheet signal) shows two transitions for the complete fusion protein, whereas CTLA 4 undergoes one transition that coincides with the first transition of Fc-CTLA 4.

Buffer System	**pH**	**2nd Virial Coefficient x 10^4 (mL*mol*g^{-2})**	**Net interaction**	**Relative Aggregation Rate**
Sodium phosphate	7.5	-6.0 ± 1.9	Attractive	Low
Sodium phosphate	6	-6.5 ± 3.7	Attractive	High
Tris/MES/acetic acid	6	6.55	Repulsive	High

Table 2-1: Comparison of colloidal stability and aggregation rate based on pH and buffer system. B_{22} values were obtained by Jonas Fast, PhD.

kDa portion (CTLA4 domain) and two 22.5 kDa portions (Fc domains) are expected if the protein was cleaved in the hinge region. However, the digestion results show one 75 kDa band and one 50 kDa band by SDS-PAGE. This indicates that the protein is not completely cleaved between the Fc and CTLA-4 portions. Figure 2-5 is a photograph of the SDS-PAGE gel showing the size of the fragments obtained from the digest.

2.3.5 E. coli Phage Display Biopanning-

Seventeen potential binding peptides were identified and are listed in Table 2-2 along with their theoretical pI values. Theoretical pI values for the peptides were calculated using SwisProt.

2.4 Discussion

Given that the two domains of the Fc-CTLA4 fusions should be oppositely charged at pH 6 and less so at pH 7.5, one might expect that protein-protein interactions and colloidal stability play a large role in the aggregation of this protein. However, since relatively high aggregation rates were observed for both buffer systems at pH 6 where the net interactions were either attractive or repulsive depending on the buffer, and low aggregation rates were observed at pH 7.5 where the net interaction is attractive, it is apparent that B_{22} does not correlate with aggregation rate. Thus colloidal stability is most likely not driving the aggregation of this protein.

Although no differences in colloidal stability between the phosphate buffer conditions at pH 7.5 and pH 6 were observed, there were large changes in conformational stability. The shift from pH 7.5 to pH 6 decreased the free energy of unfolding (ΔG_{unf}) of the first transition by over half. This pH shift had no effect on the second unfolding transition of the Fc-CTLA4 fusion.

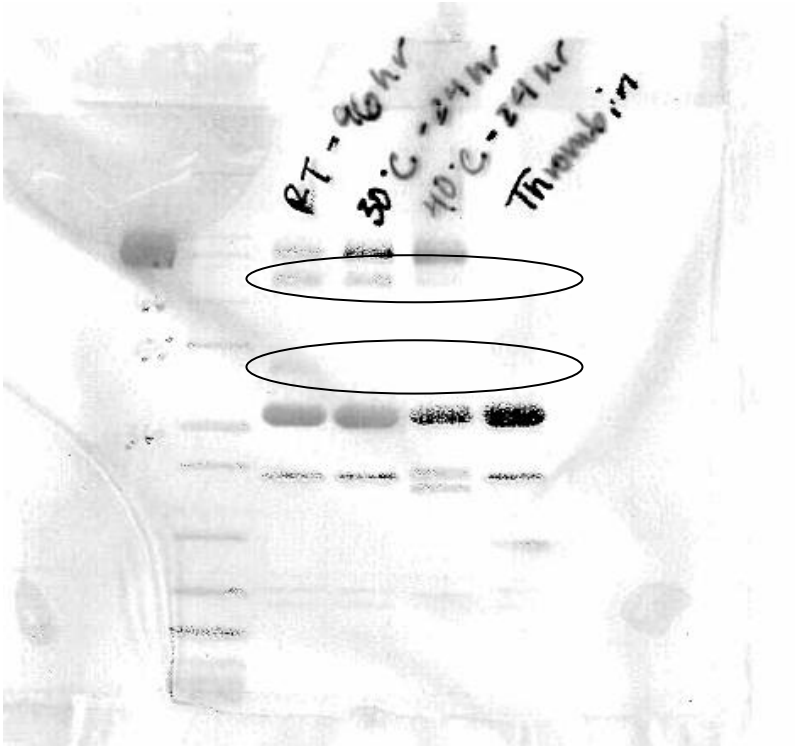

Figure 2-5: SDS-PAGE of thrombin digest samples. The upper oval is highlighting the 75 kDa band and the lower oval is highlighting the 50 kDa band. Stock Fc-CTLA4 is included in the first lane, directly to the left of the molecular weight ladder in the second land. Stock thrombin was included in the far right land for comparison with the digested samples.

Peptide Sequence	**Theoretical pI***
G N K M W R R	12.01
N M P Q R R T	12.00
R K S Y W R Q	11.00
L R G P A N K	11.00
Y K N N G R R	11.00
V C R R G F Q	10.35
G R Q C T R L	10.35
T I M N R W S	9.41
E V N K R W I	8.85
V Q K K E I S	8.56
E A T Y K E R	6.24
W V A S E W K	6.00
W M S G M D R	5.84
F K L A D T F	5.84
N V T I N F X	5.52
R I E E T T Q	4.53
L N G V D I S	3.80

Table 2-2: Peptide sequences identified by phage display that potentially bind Fc-CTLA4 and the theoretical pI values corresponding to each peptide sequence.

Two distinct unfolding transitions were also present when measured by DSC, separated by approximately 30 °C.

Since there are no tryptophan residues in the CTLA4 domain [8], the unfolding of said domain should not be detectable by intrinsic fluorescence. Thus the two transitions visible during chaotrope denaturation likely correspond to the C_H2 and C_H3 regions of the Fc domain. However, if all three domains were unfolding independently, one would expect to see three transitions during thermal denaturation. This is not the case. Only two thermal transitions are observed. When measured alone, CTLA4 at pH 7.5 show a single transition with Tm = 58 °C which is close to the first transition of the intact fusion protein. This leads to the conclusion that the CTLA4 and C_H2 domains are the least conformationally stable with overlapping unfolding transitions.

Solution conditions with an increased aggregation rate corresponded to those where the conformational stability of the CTLA4 and C_H2 domains was reduced. The shift in pH also reduced the activation energy for aggregation.

The thrombin digest did not successfully cleave the fusion protein into the separate intact Fc and CTLA4 domains. The most likely explanation of the results is that the two Fc portions are cleaved off individually, and that the 75 kDa band seen in the gel still has one Fc portion while the approximately 50 kDa band is only the CTLA4 domain. An additional complication is that the thrombin stock produces a band around 20 kDa which may mask Fc fragments. MALDI-TOF MS yielded inconclusive results on the sizes of the Fc-CTLA4 fragments. Furthermore, digestion only occurred in samples where the thrombin concentration was increased to 100 U/mL and digestion yields were too low to provide sufficient materials for further experiments. The

inability to separate the fusion domains for further experimentation limits the utility of the Fc-CTLA4 fusion as a model protein for further studies.

The *E. coli* phage display biopanning did not identify a strong candidate for a potential peptide ligand for Fc-CTLA4. There was no strong consensus between the seventeen sequences identified, although 40% of the peptides identified had a theoretical pI above 10. Additionally, since the entire Fc-CTLA4 fusion protein was used for the biopanning, the peptides may not bind the CTLA4 domain as desired for selective stabilization of the least conformationally stable domain. Another concern is that the CTLA4 domain is unlikely to be the conserved domain. Thus any peptide identified to stabilize CTLA4 is not expected to be useful beyond this fusion construct.

2.5 Conclusions

Fc-CTLA4 is highly sensitive to changes in pH. Maximizing domain conformational stability results in the most stable formulation for this fusion. However, the inability of separating the domains and the lack of domain selective stabilizing candidates makes this a difficult system to study and leaves several questions unanswered. Furthermore, the Fc domain is likely to be the conserved domain in future fusion protein products and thus work aimed at increasing the conformational stability of the CTLA4 domain may not be useful beyond this case.

2.6 References

1. Schmidt, S. R. Current Status of Fusion Protein Applications Including the Use of the Zera Peptide. AAPS National Biotechnology Conference, San Francisco, 2011.

2. Reichert, J. Antibody-based therapeutics to watch in 2011. MAbs 2010 [Epub], 3 (1).

3. In Antibody Fusion Proteins, 1st ed.; Chamow, S., Ashkenazi, A., Eds.; Wiley-Liss Inc: New York, 1999.

4. Davis, P.; Abraham, R.; Xu, L.; Nadler, S. G.; Suchard, S. J. Abatacept binds to the Fc receptor CD64 but does not mendiate complement-dependent cytotoxicity or antibody-dependent cellular cytotoxicity. J Rheumatol 2007, 34, 2204-2210.

5. Jazayeri, J.; Carroll, G. Fc-based cytokines: prospects for engineering superior therapeutics. BioDrugs 2008, 22 (1), 11-26.

6. Orencia Product Information Sheet; Bristol-Myers Squibb, 2007.

7. Orencia Product Monograph; Bristol-Myers Squibb Canada, 2006.

8. Aruffo, e. a. Inhibiting B cell activation with soluble CD40 or fusion proteins thereof. 6,376,459, April 23, 2002.

9. ProtParam Tool. http://web.expasy.org/protparam/ (accessed December 1, 2010).

10. Myers, J. K.; Pace, C. N.; Scholtz, J. M. Denaturant m values and heat capacity changes: Relation to changes in accessible surface areas of protein unfolding. Protein Science 1995, 2138-2148.

11. Pace, C. Determination and Analysis of Urea and Guanidine Hydrochloride Denaturation Curves. Methods in Enzymology 1986, 131, 266-280.

12. Sanchez-Ruiz, J. M. Theoretical analysis of Lumry-Eyring models in differential scanning calorimetry. Biophys J. 1992, 61 (4), 921-935.

13. Linsley, P. Binding Stoichiometry of the Cytotoxic T Lymphocyte-associated Molecule-4 (CLTA-4). The Journal of Biological Chemistry 1995, 270 (25), 15417-15424.

CHAPTER 3

CHOOSING APPROPRIATE ACCELERATED STABILITY STUDIES TO RANK THE STABILITY OF POTENTIAL PROTEIN FORMULATIONS

3.1 Introduction

Shelf-life requirements of therapeutic protein products necessitate aggregate levels in the very low percentages at the end of the storage period [1]. Under real storage conditions, most commonly used analytical techniques are unable to quantify the low aggregation rates implied by this requirement within a timeframe that is reasonable for development of formulations. Thus, in order to screen for formulation conditions most likely to provide acceptable long-term storage stability, accelerated degradation studies are used to screen formulations. For example, stability of proteins within formulations is often assessed by subjecting test formulations to elevated temperatures and measuring (e.g., using microcalorimetry or various optical spectroscopies) the "melting" temperature T_m at the midpoint of unfolding. Although interpretations of T_m are more complicated with multidomain proteins that may exhibit separate T_m values for each domain, formulations that result in lower T_m values generally correlate with increases in aggregation rates at temperatures less than T_m [2]. Models have also been developed to better predict low-temperature behavior from the elevated-temperature stability studies, including incubation studies [3, 4]. The recent work of Brummit, et al., has very nicely shown the predictive ability of high-temperature scans for estimating the aggregation rates observed in liquid formulations under lower-temperature storage conditions [4]. The temperature-scanning monomer loss approach predicted the observed rate coefficients for shelf-lives ranging over orders of magnitude [4]. This approach was also able to capture both the unfolding and association aspects of aggregation [4]. However, aggregation is a concern during the entire product life-cycle, including manufacturing

and transport [5, 6, 7], and accelerated stability studies at elevated temperature may still not capture all of the aggregation mechanisms involved, especially those involving interfaces. Thus there is a benefit to understanding how accelerated stability studies at elevated temperature compare with accelerated stability studies involving other stresses such as agitation or freeze/thawing.

It is very common for proteins to be exposed to air/water and water/ice interfaces, as well as freeze concentration during manufacture and shipping. Pumping or stirring of protein solutions during the manufacturing process [5] results in greater exposure of proteins to air/water interfaces. Likewise, vibrations during shipping may increase air-water interfacial surface areas, and pump cavitation can increase exposure of proteins to air/water interfaces [6, 8]. During the manufacturing process, protein may be frozen as bulk drug substance to meet the demands of the campaign schedule [9]. Additionally, products which are designed for in home administration may experience inadvertent freezing/thawing during at-home storage [10]. Not only does freezing create a water/ice interface which can induce protein damage [11], but freeze concentration of the protein in the liquid phase can also crowd molecules together and increase propensity for association and aggregation [12].

The type and duration of stress are important factors in the formation of protein aggregates. Previous studies have shown that different stresses can lead to differences in the amount and type of aggregates produced. Freeze-thaw cycling has been shown to produce different protein aggregate types and amounts than are produced by heating, [13, 14] and to produce fewer particles than agitation [14]. Subcutaneously injected protein aggregates produced by freeze-thawing elicited different immune responses from those formed by agitation [15]. Stirring has been shown to be a more harsh agitation stress than shaking [16]. Even when stirring is considered

alone, the orientation of the stirring mechanism itself (e.g. top versus bottom) can lead to differences in aggregate formation [17].

Further complicating analysis of the aggregation is that protein aggregates may be found at low concentration and span a broad range of sizes, making their quantitation problematic. Size exclusion chromatography (SEC) can provide accurate quantification of monomer and lower-order aggregates (e.g., dimers, trimers) but may miss subvisible particles that are filtered out by the column resin [18]. Characterizing these subvisible particles is desirable since they have been implicated in potentially causing adverse immune responses [19, 20, 21]. Utilizing flow imaging in conjunction with SEC can help provide a more complete picture of product behavior upon exposure to process changes/stresses [22].

Here we compare the previously determined mechanism responsible for thermally-induced aggregation of abatacept, an Fc-CTLA4 fusion protein, to the aggregation induced by agitation or freeze/thawing in solutions at both pH 7.5 and pH 6.0. Previously, conformational instability was determined to be the main factor leading to aggregation of abatacept during accelerated stability studies conducted at elevated temperatures [23]. At elevated temperatures, the domains of abatacept sequentially unfold. The CTLA4 domain and the C_H2 region of the Fc domain unfold during the first transition, and the C_H3 region of the Fc domain unfolds during the second transition. Abatacept was found to be less conformationally stable (i.e., the free energy of unfolding for the first unfolding transition was approximately 8.5 kJ/mol lower) and more aggregation-prone in solutions at pH 6.0 relative to solutions at pH 7.5 [23]. Given that several accelerated methods often are used to predict long term storage behavior, it is useful to understand how the choice of accelerated method influences the ranking of formulation stabilities. Here, freeze/thaw and agitation studies were used to evaluate the stability of abatacept

formulations to stresses beyond elevated temperature and compare how differences in conformational stabilities between formulations influence the aggregation of abatacept.

3.2 Materials and Methods

3.2.1 Stock Protein Preparation

Abatacept, an Fc-CTLA4 fusion protein, was obtained as a lyophilized white powder (marketed as Orencia®, Bristol Myers Squibb, New York, New York). After reconstitution according to package instructions, abatacept was dialyzed into the experimental buffer: 50 mM Tris, 25 mM MES, 25 mM acetic acid and 25 mM NaCl (pH 6.0 or pH 7.5) as noted. All buffers contained 0.01% w/v sodium azide to inhibit microbial growth and were filtered with a 0.22 μm nitrocellulose filter (Millipore, Cork, Ireland) prior to dialysis.

3.2.2 Agitated sample preparation

Stock protein was diluted to a final concentration of 1 mg/mL. 400 μL aliquots were placed in 0.6 mL polypropylene microcentrifuge tubes (Fisher brand). The centrifuge tubes were secured horizontally on an orbital titer plate shaker (Lab-Line Instruments, Inc., Melrose Park, IL). Samples were agitated for 1, 3 or 6 hours at shaker intensity setting 5 or 10.

3.2.3 Freeze thaw sample preparation

400 μL of solutions containing abatacept at a concentration of 1 mg/mL were aliquoted into 0.6 mL polypropylene microcentrifuge tubes. One of two freeze/thaw protocols was used. Samples were either frozen in liquid nitrogen for 1 minute and then thawed for five minutes in a water bath at 23.5 °C (fast protocol) or frozen at -20 °C for 30 minutes and thawed at 4 °C on a

refrigerator shelf for two hours (slow protocol). The liquid nitrogen freezing protocol was repeated for a total of 5 or 20 cycles and the -20 °C freezing protocol was repeated for a total of 5 cycles.

3.2.4 Stressed sample storage

After application of the respective stress, freeze thaw- or agitation-stressed samples were stored in the original microcentrifuge tubes for 24 hours at 4 °C before analysis to observe if any changes in aggregate profile occurred. Samples were stored quiescently in a vertical orientation.

3.2.5 Size exclusion chromatography (SEC)

Prior to SEC analysis, samples were centrifuged for 5 minutes to remove larger aggregates. Samples were then injected onto a Tosoh Bioscience 3000swxl gel column (Montgomeryville, PA) using a Waters 717plus autosampler (Waters Technologies Corporation, Milford, MA). A Beckman System Gold with a 166 detector (Beckman Coulter, Brea, CA) was used to control the flow rate and measure the absorbance of the eluate. The mobile phase consisted of 100 mM sodium phosphate, 200 mM sodium chloride at pH 7.0 and the flowrate was 0.6 mL/min. The mass of protein in the peak of interest was calculated using Equation 1:

$$(1) \qquad \text{Mass} = \frac{(\text{Peak Area})(V_f)}{(\varepsilon_{280})10^6}$$

where V_f is the flowrate in mL/s and ε_{280} is the extinction coefficient of the protein in cm^2/mg.

3.2.6 Micro Flow Imaging (MFI) Analysis

The Brightwell Dynamic Particle Analyzer 4100 particle imaging system (Ottawa, Ontario, Canada) was used to collect particle counts for the stressed and unstressed samples. The instrument was operated in normal mode with low magnification and a vertical cell orientation. For each sample, 0.15 mL were dispensed prior to analysis in order to minimize dead-volume effects. The cell was flushed with filtered water between protein samples until particle counts returned to the original pre-sample levels. Samples were not centrifuged prior to analysis by MFI. The total mass of aggregates present in each sample was estimated as previously described [22]. Briefly, binned particle counts reported from MFI analysis were converted to particle mass per bin by assuming that each size bin represented spherical particles with a diameter equal to the bin midpoint. The volume of particles in each size bin was calculated, and then converted to mass concentration (M_p) by multiplying by an effective protein density using Equation 2:

$$(2) \qquad M_P = \sum_{\text{all i}} V\varphi\rho n_i$$

where V is particle volume, φ is fraction of protein within particle, ρ is the protein density, and n_i is particle population density in size bin i. For these estimations, a protein fraction within the particles of ¾ and a protein density of 1.43 g/mL were used [22].

3.2.7 Conformational stability of abatacept at 4 °C

Conformational stability of abatacept at 4 °C was determined using the chaotrope perturbation method described previously [24] to calculate the free energies of unfolding. Abatacept samples at a concentration of 0.1 mg/mL were incubated overnight in guanidine hydrochloride (0-6 M) prior to fluorescence measurement. To measure intrinsic fluorescence, the samples were

excited by light at a wavelength of 293 nm and the resulting emission spectra from 300-400 nm were recorded using an Aminco Bowman Series 2 fluorescence spectrophotometer (SLM Aminco, Urbana, Illinois). The center of spectral mass (CSM) of each emission spectrum was calculated using Equation 3:

$$(3) \qquad \mathrm{CSM} = \frac{\sum F_i V_i}{\sum F_i}$$

In Equation 3, F_i is the fluorescence intensity at a given wavenumber, v_i. Plots of CSM values versus chaotrope concentration were then fit to a two state unfolding model using a linear least-squares fit to Equation 4 to calculate the free energies of unfolding (ΔG_{NU}) [25]. Equation 5 represents the linear approximation for ΔG_{NU} for chaotrope-induced denaturation [25].

$$(4) \qquad Y_0 = \frac{(k_N[D] + b_N) + (k_U[D] + b_U)\exp\left(\frac{-\Delta G_{NU}}{RT}\right)}{1+\exp\left(\frac{-\Delta G_{NU}}{RT}\right)}$$

$$(5) \qquad \Delta G_{NU}(D) = \Delta G_{NU}(H_2O) + m[D]$$

In Equation 4, k_N and k_U are the slopes of the baselines of the native and unfolding states respectively, b_N and b_U are the intercepts of these baselines, Y_0 is the center of spectral mass value, T is temperature, and R is the molar gas constant. In Equation 5, [D] is the concentration of the chaotrope and m represents $d\Delta G_{NU}/d[D]$ (i.e., the sensitivity of ΔG_{NU} to chaotrope concentration). $\Delta G_{NU}(D)$ is the free energy of the unfolding with chaotrope present and $\Delta G_{NU}(H_20)$ is the free energy of unfolding at a zero chaotrope concentration.

3.2.8 Colloidal stability of abatacept at 4 ℃

Zeta potential values were calculated at 4 ℃ to serve as an indicator of colloidal stability. The Malvern Zetasizer Nano ZS (Worcestershire, United Kingdom) was used to measure electrophoretic mobility of the protein samples. These data were converted to zeta potential values using the Smoluchoski approximation to Henry's equation (Equation 6) [26].

$$(6) \qquad \mu_e = \frac{2\varepsilon k_s \zeta}{3\eta}$$

In Equation 6, μ_e is the elecrophoretic mobility, η is the solution viscosity, ε is the dielectric constant, ζ is the zeta potential and k_s equals 1.5 in the Smoluchoski approximation. Protein samples at 4 ℃ and a concentration of 1 mg/mL were placed in disposable folded capillary cells (Malvern Instruments Ltd, Worcestershire, United Kingdom). Three separate samples were measured for each solution condition and the reported values represent the average ± the standard deviation.

3.3 Results

3.3.1 Thermal stability of abatacept

For ease of comparison, we first summarize the major experimental result of a previously reported study on the stability of abatacept against aggregation accelerated by incubation at elevated temperatures [23]. In these earlier studies, a two order of magnitude increase in the aggregation rates at pH 6.0 relative to pH 7.5 conditions was seen during accelerated stability studies at 40 ℃ [23].This increase in aggregation correlated with the decreased activation energy (measured by scanning calorimetry) and decreased free energy of unfolding for the first structural transition at pH 6.0 versus pH 7.5 [23]. The first structural transition corresponds to the unfolding of the CTLA4 domain and the C_H2 region of the Fc domain [23].

3.3.2 Conformational stability of abatacept at 4 °C

ΔG_{NU} values for abatacept measured at 4 °C are lower in solutions at pH 6.0 than values measured in solutions at pH 7.5 (Table 3-1). Lower conformational stability at pH 6.0 compared to pH 7.5 was also observed previously at 25 °C (Table 3-1) [23]. However, although the relative order of stabilities with respect to pH remains the same between the two solution conditions at either temperature (i.e., the protein is less conformationally stable at pH 6.0 than at pH 7.5), the conformational stability was increased at 4 °C compared to 25 °C (Table 3-1).

3.3.3 Colloidal stability of abatacept at 4 °C

Although colloidal instability was determined not to be a major contributor to the aggregation of abatacept at elevated temperature [23], it still may be an important factor in the freeze thaw studies here. Since pKa values are a function of temperature [27], the potential exists for protein-protein electrostatic interactions to vary between 4 °C and 25 °C because the charge state of the molecule may change. However, that was not seen to be the case. Zeta potential values are the same at 4 °C and 25 °C (Table 3-1), indicating that there is not a large temperature dependence on the electrostatic contributions to colloidal stability of abatacept in the range 2-25 °C.

3.3.4 Freeze/thaw induced aggregation

No significant changes in monomer concentration were detected by SEC for samples stressed by either freeze/thaw protocol. This observation held in formulations at both pH 6.0 and 7.5. When the freeze-thaw cycled samples were stored at 4 °C for 24 hours and then analyzed by

pH	ΔG_{NU} (kJ/mol) at 4 °C	ΔG_{NU} (kJ/mol) at 25 °C*	Zeta potential (mV) at 4 °C	Zeta potential (mV) at 25 °C
6.0	12.1 ± 1.4	7.1 ± 0.6	-2.7 ± 1.3	-2.7 ± 1.4
7.5	21.4 ± 2.3	15.6 ± 1.2	-1.3 ± 0.5	-2.9 ± 2.8

Table 3-1: Conformational and colloidal stability of abatacept as a function of temperature at pH 6.0 and pH 7.5. Values represent the average of three samples ± the standard deviation. *ΔG_{NU} values for abatacept at 25 C are from Fast et al. 2009.

SEC, no changes were observed. There were no soluble high molecular weight aggregates detected by SEC at either pH condition.

Although no high molecular weight aggregates could be detected by SEC, MFI analysis showed increased numbers of particles in solution for samples subjected to freeze-thaw cycling. After five slow freeze thaw cycles, average particle counts increased by a larger degree at pH 6.0 than at pH 7.5 in most of the size ranges analyzed, with the exception of particles larger than 25 μm (Figure 3-1). After five freeze thaw cycles, the average particle concentration in the 2-5 μm range increased by 5.2x at pH 6.0 and by 1.6x at pH 7.5. Particles per mL in the 5-10 μm range increased by 10.1x at pH 6.0 and 1.2x at pH 7.5. Particles per mL in the 10-25 μm size range increased by 6.7x at pH 6.0,and doubled at pH 7.5. The concentration of particles larger than 25 μm increased by only 10% at pH 6.0 and 50% at pH 7.5.

Samples stressed by application of 20 cycles of the fast freeze/thaw protocol contained large numbers of air bubbles, complicating the analysis by MFI. However, after only 5 fast freeze/thaw cycles, an increase in particles was observed at both pH conditions, with a larger number of particles detected in the pH 6.0 samples (Figure 3-2). After 24 hours of storage the samples stressed by 5 fast freeze thaw cycles exhibited greater differences in particle concentrations between solutions at the two pH values compared to unstressed samples. The concentration of particles in each size range decreased significantly after 24 hours storage at pH 7.5, with over a 50% loss of particles upon storage for all size ranges. For samples formulated at pH 6.0, this decrease in particle numbers upon storage was not seen.

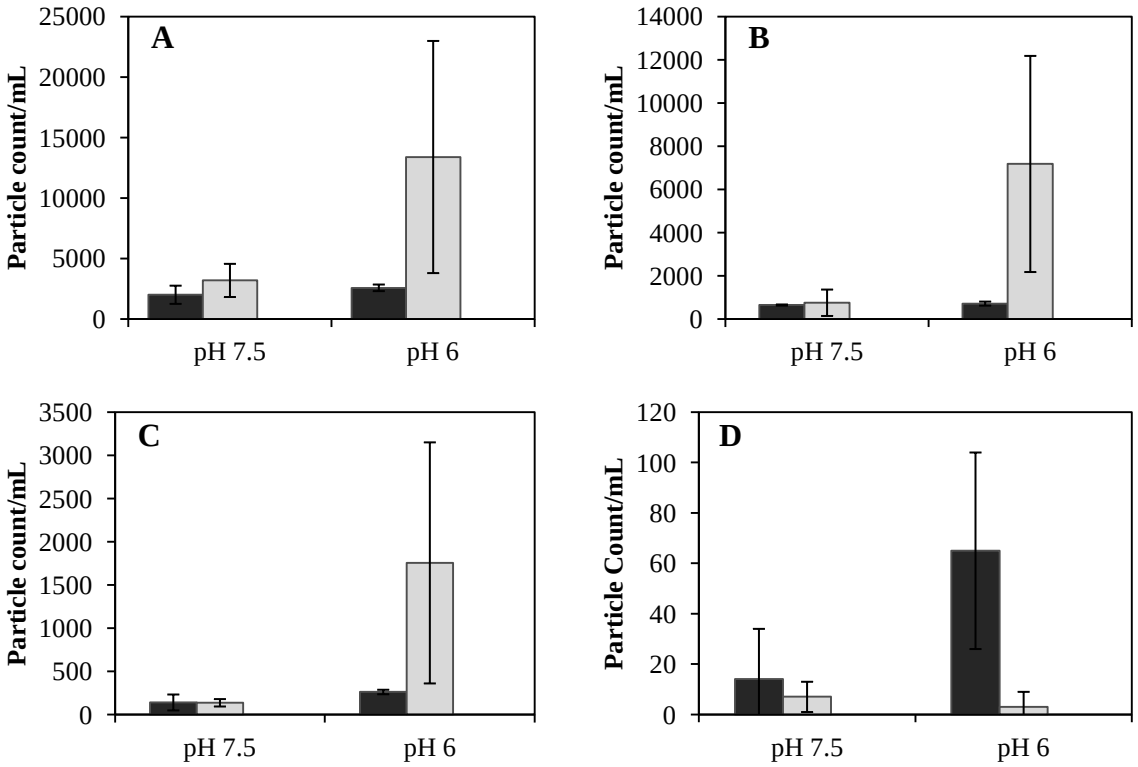

Figure 3-1: Slow freeze thaw stressed samples (5x) showing particle concentrations for each equivalent spherical diameter size range. Panel A represents the 2-5 μm size range, panel B the 5-10 μm range, panel C the 10-25 μm range and panel D represents particles 25 μm and above. Samples include stock protein (black) and protein after 5 freeze-thaw cycles (gray). In panels A-C (i.e., particles up to 25 μm), freeze thaw stress increases particle concentrations in solutions at pH 6.0 but not in solutions at pH 7.5. The concentration of particles greater than 25 μm did not increase after freeze thawing at either pH condition; however, the concentration of particles at pH 6.0 was high initially.

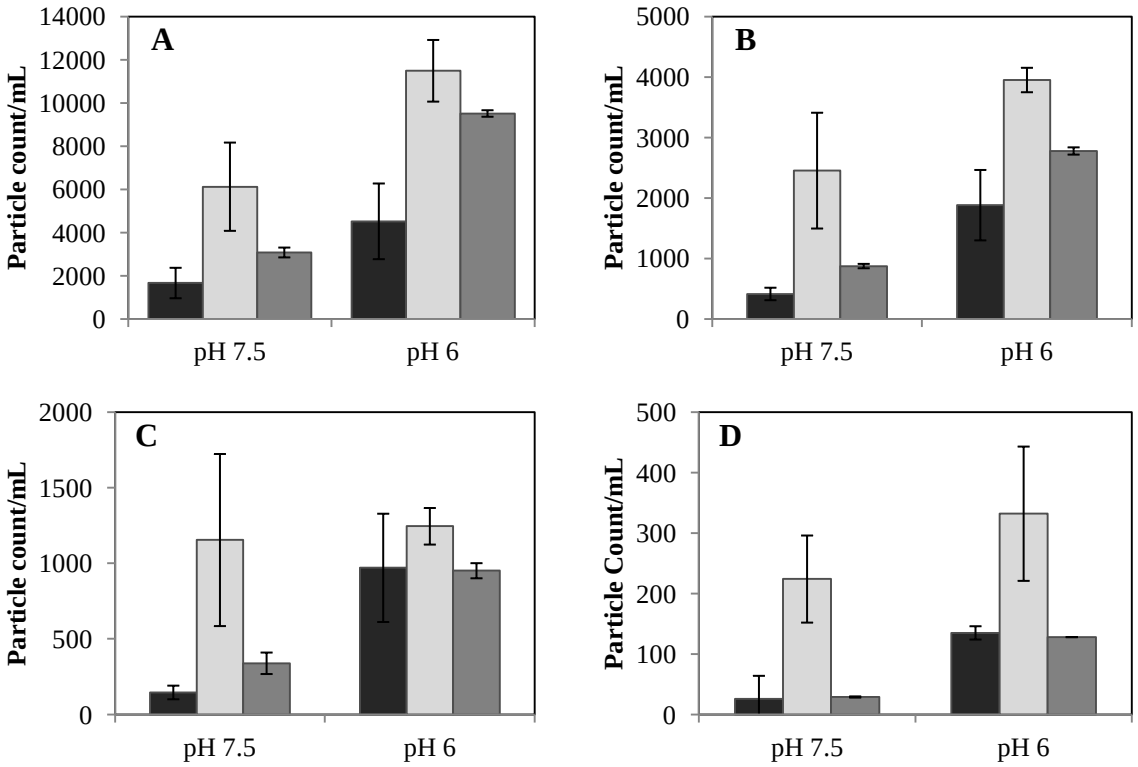

Figure 3-2: Fast freeze thaw stressed samples (5x) showing particle concentrations for the 2-5 µm size range (Panel A), the 5-10 µm size range (Panel B), the 10-25 µm size range (Panel C) and the greater than 25 µm size range (Panel D). Samples include stock protein (black), protein after 5 freeze-thaw cycles (light gray) and the freeze thaw stressed protein after 24 hours storage (medium gray). Although particle concentrations increased in all size ranges after 5 fast freeze thaw cycles for both pH conditions, the particle concentrations decreased much more at pH 7.5 than at pH 6.0 after 24 hours of storage.

3.3.5 Agitation induced aggregation

Agitated samples exhibited significant amounts of monomer loss as measured by SEC after only one hour of agitation at an orbital shaker setting of level 10, as seen in Figure 3-3. Despite the similarities in monomer loss between the two pH conditions after only one hour agitation, larger differences in aggregation were detected at later time points. Soluble higher molecular weight species were also detected by SEC at pH 6, but not at pH 7.5. In the samples formulated at pH 6.0 where higher molecular weight species were detected, there was still incomplete recovery of the initial mass. After 6 hours of agitation at pH 6.0, approximately 87.8 ± 3.0% of the initial mass was recovered. No changes in monomer levels were seen after the stressed samples were stored for 24 hours at 4 °C (data not shown).

When MFI was used to analyze samples agitated for three hours, it was found that the pH 6.0 formulation did not show as great of an increase in particle number as that seen in the pH 7.5 formulation, even though initial particle numbers were comparable. For example, the amount of particles per mL in the 2-5 μm size range increased by only 5x at pH 6.0 compared to an 11x increase at pH 7.5. However, the standard deviation for the particle count was very large, with the particle number per mL differing by an order of magnitude over the three agitated samples. The amount of particles detected in solutions at either pH did not change significantly after 24 hours of storage (Figure 3-4).

The mass of protein present in the particles was also estimated from MFI measurements for samples agitated three hours at either pH 6.0 or pH 7.5, and compared with the monomer loss detected by SEC. The results of these calculations indicated there were 8.4 ± 5.5 μg/mL of protein present in the particles detectable by MFI at pH 6.0. However, the amount of monomer loss detected by SEC at pH 6.0 was approximately 160 ± 20 μg /mL. The mass of the high

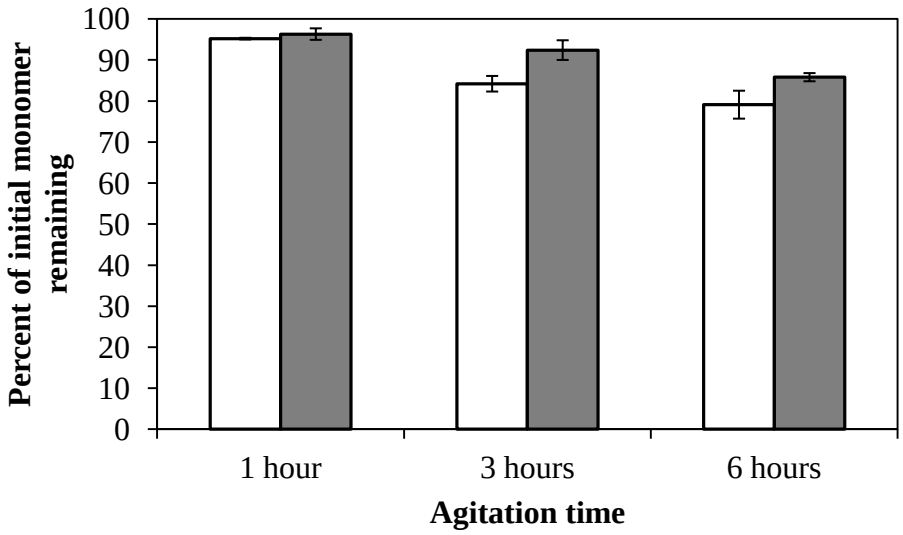

Figure 3-3: Percent of initial monomer remaining after agitation for 1, 3 or 6 hours. Monomer loss increases the longer samples are exposed to agitation. As the time over which samples were exposed to agitation increased, samples formulated at pH 6.0 (white bars) exhibited greater amounts of monomer loss than those formulated at pH 7.5 (gray bars).

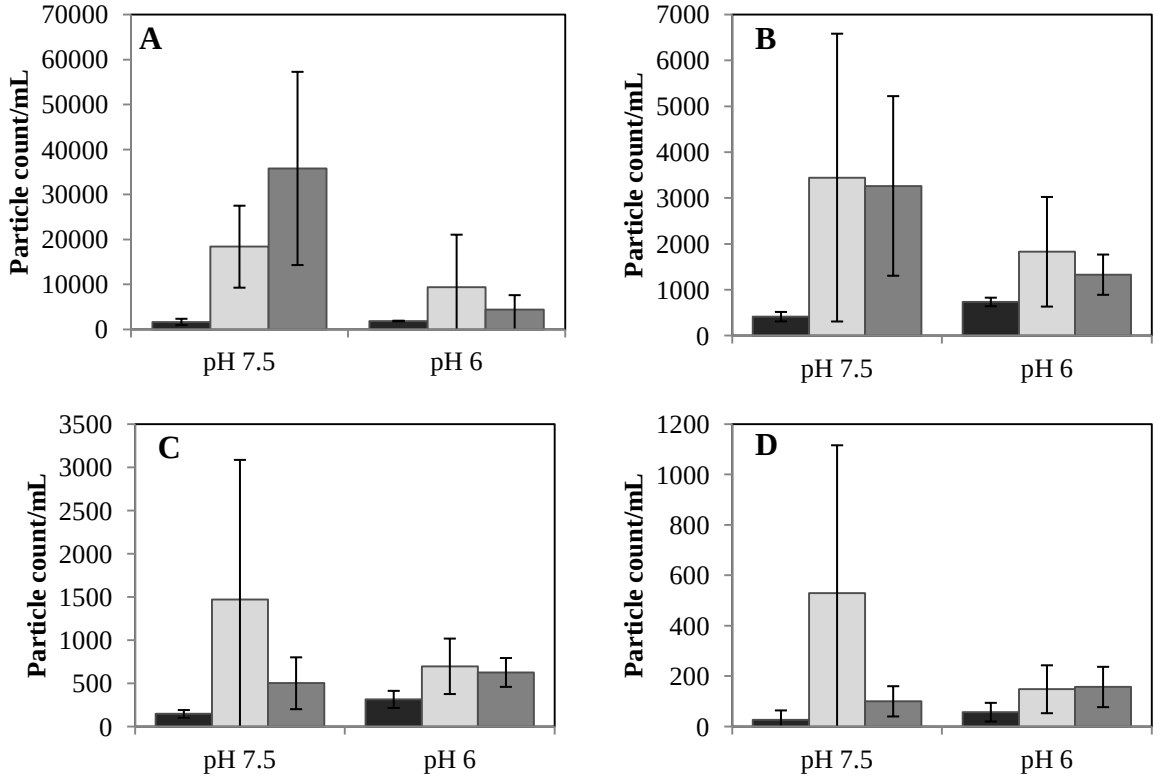

Figure 3-4: Agitation stressed samples showing particle concentrations for the 2-5 μm size range (Panel A), the 5-10 μm size range (Panel B), the 10-25 μm size range (Panel C) and the greater than 25 μm size range (Panel D). Samples include stock protein (black), samples agitated for 3 hours (light gray) and the 3 hour agitated samples stored for 24 hours (medium gray). In solutions at pH 7.5, particle concentrations increase for all size ranges after three hours of agitation. For samples in solution conditions at pH 6.0, the increase in particle count is lower than at pH 7.5. Significant decreases in particle concentrations are not observed in either solution condition after 24 hours storage.

molecular weight species (HMWS) detected accounts for 40 μg/mL of the initial monomer lost, but there is still incomplete mass recovery in samples at pH 6.0. At pH 7.5, 86 ± 110 μg/mL of protein was present in the particles, which is similar to the 80 ± 3 μg/mL monomer loss detected by SEC. Furthermore, no HMWS were detected by SEC in the pH 7.5 samples.

3.4 Discussion

Although calorimetry is frequently used as a formulation screening tool, the relatively high temperatures required for calorimetric assessment of conformational stability raises the question as to whether the results are relevant for predicting aggregation induced by stresses other than temperature. Differences in aggregation mechanisms might be expected, because aggregation during thermal stability studies occurs in the bulk, whereas aggregation during freeze/thaw cycling or agitation is likely influenced by conformational stability at air-water or ice-water interfaces. For these routes of damage, the propensity of a protein to adsorb to an interface and its stability at that interface would be important and not necessarily captured by thermal studies, as thermal stability of proteins has been shown to decrease upon surface adsorption [28]. For example, recombinant human growth hormone aggregates rapidly at air-water interfaces in spite of its relatively high thermal stability (T_m approximately 80 C at pH 6.0) [29, 30].

However, for abatacept, the use of elevated temperatures to accelerate degradation [23] appears to be relevant to aggregation induced by freeze/thaw or agitation interfacial stresses. At elevated temperature, greatly increased aggregation was observed at pH 6.0 compared to pH 7.5. Calorimetric analysis showed that activation energies for unfolding decreased at the lower pH condition, and the free energy of unfolding was reduced. In the current study, during agitation and freeze/thaw studies, decreased monomer loss and reduced particle formation rates were

observed in solutions at pH 7.5 compared to those at pH 6.0. Since the rate limiting step for aggregation during thermally-accelerated stability studies was related to abatacept conformational stability [23], it is not surprising that the thermal screening results correlate with what was seen here; interfaces faces might serve only to further destabilize the conformation of abatacept. It is possible the results from accelerated stability studies based on thermal stress, agitation, and freeze-thawing would not correlate as well in cases where association is the rate limiting step for aggregation, since conformational instability would not be playing as large a role in the aggregation pathway.

Capturing the interfacial component in accelerated stability studies is important because the extent of damage caused by the agitation and freeze/thaw stresses appears to be a function not only of the conformational stability, but also a function of the fluidity of the interface. Previous work studying the agitation-induced aggregation of abatacept in syringes showed increased particle counts when silicone oil contributed a fluid-fluid interface, but no increases in particle counts for agitation in syringes without silicone oil at pH 7.2 [31]. In this current study, agitation exposed abatacept to large amounts of dynamic air/water interfacial area. At this fluid-fluid interface, large amount of aggregates were formed. The amount of monomer loss at pH 7.5 was less than at pH 6 and correlates with the increased conformational stability of the protein at pH 7.5. Unlike the results seen in agitation studies, freeze/thaw cycling did not result in large amounts of aggregation. As no significant difference in colloidal stability was detected between 4 °C and 25 °C, it is possible the increased conformational stability at 4 °C is responsible for the decreased amounts of monomer loss observed. However, the fluidity of the interface is likely an important factor as well, with the solid/liquid interface of ice/water being less fluid than the air/water interface. Increased turnover of a fluid interface would return unfolded or

conformationally perturbed proteins at the surface to the bulk formulation, accounting for the increased aggregation seen in the agitation studies. This observation fits with the results of a previous study of abatacept aggregation in the presence of silicone oil [31]. Abatacept aggregation increased with the addition of silicone oil and this fluid/fluid interface (i.e., buffer/silicone oil) appears to be more damaging than the solid/fluid interface of the glass/buffer alone [31]. Although shear by itself typically is not sufficient to damage therapeutic proteins [8, 32, 33], similar effects of air/water interfacial turnover have also been seen in the aggregation of recombinant human growth hormone (rhGH) [34]. rhGH exposed to shear in the absence of an air/water interface did not aggregate significantly, but aggregated to a large degree when the air/water interface was present. Aggregation of rhGH in the presence of an air/water interface increased with increasing shear rate, likely due to greater interfacial turnover. The observed aggregation rate was first order with respect to protein concentration, indicating that conformational stability plays a large role in the aggregation of rhGH induced by interfacial turnover [34].

The differences in reversibility of particles formed by freeze thawing at pH 7.5 versus those formed by agitation are likely the result of the milder freeze thaw stress compared to air/water interfacial turnover during agitation and the increased conformational stability of the protein at pH 7.5. If the protein is less structurally perturbed, the particles formed will then be less stable compared to particles formed from a more unfolded protein structure.

Although MFI was useful in examining differences in formulation conditions where aggregation was undetectable by SEC, it bears mention that there were still limitations with this method. Unlike previously reported studies [22], the amount of protein in particles detected by MFI did not agree with the monomer loss as detected by SEC in all cases. After a three hour agitation of samples at pH 7.5, where no higher molecular weight aggregates were detected by SEC, there

is close agreement between the MFI and SEC results (86 ± 110 μg/mL of protein in particles versus 80 ± 3 μg/mL of monomer lost). However, at pH 6.0, there is not a good agreement between the monomer lost and the amount of protein in the particles after agitation. The 160 ± 20 μg /mL loss of monomeric abatacept at pH 6.0 was greater than that observed at pH 7.5 (80 ± 3 μg/mL) after three hours of agitation, but only 8.4 ± 5.5 μg/mL of protein in particles were detected. The mass of the soluble aggregates detected by SEC is not enough to account for the difference. Since there is still a gap in particle detection in the 0.1-1 μm size range, it is possible that if these particles could be included that the particle mass balance would accurately reflect the monomer loss at pH 6.0 and give a more complete picture of the aggregation.

3.5 Conclusions

Thermal stability studies were predictive of the relative stabilities of formulations subjected to freeze/thaw and agitation stresses. Conformational stability of this protein controlled the rate limiting step during aggregation at elevated temperature, and damage as a result of agitation or freeze/thaw cycling also was increased in formulations where the protein had a lower conformational stability.. While all three methods provided the same relative ranking of formulation stability, the differences in damage due to interfacial fluidity suggest careful selection of an appropriate accelerated stability study is still important.

3.6 References

1. Randolph, T. W.; Carpenter, J. F. Engineering Challenges of Protein Formulations. *AIChE Journal* **2007,** *53* (8), 1902-1907.

2. Roberts, C.; Das, T. K.; Sahin, E. Predicting solutoin aggregation rates for therapeutic proteins: Approaches and challenges. *International Journal of Pharmaceutics* **2011,** *doi:10.1016/j.ijpharm.2011.03.064*.

3. Remmele, R. L.; Zhank-van Enk, J.; Dharmavaram, V.; Balaban, D.; Durst, M.; Shoshitaishvili, A.; Rand, H. Scan-Rate Dependent Melting Transitions of Interleukin-1 Receptor (Type II): Elucidation of Meaningful Thermodynamic and Kinetic Parameters of Aggregation Acquired from DSC Simulations. *J. Am. Chem. Soc.* **2005,** *127*, 8328-8339.

4. Brummitt, R. K.; Nesta, D. P.; Roberts, C. J. Predicting Accelerated Aggregation Rates for Monoclonal Antibody Formulations, and Challenges for Low-Temperature Predictions. *Journal of Pharmaceutical Sciences* **2011,** *DOI 10.1002/jps.22633*.

5. Cromwell, M.; Hilario, E.; Jacobson, F. Protein Aggregation and Bioprocessing. *The AAPS Journal* **2006,** *8* (3), 572-579.

6. Rathore, N.; Rajan, R. S. Current Perspectives on Stability of Protein Drug Products during Formulation, Fill and Finish Operations. *Biotechnol. Prob.* **2008,** *24* (3), 504-514.

7. Bee, J.; Randolph, T. W.; Carpenter, J.; Bishop, S.; Dimitrova, M. Effects of Surfaces and Leachables on the Stability of Biopharmaceuticals. *J Pharm Sci* **2011**.

8. Bee, J. S.; Stevenson, J. L.; Mehta, B.; Svitel, J.; Pollastrini, J.; Platz, R.; Freund, E.; Carpenter, J. F.; Randolph, T. W. Response of a Concentrated Monoclonal Antibody Formulation to High Shear. *Biotechnol Bioeng* **2009,** *103* (5), 936-943.

9. Shire, S. Formulation and manufacturability of biologics. *Current Opinion in Biotechnology* **2009,** *20* (6), 708-714.

10. Eugene, J.; McNally, C. The imporance of a thorough preformulation study.. In *Protein Formulation and Delivery*, 1st ed.; McNally, E., Ed.; Marcel Dekker: New York, 1999; pp 111-138.

11. Strambini, G. B.; Gabellieri, E. Proteins in Frozen Solutions: Evidence of Ice-Induced Partial Unfolding. *Biophysical Journal* **1996,** *70*, 971-976.

12. Bhatnagar, B. S.; Bogner, R. H.; Pikal, M. J. Protein Stability During Freezing: Separation of Stresses and Mechanisms of Protein Stabilization. *Pharmaceutical Development and Technology* **2007,** *12*, 505-523.

13. Hawe, A.; Kasper, J. C.; Friess, W.; Jiskoot, W. Structural properties of monoclonal antibody aggregates induced by freeze-thawing and thermal stress. *European Journal of Pharmaceutical Sciences* **2009,** *38*, 79-87.

14. Joubert, M. K.; Luo, Q.; Nashed-Samuel, Y.; Wypych, J.; Narhi, L. O. Classification and Characterization of Therapeutic Antibody Aggregates. *Journal of Biological Chemistry* **2011,** *286* (28), 25118-25133.

15. Fradkin, A. H.; Carpenter, J. F.; Randolph, T. W. Immunogenicity of Aggregates in Recombinant Human Growth Hormone in Mouse Models. *Journal of Pharmaceutical Sciences* **2009,** *98* (9), 3247-3264.

16. Kiese, S.; Pappenberger, A.; Friess, W.; Mahler, H.-C. Shaken, Not Stirred: Mechanical Stress Testing of An IgG1 Antibody. *Journal of Pharmaceutical Sciences* **2008,** *97* (10), 4347-4366.

17. Ishikawa, T.; Kobayashi, N.; Osawa, C.; Sawa, E.; Wakamatsu, K. Prevention of Stirring-Induced Microparticle Formation in Monoclonal Antibody Solutions. *Biol. Pharm. Bull.* **2010,** *33* (6), 1043-1046.

18. Philo, J. S. A Critical Review of Methods for Size Characterizatio of Non-Particulate Protein Aggregates. *Current Pharmaceutical Biotechnology* **2009,** *10,* 359-372.

19. Rosenberg, A. Effects of Protein Aggregates: An Immunologic Perspective. *The AAPS Journal* **2006,** *8* (3), 501-507.

20. Carpenter, J. F.; Randolph, T. W.; Jiskoot, W.; Crommelin, D. J.; Middaugh, C. R.; Winter, G.; Fan, Y.-X.; Kirshner, S.; Verthelyi, D.; Kozlowski, S.; Clouse, K. A.; Swann, P. G.; Rosenberg, A.; Cherny, B. Overlooking Subvisible Particles in Therapeutic Protein Products: Gaps That May Compromise Product Quality. *Journal of Pharmaceutical Sciences* **2009,** *98* (4), 1201-1205.

21. Fradkin, A.; Carpenter, J. F.; Randolph, T. W. Glass particles as an adjuvant: A model for adverse immunoenicity of therapeutic proteins. *Journal of Pharmaceutical Sciences* **2011,** doi: 10.1002/jps.22683.

22. Barnard, J. G.; Singh, S.; Randolph, T. W.; Carpenter, J. F. Subvisible Particle Counting Provides a Sensitive Method of Detecting and Quantifying Aggregation of Monoclonal Antibody Caused by Freeze-Thawing: Insigns Into the Roles of Particles in the Protein Aggregation Pathway. *Journal of Pharmaceutical Scinces* **2011,** *100* (2), 492-503.

23. Fast, J.; Cordes, A. A.; Carpenter, J. F.; Randolph, T. W. Physical Instability of a Therapeutic Fc Fusion Protein: Domain Contributions to Conformational and Colloidal Stability.

Biochemistry **2009,** *48,* 11724-11736.

24. Pace, C. Determination and Analysis of Urea and Guanidine Hydrochloride Denaturation Curves. *Methods in Enzymology* **1986,** *131,* 266-280.

25. Myers, J. K.; Pace, C. N.; Scholtz, J. M. Denaturant m values and heat capacity changes: Relation to changes in accessible surface areas of protein unfolding. *Protein Science* **1995,** 2138-2148.

26. Faude, A.; Zacher, D.; Muller, E.; Bottinger, H. Fast determination of conditions for maximum dynamic capacity in cation-exchange chromatography of human monoclonal antibodies. *Journal of Chromatography A* **2007,** *1161,* 29-35.

27. Berg, J. M.; Tymoczko, J. L.; Stryer, L. Protein Structure and Function. In *Biochemistry,* 5th ed.; W.H. Freeman and Company: New York, 2002; pp 41-73.

28. Steadman, B. L.; Thompson, K. C.; Middaugh, C. R.; Matsuno, K.; Vrona, S.; Lawson, E. Q.; Lewis, R. V. The effects of surface adsorption on the thermal stability of proteins. *Biotechnology and Bioengineering* **1991,** *40* (1), 8-15.

29. Katakam, M.; Bell, L. N.; Banga, A. K. Effect of surfactants on the physical stability of recombinant human growth hormone. *J Pharm Sci* **1995,** *84* (6), 713-716.

30. Bam, N. B.; Cleland, J. L.; Yang, J.; Manning, M. C.; Carpenter, J. F.; Kelley, R. F.; Randolph, T. W. Tween protects recombinant human growth hormone against agitation-induced damage via hydrophobic interactions. *J Pharm Sci* **1998,** *87* (12), 1554-1559.

31. Majumdar, S.; Ford, B. M.; Mar, K. D.; Sullivan, V. J.; Ulrich, R. G.; D'Souza, A. J. M. Evaluations of the Effect of Syringe Surfaces on Protein Formulations. *Journal of Pharmaceutical Sciences* **2011,** *100* (7), 2563-2573.

32. Jaspe, J.; Hagen, S. J. Do Protein Molecules Unfold in a Simple Shear Flow? *Biophysical Journal* **2006,** *91,* 3415-3424.

33. Thomas, C. R.; Geer, D. Effects of shear on proteins in solution. *Biotechnol Lett* **2011,** *33,* 443-456.

34. Maa, Y.-F.; Hsu, C. C. Protein Denaturation by Combined Effect of Shear and Air-Liquid Interface. *Biotechnology and Bioengineering* **1997,** *54* (6), 503-512.

35. Roberts, C. Non-Native Protein Aggregation Kinetics. *Biotechnology and Bioengineering* **2007,** *98* (5), 927-937.

36. Chi, E. Y.; Krishnan, S.; Randolph, T.; Carpenter, J. Physical Stability of Proteins in

Aqueous Solution: Mechanism and Driving Forces in Nonnative Protein aggregation. *Pharmaceutical Research* **2003,** *20* (9), 1325-1336.

37. Lumry, R.; Eyring, H. Conformation changes of proteins. *J Phys Chem* **1954,** *58*, 110-120.

CHAPTER 4

SELECTIVE DOMAIN STABILIZATION AS A STRATEGY TO REDUCE FUSION PROTEIN AGGREGATION

(This work has been submitted as Amanda A. Cordes, Christopher W. Platt, John F. Carpenter, Theodore W. Randolph. Selective domain stabilization as a strategy to reduce fusion protein aggregation.)

4.1 Introduction

Fusion proteins are a growing class of protein therapeutics [1]. These are molecules which combine unrelated proteins, or domains from unrelated proteins, to create a new therapeutic protein. Etanercept, romiplostim, abatacept and rilonacept are all examples of current FDA-approved fusion proteins, and there are others in late-stage clinical trials [2]. Compared to other protein therapeutics, there can be several benefits to fusion proteins, such as extended serum half-life[3, 4] or added functionality [5]. Despite these benefits, there are also inherent challenges in creating stable formulations of fusion proteins. The increasing numbers of fusion proteins in development make it desirable to understand and improve fusion protein formulations.

As with other therapeutic proteins, fusion proteins are susceptible to instabilities such as a propensity to aggregate that can negatively impact production and product quality[6]. Aggregation has been implicated in causing adverse immune responses in patients [7, 8, 9]. Aggregation also can cause loss of protein during manufacture, transportation and storage [10, 11], leading to decreased product yields and profits [12].

The Lumry-Eyring model has been extensively used as the basis for the understanding of protein aggregation [11, 13, 14]. Roberts et al. have described an extended model of non-native protein aggregation composed of six steps [15, 16], although any specific protein need not go

through all steps in order to form aggregates. The initial step involves some conformational change to form an aggregation-competent species and the second step involves the association of aggregation-competent monomers to a reversible aggregate. Later steps describe further conformational changes that result in irreversibility of the initial aggregate and then growth to larger aggregates. The two initial steps are essentially the Lumry-Eyring framework of protein aggregation, which may be depicted schematically as [11, 13, 15]:

$$(1) \quad N \leftrightarrow N^*$$

$$(2) \quad 2N^* \leftrightarrow A_2$$

where N* is an aggregation competent conformation of the native protein and A is the initial aggregate. The rate of the initial step is impacted by the conformational stability of the protein, which is measured experimentally as the free energy of unfolding (ΔG_{unf}); larger ΔG_{unf} values indicate proteins or protein domains with increased conformational stability and thus lower equilibrium populations[11] of aggregation-competent species N*.

The rate constant for the association step is affected by the energetics of protein-protein interactions, i.e., colloidal stability. Experimentally, second osmotic virial coefficient values (B_{22}) are used to reflect the net contribution of all protein-protein interactions (e.g. hard sphere, electrostatic, Van der Waals). Positive B_{22} values indicate that protein-protein self interactions are repulsive, whereas negative B_{22} values indicate self-interactions are attractive. Either the unfolding or association step can be rate limiting in the formation of the initial aggregates [17], depending on the solution conditions. Both steps are potential targets for strategies to reduce protein aggregation. For example, excipients may be added that increase ΔG_{unf}, and solution conditions such as pH may be adjusted to increase repulsive protein-protein interactions[17].

Fusion proteins face an additional set of unique stability challenges that can contribute to their propensity to aggregate. Unlike naturally-occurring multidomain proteins, the individual domains in fusion proteins have not co-evolved for stability and may lack stabilizing intra-domain interactions, thus reducing ΔG_{unf}. Formulation conditions that favor the conformational stability of one domain may not adequately stabilize other domains [18]. In addition, under solutions conditions where the domains have different net charges, large dipoles may be created, adding additional attractive protein-protein interactions and colloidally destabilizing the protein solution [18].

Previous work by our group on an Fc- fusion protein showed increases in aggregation rates that correlated with decreased domain conformational stability [18]. The model protein for those studies was Fc-CTLA-4, an IgG Fc domain fused with the extracellular domain of CTLA-4 (human cytotoxic T-lymphocyte associated factor). During accelerated stability studies, Fc-CTLA4 exhibited markedly different aggregation rates with only a small shift in pH. Conditions that increased aggregation also reduced the conformational stability of the CTLA-4 domain and the C_H2 region of the Fc domain. Thermally- and chaotrope-induced denaturation studies showed that these two domains were the least conformationally stable of the protein's domains, leading to the conclusion that domain conformational instability was the primary driving force for Fc-CTLA4 aggregation.

These previous findings now lead us to develop two hypotheses regarding fusion protein behavior. We hypothesize that the overall stability and aggregation behavior of multi-domain proteins can be controlled by choosing formulation conditions that favor the stability of the least conformationally stable domain, and that selective stabilization of this domain will reduce overall aggregation rates of the entire fusion protein. In this work, we use protein comprising a

fusion of human serum albumin with human growth hormone (HSA-hGH) as a model system to determine the impact of domain stability on overall protein stability.

To test our hypotheses, we measured the conformational stabilities of the least conformationally stable domain and of the complete fusion protein. In addition, we measured B_{22} values for the fusion protein. During these studies, cosolute addition was investigated as a way to achieve selective domain conformational stabilization through the preferential binding of the cosolutes to the native state [11]. HSA is the least conformationally stable domain in the thermodynamic sense because it has a lower free energy of unfolding than hGH. The free energy of unfolding for hGH has been reported as 60.7 ± 4.2 kJ/mol and 62.3 kJ/mol at pH 7.5 [19, 20] and 62.3 kJ/mol at pH 6.0 [21]. These relatively high stabilities can be compared to 17.2 ± 4.2 kJ/mol at pH 7.4 and 14.6 ± 1.3 at pH 5.3 for HSA, as reported by Faruggia and Pico [22]. Based on these data, the HSA domain was chosen as the target for selective stabilization. Additionally, since there are other HSA fusion proteins that have either been patented or commercially developed to varying degrees [25, 26], this approach has the potential to be useful on a platform level. Conformational and colloidal stability of the fusion protein with the cosolute were measured to determine cosolute influence on overall protein stability.

Octanoic acid was used as a cosolute to selectively stabilize the HSA domain. Although HSA binds long chain fatty acids with a higher affinity than octanoic acid [27, 28], octanoic acid was chosen for its historical role as a stabilizer during heat treatment of HSA [29, 30], and for its higher solubility compared to long chain fatty acids [30]. Most of association constants [28, 29, 31] that have been measured under solution conditions similar to those used in the present study are on the order of 10^6 M^{-1}, although a binding constant of 2.6×10^4 M^{-1} has also been reported [27]. Binding of octanoic acid to HSA is consistent with a single binding site in the HSA sub domain IIIA [28, 29],

which is a very active binding site on the molecule[32]. Based on the Wyman linkage function [33, 34], one would expect an increase in HSA conformational stability when octanoic acid binds to the protein. This increase in stability is presumably reflected in the 8 °C increase in apparent T_m at pH 7.4 seen with a 5:1 molar ratio of octanoic acid to protein [29], although apparent Tm values reflect a mixture of both aggregation and unfolding.

4.2 Materials and Methods

4.2.1 Stock protein preparation

The HSA-hGH fusion protein was donated by Teva Biopharmaceuticals (Rockville, MD) and recombinant HSA was donated by Novozymes (Bagsvaerd, Denmark). Protein was dialyzed into the buffer of choice: 10 mM sodium phosphate (pH 7.0) or 10 mM sodium acetate (pH 5.0).All buffers contained 0.01% sodium azide as an antimicrobial agent. The hGH was expressed and purified in-house as described previously [35] and dialyzed into one of the above buffers for experimentation.

4.2.2 Addition of octanoic acid

Octanoic acid stock was prepared at a concentration of 4 mM in the buffer of choice prior to each experiment. Appropriate volumes of stock were added to protein samples to obtain either a constant 5:1 molar ratio of octanoic acid to protein, or a bulk concentration of 0.5 mM octanoic acid. When the molar ratio of octanoic acid to protein is held constant, the concentration of octanoic acid must necessarily be different at the different protein concentrations required for various experimental techniques. In addition, due to the different molecular weights of HSA and HSA-hGH, bulk concentrations of octanoic acid will be different at a constant octanoic

acid/protein ratio. A comparison of molar ratio versus octanoic acid concentration for HSA and HSA-hGH across techniques is given in Table 4-1. All experimental results are reported in initial mM concentration of octanoic acid.

4.2.3 Aggregation studies

Protein samples, either HSA, hGH, or HSA-hGH, were incubated at an initial concentration of 5 mg/mL at 50 °C in buffer alone or with octanoic acid. Octanoic acid concentrations were maintained at either 0.5 mM in the bulk or a 5:1 molar ratio of octanoic acid to protein. Size exclusion chromatography was used to measure the amount of monomer remaining after incubation as well as to detect the presence/amount of soluble aggregates. Prior to analysis by size exclusion-high performance liquid chromatography (SEC-HPLC), samples were centrifuged for five minutes at 15400*g* to remove insoluble aggregates. A Beckman System Gold HPLC (Beckman Coulter, Brea, CA) with a 717plus autosampler (Waters Technologies Corporation, Milford, MA) and a G3000SWXL size exclusion column (Tosoh Bioscience LLC, Montgomeryville, PA) were used. The mobile phase was 100 mM sodium phosphate, 200 mM sodium chloride (pH 7.0) for the HSA-hGH samples and 20 mM sodium phosphate, 100 mM sodium chloride (pH 6.8) for the HSA samples with a flow rate of 0.6 mL/min. Column elution was monitored by UV absorbance at 280 nm and Bomem Grams software version 7.0 was used to integrate the peaks. Concentration of the peak species was calculated from the integrated peak area. For analysis of apparent first order rate constants for aggregation, the only points used were those where at least 90% of initial monomer remained. Apparent first order reaction rate constants were determined from the slope of a plot of the

Experiment	Protein concentration	HSA		HSA-hGH	
		Octanoic acid concentration (mM)	*Molar ratio of octanoic acid to protein*	*Octanoic acid concentration (mM)*	*Molar ratio of octanoic acid to protein*
Aggregation Studies	5 mg/mL	0.38	5:1	0.28	5:1
		0.5	6.6:1	0.5	8.9:1
Far UV CD/Intrinsic fluorescence	0.1 mg/mL	0.008	5:1	0.006	5:1
		0.5	330:1	0.5	445:1
Near UV CD	1 mg/mL	---	---	0.056	5:1
		---	---	0.5	44.5:1
Static Light Scattering	1-3 mg/mL	0.076 – 0.230	5:1	0.056 – 0.170	5:1
		0.5	33:1 – 11:1	0.5	44.5:1 – 15:1

Table 4-1: Comparisons of mM octanoic acid concentrations to molar ratios of octanoic acid to protein at varying experimental protein concentrations

natural log of monomer concentration versus time and represent the average of rate constants from three incubation experiments. Errors represent the standard deviation.

4.2.4 Static light scattering

HSA-hGH was dialyzed into 10 mM sodium phosphate (pH 7.0) or 10 mM sodium acetate (pH 5.0) at five different target concentrations: 1, 1.5, 2, 2.5 and 3 mg/mL. Samples were filtered using either a 0.02 um inorganic filter (Whatman Anotop, Kent, UK) for the blank (buffer only) or a 0.1 um filter for samples containing protein. For samples containing octanoic acid, the octanoic acid stock was added to the filtered protein sample as described above. The static light scattering of the samples was measured with a Brookhaven light scattering system (Holtsville, NY) with a 633 nm laser. The detector aperture was set to 1 cm. The actual sample concentrations after dialysis and filtration were determined from the absorbance at 280 nm following completion of the experiments. During all experiments, the temperature of the sample chamber was set to 25 °C using a water bath connected to the sample chamber. Equations 1 and 2 were used to calculate the osmotic second virial coefficient (B_{22}) [36]. B_{22} values are reported as the average of three experiments ± standard deviation. Equation 1 can be used to determine the B_{22} from a graph of excess Raleigh ratio versus concentration, where M_w is the mass averaged molecular weight, R_{90} is the excess Rayleigh ratio at 90°, and K is the optical constant described by Equation 2. In Equation 2, n_0 is the solvent refractive index, dn/dc is the refractive index increment, λ is the incident wavelength and N_A is Avogadro's number. For these calculations, a dn/dc value of 0.185 was used [37].

$$\frac{Kc}{R_{90}} = \frac{1}{M_w} + 2(B_{22})c \qquad (1)$$

$$K = \frac{4\pi^2 n_0^2 (dn/dc)^2}{N_A \lambda^4} \qquad (2)$$

4.2.5 Fluorescence spectroscopy

Fluorescence spectroscopy was used to measure the free energy of unfolding (ΔG_{NU}) of the proteins according to the chaotrope perturbation method described previously [38]. Intrinsic fluorescence of HSA and HSA-hGH were monitored as a function of urea or guanidine hydrochloride concentration at 25 °C. Protein samples (either alone or with excess molar octanoic acid as noted) at a concentration of 0.1 mg/mL were incubated for 12 hours with urea concentrations varying from 0-9.5 M or with guanidine hydrochloride concentrations from 0-6.5 M. Samples were prepared by mixing stock protein, buffer and buffer with 10 M urea or 7 M guanidine hydrochloride to generate the range of chaotrope concentrations for the incubation. Stock buffers with chaotrope were freshly prepared for each incubation. Chaotrope concentrations were determined from the difference in refractive index between the buffer and the buffer with chaotrope [38]. After incubation, each sample was excited with 293 nm wavelength light and the emission spectrum from 300-400 nm was recorded using an Aminco Bowman Series 2 fluorescence spectrophotometer (SLM Aminco, Urbana, Illinois). For each emission scan, the center of spectral mass (CSM) was calculated using Equation 3:

$$\mathrm{CSM} = \frac{\sum F_i V_i}{\sum F_i} \qquad (3)$$

where F_i is the fluorescence intensity and v_i is the wavenumber. Unfolding curves were generated by graphing the center of spectral mass versus denaturant concentration. The incubations were repeated a total of three times to generate each unfolding curve. Free energies

of unfolding for HSA were calculated in Sigma Plot (Version 7.0, 2001) by a non-linear least squares fit to a two state model of protein unfolding using Equation 4 as previously described [39]:

$$Y_0 = \frac{(k_N[D] + b_N) + (k_U[D] + b_U)\exp\left(\frac{-\Delta G_{NU}}{RT}\right)}{1+\exp\left(\frac{-\Delta G_{NU}}{RT}\right)} \qquad (4)$$

In this equation, Y_0 is the center of spectral mass value, k_N and k_U are the slopes of the baselines of the native and unfolding states respectively, b_N and b_U are the intercepts of these baselines, T is temperature, R is the molar gas constant and ΔG_{NU} is the free energy of unfolding. For chaotrope-induced unfolding, ΔG_{NU} can be described by Equation 5 [39].

$$\Delta G_{NU}(D) = \Delta G_{NU}(H_2O) + m[D] \qquad (5)$$

$\Delta G_{NU}(D)$ is the free energy of the unfolding in the chaotrope, $\Delta G_{NU}(H_20)$ is the free energy of unfolding at a zero chaotrope concentration, [D] is the concentration of the chaotrope and m reflects the sensitivity of ΔG_{NU} to chaotrope concentration (i.e., $d\Delta G_{NU}/d[D]$).

4.2.6 Thermally Induced Unfolding Monitored by Circular Dichroism

Secondary and tertiary structural changes of HSA, hGH and HSA-hGH were inferred from far- and/or near-UV circular dichroism (CD) spectra, obtained as a function of temperature using a Chirascan Plus CD spectrometer (Applied Photophysics, Surrey, UK) fitted with a Peltier temperature control. The protein secondary structure was measured with far UV scans from 200-250 nm, at a protein concentration 0.1 mg/mL and quartz cell path length of 1 mm. Fusion protein tertiary structures were measured with near UV scans from 240-350 nm using a 10 mm pathlength quartz cuvette at a protein concentration of 1 mg/mL. For thermally-induced

unfolding scans, a one degree C step was used, with a one minute hold at each temperature. An unfolding curve was measured at each wavelength in the range of interest (200-250 nm or 240-350 nm) during thermal unfolding. The loss of tertiary structure was determined by following the signal of the tryptophan (295 nm) or tyrosine (280 nm) residues. Octanoic acid was added to protein samples in a 5:1 molar ratio of octanoic acid to protein (6 μM) or at a bulk concentration of 0.5 mM to investigate the effects of octanoic acid on protein structure and thermal stability. The apparent midpoints of unfolding (T_m) were calculated using the Global Analysis software (Applied Photophysics, Surrey, UK), with the average values of three replicates ± the standard deviation listed in the results.

4.3 Results

4.3.1 Aggregation Studies

HSA-hGH aggregates much more rapidly at pH 5.0 than at pH 7.0 (see Table 4-2) during incubation at 50 °C. Under the same solution conditions used for the HSA-hGH studies, HSA aggregation rates are lower than those of HSA-hGH. Incubation of HSA at pH 5.0 in 10 mM sodium acetate buffer results in an almost no loss of monomer, as seen in Figure 4-1. Additionally, at pH 7.0, no aggregation of HSA is detected during the 17 days of incubation at 50 °C. However, at pH 5.0, the aggregation behavior of hGH appears to be similar to that of the HSA-hGH fusion protein. At pH 7.0, hGH aggregation proceeds more slowly than at pH 5.0.

The addition of octanoic acid results in a large reduction of HSA-hGH aggregation rates (Figure 4-2), but does not reduce the aggregation rates of either HSA or hGH. No changes were observed in the aggregation rate of HSA with the addition of 0.38 mM octanoic acid (5:1 molar ratio) or 0.5 mM octanoic acid at pH 5.0. Addition of octanoic acid does not reduce hGH

	Apparent first order reaction rate constants (day $^{-1}$) measured at 50 °C			
Protein	pH 7.0	pH 7.0 + 0.5 mM octanoic acid	pH 5.0	pH 5.0 + 0.5 mM octanoic acid
HSA-hGH	0.01 ± 0.002	0.004 ± 0.004	0.77 ± 0.16	0.002 ± 0.001
HSA	Zero	Zero	Zero	N/D
hGH	0.1 ± 0.02	0.17 ± 0.02	0.6 ± 0.2	0.7 ± 0.2

Table 4-2: Apparent first order reaction rate constants (day $^{-1}$) for the three proteins under various solution conditions. The rate of HSA aggregation detected was zero, within error at both pH 7.0 and pH 5.0. Addition of octanoic acid reduced the aggregation of HSA-hGH, but did not appear to reduce the aggregation of HSA or hGH alone.

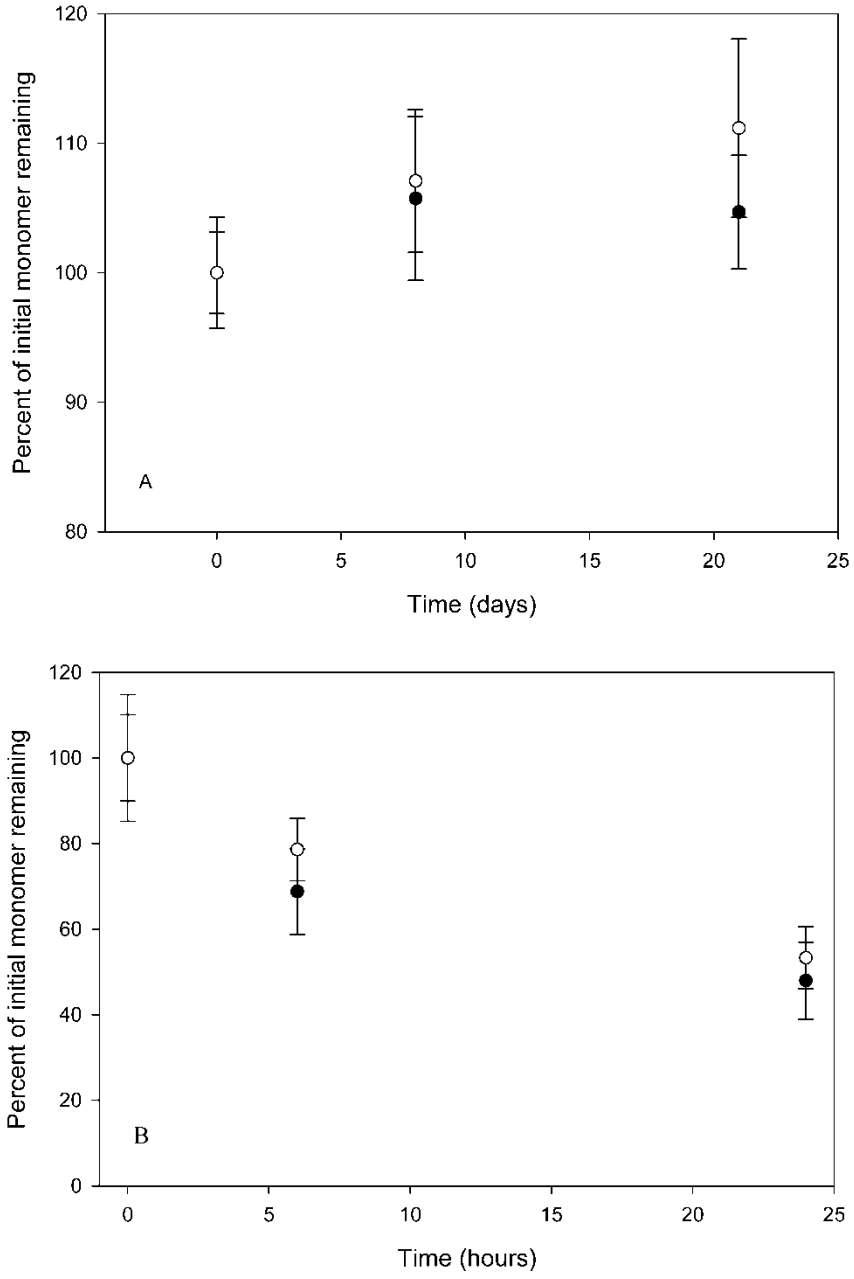

Figure 4-1: Percent of initial monomer remaining versus time for HSA (Panel A) and hGH (Panel B) incubation at pH 5.0 and 50 °C for the protein alone (●) and with (○)octanoic acid. Data points represent the average value ± the standard deviation.

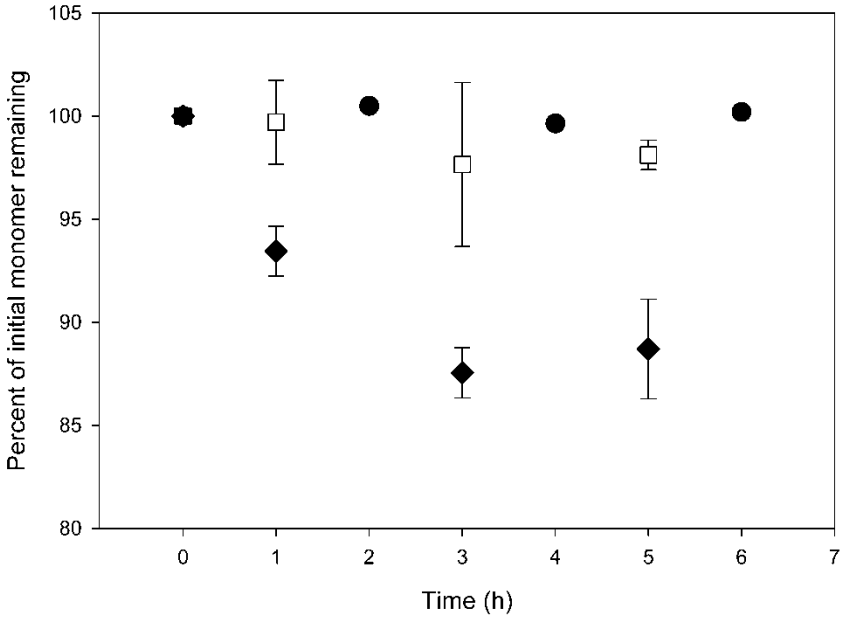

Figure 4-2: Percent of initial monomer remaining versus time during HSA-hGH incubation at pH 5, 50 °C for the protein alone (◆), with 0.28 mM octanoic acid (□) and with 0.5 mM octanoic acid(●). Aggregation of HSA-hGH is reduced as octanoic acid concentration increases, as evidenced by the increased amounts of monomer remaining in solution after incubation when octanoic acid is present. Data points represent the average value ± the standard deviation.

aggregation. At pH 5.0, in the presence of 0.5 mM octanoic acid, the apparent first order reaction rate constant is essentially the same as the rate constant without octanoic acid present. At pH 7.0, the rate of hGH aggregation in the presence of 0.5 mM octanoic acid appears to increase slightly compared to at pH 7.0 alone.

Additionally, longer incubations of HSA-hGH at pH 5.0 and 50 °C with and without octanoic acid showed differences in the amount and type of aggregate species present. For HSA-hGH in the absence of octanoic acid, only 15% of the initial monomer remained after five days and no soluble aggregates were detected. The samples containing HSA-hGH and 0.28 mM octanoic acid had 30% of the initial monomer remaining, with a small amount of soluble aggregates present as well, as shown in Figure 4-3.

4.3.2 Measurement of B_{22} by Static Light Scattering

For all HSA-hGH samples at 25 °C, the net protein-protein self interactions are repulsive, as evidenced by the positive values for the second virial coefficients in Table 4-3. When octanoic acid is added to HSA-hGH at pH 5.0 at a 5:1 molar ratio of octanoic acid (equivalent to an octanoic acid concentration range of 0.078 to 0.17 mM, see Table 4-1), the magnitude of the repulsive interaction increases. However, at pH 7.0, the addition of octanoic acid does not appear to change the net interaction. The self interactions remain repulsive and the magnitudes of these interactions remain the same as the samples without octanoic acid. Static light scattering measurements of HSA-hGH with a constant 0.5 mM octanoic acid at pH 5.0 indicate that the additional octanoic acid does not change the self interactions significantly compared to the experiments where the molar ratio was held constant (data not shown).

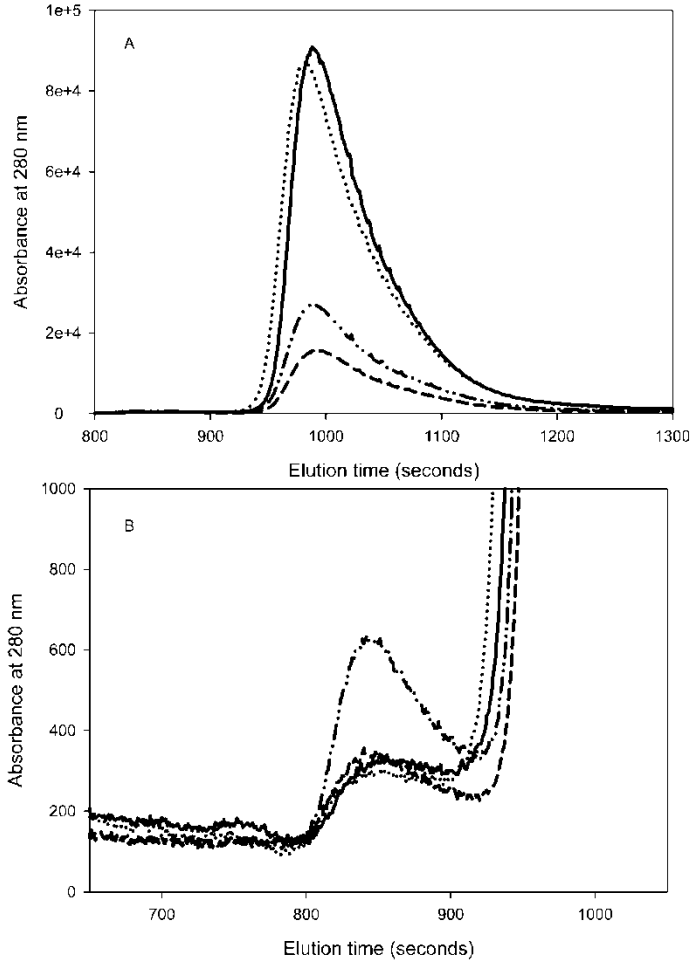

Figure 4-3: A) SEC chromatogram of HSA-hGH (solid line) and HSA-hGH with 0.28 mM octanoic acid (5:1 molar ratio) (dotted line) at time zero and HSA-hGH (dashed line) and HSA-hGH with 0.28 mM octanoic acid (dash-dotted line) post 5 day, 50 °C incubation. B) Close up of soluble aggregate peak. Addition of octanoic acid reduces the extent of monomer loss (A) and changes the distribution of aggregate species, with soluble aggregates being detected when octanoic acid is present (B).

pH	SVC x 10^4 (mL mol g^{-2})	SVC x 10^4 (mL mol g^{-2}) with 5:1 octanoic acid
5.0	0.4 ± 2.1	6.0 ± 0.4
7.0	3.1 ± 0.9	2.9 ± 1.4

Table 4-3: Osmotic second virial coefficients for HSA-hGH calculated from static light scattering with and without octanoic acid. Values represent the average of three replicates ± the standard deviation.

4.3.3 Protein conformational stability

HSA-hGH unfolding curves exhibit two transitions during chaotrope denaturation. Although it is difficult to calculate the free energies of HSA-hGH unfolding due to the non-zero slope of the baseline at urea concentrations greater than 9.5 M (shown in Figure 4-4), it is still possible to compare the onset of unfolding and the transitions that are present as a function of urea concentration. Although guanidine hydrochloride is a stronger chaotrope than urea, urea is used here because chloride ion binding may interfere with the binding of other molecules (e.g., octanoic acid) to HSA[31]. Previously, the free energy values for guanidine hydrochloride denaturation of HSA-hGH were reported as 16.7 ± 0.8 kJ/mol for the first transition and 24.6 ± 2.5 kJ/mol for the second transition[40]. In the current study, at pH 7.0 and 25 °C, the first HSA-hGH unfolding transition begins at approximately 5 M urea, and the second transition begins at approximately 7 M urea. Addition of 0.006 mM octanoic acid does not change the transitions with regard to denaturant concentration at onset of unfolding or curve shape (Figure 4-4). The first unfolding transition at pH 5.0 also begins at 5 M urea, and the unfolding curve is similar in shape to the unfolding curve at pH 7.0.

Chaotrope-induced denaturation curves for HSA exhibit only one unfolding transition and the onset of this transition coincides with that of the first transition of the HSA-hGH fusion (Figure 4-5), as observed previously [40]. The free energy of unfolding is 20.7 ± 3.6 kJ/mol at pH 7.0. Previously, the conformational stability of HSA has been shown to be nearly independent of pH between pH 7.4 and pH 5.3, with a ΔG_{NU} value of 17.1 ± 4.2 kJ/mol at pH 7.4 and a ΔG_{NU} value of 14.6 ± 1.3 kJ/mol at pH 5.3 [22].The onset of unfolding for HSA increases by an increment of 2 M urea with the addition of 0.5 mM octanoic acid at pH 5.0, but the baseline at high urea concentrations is not sufficient for calculations of ΔG_{unf}. Assuming the m value (which

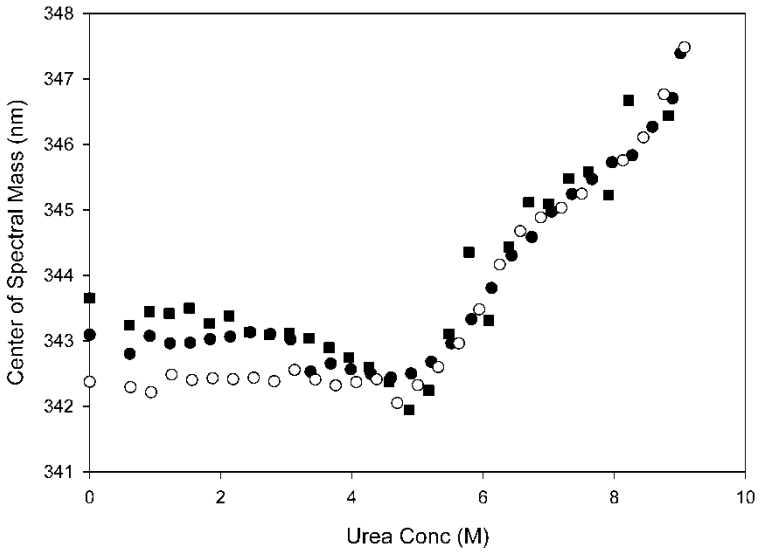

Figure 4-4: Representative plots of the center of spectral mass versus urea concentration during fluorescence spectroscopy monitored denaturation of HSA-hGH by urea at pH 7.0 either with (○) or without (●) 0.006 mM octanoic acid and at pH 5.0 (■). No change in the onset of denaturation or with regard to the two transitions is observed between the pH two conditions or with the addition of octanoic acid.

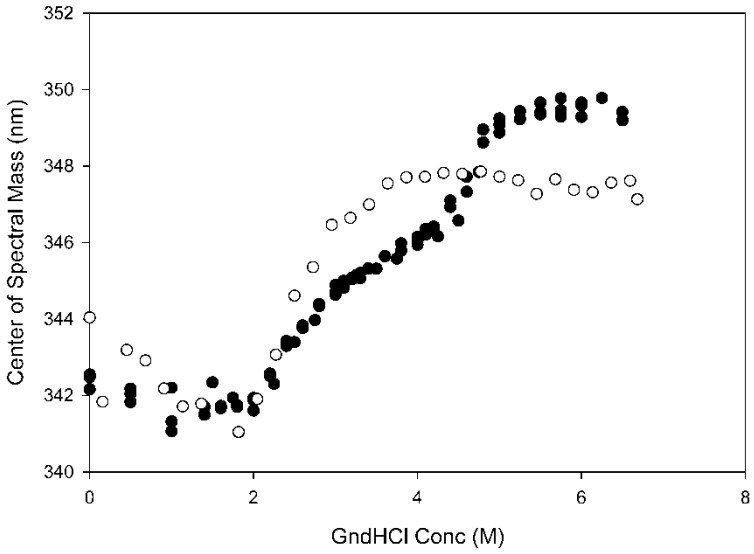

Figure 4-5: Denaturation of HSA (○) and HSA-hGH (●) at pH 7.0 by guanidine hydrochloride monitored by fluorescence spectroscopy, showing the center of spectral mass versus molar chaotrope concentration. Onset of HSA unfolding occurs at the same GndHCl concentration as that of the first transition of HSA-hGH.

was reported as 15.0 kJ/mol[21]) remains unchanged with the addition of octanoic acid, the observed 2M increase in the concentration of urea at the onset of unfolding represents an increase in stability, $\Delta\Delta G_{NU}$, of 30 kJ/mol.

4.3.4 Protein structure and apparent midpoints of unfolding

The far UV CD scans from 200-250 nm show that HSA-hGH has a predominantly α-helical structure and that secondary structure is not affected by the addition of 0.5 mM octanoic at either pH condition (Figure 4-6). The structure of the HSA domain was also unaffected by the addition of 0.5 mM octanoic acid at pH 5.0 (data not shown). Values for the apparent midpoint of the unfolding transition (T_m) are listed in Table 4-4. An increase in HSA-hGH T_m is seen upon addition of 0.5 mM octanoic acid; the apparent T_m increases by one degree at pH 5.0 and by approximately four degrees at pH 7.0. The apparent T_m for HSA increases in the presence of 0.5 mM octanoic acid at pH 5.0; however, there is no significant change to the apparent T_m for hGH under these conditions. Apparent T_m values are not equilibrium values. The protein aggregates during heating, and thus the apparent T_m values reflect both unfolding and aggregation processes[41].

No change in the tertiary structure of HSA-hGH is observed by near UV CD after the addition of octanoic acid at 25 °C (data not shown). The apparent T_m for the loss of HSA-hGH tertiary structure could not be calculated due to the signal from the aggregates, but the onset of thermal denaturation occurred at 63 °C without octanoic acid at pH 5.0 (Figure 4-7). A two degree increase in the temperature of the onset of unfolding is seen with the addition 0.5 mM octanoic acid at pH 5.0.

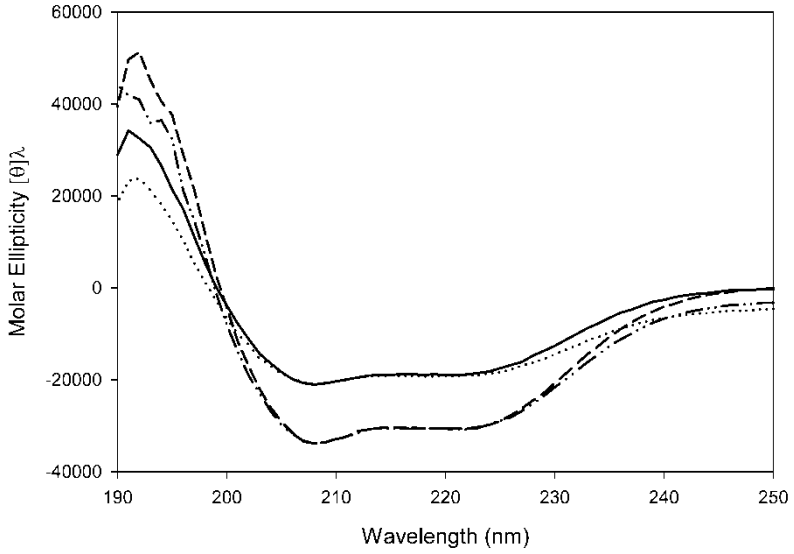

Figure 4-6: Far UV CD of HSA-hGH comparing the secondary structure of samples at pH 5.0 with 0.5 mM octanoic acid (dotted) and without (solid) to samples at pH 7.0 with (dash-dotted) and without (dashed) 0.5 mM octanoic acid. Addition of octanoic acid does not noticably change the protein secondary structure.

Protein	**pH**	**Tm (°C)**	**Tm in the presence of 0.5 mM octanoic acid (°C)**
HSA-hGH	5.0	69.0 ± 0.1	70.4 ± 0.1
HSA-hGH	7.0	69. 3 ± 0.2	73.9 ± 0.5
has	5.0	70.0 ± 0.3	72.0 ± 0.1
hGH	5.0	66.3 ± 1	67.4 ± 2.3

Table 4-4: Tm values for HSA-hGH, HSA and hGH with and without octanoic acid. Addition of 0.5 mM octanoic acid increases the conformational stability of HSA-hGH and HSA. In order to bridge the different octanoic acid concentrations used for aggregation studies versus conformational stability studies, the T_m was also measured for HSA and HSA-hGH at concentrations of 0.38 mM and 0.28 mM octanoic acid concentrations. T_m values under these conditions are 70.1 ± 0.1 °C for HSA-hGH and 73.2 ± 1.7 °C for HSA.

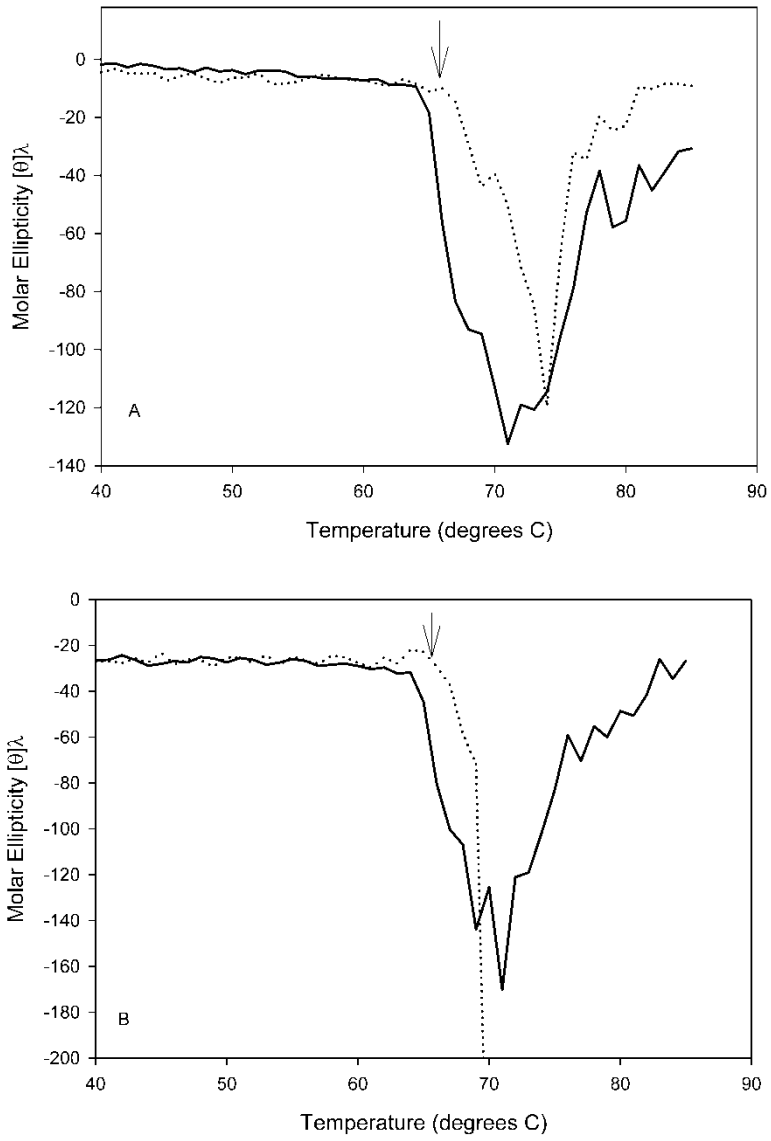

Figure 4-7: Loss of HSA-hGH tertiary structure during thermal denaturation at pH 5.0, followed by near UV CD spectroscopy at 295 nm (A) or 280 nm (B) of the protein alone (solid line) or with 0.5 mM octanoic acid (dotted). The onset of the thermal transition is shifted from 63 °C to 65 °C with 0.5 mM octanoic acid.

4.4 Discussion

Human growth hormone is a therapeutic protein used to treat endogenous growth hormone deficiency in both children and adults [24]. HSA-hGH fusion proteins were created with the goal of increasing the circulation half-life of hGH [25]. Although HSA aggregates more slowly than hGH at both pH 5.0 and pH 7.0, the addition of the HSA domain to hGH does not result in improved kinetic stability of the therapeutic molecule against aggregation. The HSA-hGH fusion protein aggregates much more rapidly than HSA alone at pH 5.0 and aggregates more at pH 7.0 as well, with rate constants similar to those exhibited by hGH. However, although addition of HSA to hGH does not result in improved stability against aggregation, it does appear to stabilize the hGH structure within the fusion protein, as HSA-hGH shows increased resistance to thermal melting compared to hGH alone.

Octanoic acid presumably increases the conformational stability of HSA as evidenced by the previously reported increase in T_m in the presence of octanoic acid [29], and it is used during viral inactivation steps to protect against the precipitation of HSA [30]. Octanoic acid also increases the apparent T_m of HSA-hGH. Even though the aggregation rates of HSA-hGH are more similar to the aggregation rates of hGH than to the aggregation rates of HSA, HSA-hGH aggregation is reduced and the apparent T_m is increased with addition of 0.28 mM octanoic acid. Repulsive HSA-hGH protein-protein interactions also increase with the addition of octanoic acid, as evidenced by the increase in B_{22}.

Under the solution conditions tested, HSA is relatively stable against aggregation. Even in the absence of octanoic acid, aggregation for HSA alone was much slower than that of the fusion protein. No changes in aggregation rates of HSA alone were detected at the different pH

conditions or with the addition of octanoic acid, even though increases in conformational stability were seen with the addition of octanoic acid.

Although the addition of octanoic acid increases both the colloidal stability and stability against thermal unfolding of HSA-hGH, it is apparent that colloidal instability dominates the aggregation behavior. This can be seen from the behavior of the fusion protein at pH 5.0 and pH 7.0. No significant changes in the conformational stability of HSA-hGH were observed between pH 5.0 and pH 7.0; the onset of unfolding during chaotrope denaturation occurs at the same urea concentrations and the unfolding transitions overlap. However, the aggregation rate at pH 5.0 was an order of magnitude larger than the aggregation rate at pH 7.0. Consistent with the dominant influence of colloidal interactions, net interactions were more attractive at pH 5.0 than at pH 7.0.

Similar dependence on colloidal stability was seen previously with GCSF where under two pH conditions nearly identical conformational stabilities were observed but dramatic differences in aggregation rates correlated with B_{22} values [17]. The aggregation of recombinant human interleukin-1 receptor antagonist (rhIl1-ra) also is driven by colloidal instabilities [42]. rhIl1-ra conformational stability was independent of formulation conditions, but the colloidal stability was reduced at low ionic strengths. The attractive protein self interactions were not screened at low ionic strength, resulting in the formation of dimers and trimers [42]. Still, colloidal stability is not always the driving force for aggregation. Increases in aggregation that correspond to activation energy decreases for structural transitions have been seen both for large, multidomain proteins [18] as well as smaller proteins (~ 50 kDa) with a single unfolding transition [43, 44].To help understand the contribution so individual domains to the stability of fusion proteins, , ΔG_{NU} values for individual protein domains may be measured. In contrast, however,

B_{22} values cannot be ascribed to individual domains. Furthermore, it is unlikely that the colloidal stability of a fusion protein formulation could be predicted from the colloidal stability of formulations of individual domains. B_{22} includes the effects of electrostatic, steric and short range interactions and is impacted by charge distribution and protein geometry [45]. In other multidomain proteins, such as antibodies, it has been shown that the self association can change significantly with relatively small changes in amino acid sequence. For example, two monoclonal antibodies were studied that only differed in sequence in the Fab domain [46]; mAb1 self associated while mAb2 did not. By swapping the charged residues in mAb1 with the residues at the corresponding position in mAb2, the self association behavior of mAb1 was reduced [46]. Since mAb1 and mAb2 only differed in sequence in the Fab region, it would be expected by analogy that the colloidal properties of a fusion protein would differ depending on the domain partnered with HSA. Better predictive models of colloidal stability would be useful to help understand the changes in colloidal stability that may occur with a fusion protein compared to the therapeutic protein alone.

4.5 Conclusions

In contrast to our original hypothesis, we found that stabilizing the HSA domain does not reduce the aggregation of HSA-hGH. However, increasing colloidal stability reduces aggregation significantly. Additional work is needed to determine the applicability of these results across the HSA fusion class of proteins.

4.6 Acknowledgements

The authors gratefully acknowledge Teva Biopharmaceuticals and Novozymes for their generous donation of material. HSA-hGH was supplied by Teva Biopharmaceuticals and HSA was supplied by Novozymes. AAC would especially like to thank Yemin Xu for the production of the hGH used in these experiments. NIH grant R01 EB006006 is gratefully acknowledged for funding this work.

4.7 References

1. Jazayeri JA, Carroll GJ 2008. Fc-based cytokines: prospects for engineering superior therapeutics. BioDrugs 22:11-26.

2. Reichert JM 2011. Antibody-based therapeutics to watch in 2011. MAbs 3:76-99.

3. Muller N, Schneider B, Pfizenmajer K, Wajant H 2010. Superior serum half life of albumin tagged TNF ligands. Biochem Biophys Res Commun 396:793-799.

4. Syed S, Schuyler PD, Kulczycky M, Scheffield WP 1997. Potent antithrombin activity and delayed clearance from the circulation characterize recombinant hirudin genetically fused to albumin. Blood 89:3243-3252.

5. Chamow SW, Ashkenazi A. 1999. Overview. In Chamow SW, Ashkenazi A, editors. Antibody Fusion Proteins, New York: Wiley-Liss Inc.

6. Manning MC, Patel K, Borchardt RT 1989. Stability of Protein Pharmaceuticals. Pharm Res 6:903-918.

7. Rosenberg AS 2006. Effects of Protein Aggregates: An Immunologic Perspective. AAPS J 8:501-507.

8. Stravitz RT, Chung H, Sterling RK, Luketic VA, Sanyal AJ, Price AS, Purrington A, Shiffman ML 2005. Antibody-Mediated Pure Red Cell Aplasia Due to Epoetin Alfa During Antiviral Therapy of Chronic Hepatitis C. Am J Gastroenterol 100:1415-1419.

9. Bunn HF 2002. Drug-Induced Autoimmune Red-Cell Aplasia. N Engl J Med 346:522-523.

10. Shire SJ 2009. Formulation and manufacturability of biologics. Curr Opin Biotechnol 20:708-714.

11. Chi EY, Krishnan S, Randolph TW, Carpenter JF 2003. Physical Stability of Proteins in Aqueous Solution: Mechanism and Driving Forces in Nonnative Protein aggregation. Pharm Res 20:1325-1336.

12. Randolph TW, Carpenter JF 2007. Engineering Challenges of Protein Formulations. AIChE Journal 53:1902-1907.

13. Lumry R, Eyring H 1954. Conformation changes of proteins. J Phys Chem 58:110-120.

14. Kendrick BS, Carpenter JF, Cleland JL, Randolph TW 1998. A transient expansion of the native state precedes aggregation of recombinant human interferon-gamma. Proc Natl Acad Sci USA 95:14142-14146.

15. Roberts CJ 2007. Non-Native Protein Aggregation Kinetics. Biotechnol Bioeng 98:927-937.

16. Roberts CJ, Das TK, Sahin E 2011. Predicting solution aggregation rates for therapeutic proteins: Approaches and challenges. Int J Pharm doi: 10.1016/j.ijpharm.2011.03.064.

17. Chi EY, Krishman S, Kendrick BS, Chang BS, Carpenter JF, Randolph TW 2003. Roles of Conformational Stability and Colloidal Stability in the Aggregation of Recombinant Human Granulocyte Colony Stimulating Factor. Protein Sci 12:903-913.

18. Fast JL, Cordes AA, Carpenter JF, Randolph TW 2009. Physical Instability of a Therapeutic Fc Fusion Protein: Domain Contributions to Conformational and Colloidal Stability. Biochemistry 48:11724-11736.

19. Brems DN, Brown PL, Becker GW 1990. Equilibrium Denaturation of Human Growth Hormone and Its Cysteine-modified Forms. J Biol Chem 265:5504-5511.

20. DeFelippis MR, Alter LA, Pekar AH, Havel HA, Brems DN 1993. Evidence for a self-associating equilibrium intermediate during folding of human growth hormone. Biochemistry 32: 1555-1562.

21. Bam, NB.Cleland, JL, Randolph, TW 1996. Molten globule intermediate of recombinant human growth hormone: stabilization with surfactants. Biotechnol Prog 12: 801-809.

22. Farruggia B, Pico GA 1999. Thermodynamic Features of the Chemical and Thermal Denaturations of Human Serum Albumin. Int J Biol Macromol 26:317-323.

23. Kosa T, Maruyama T, Otagiri M 1998. Species Differences of Serum Albumins: II. Chemical and Thermal Stability. Pharm Res 15:449-454.

24. Mulinacci F, Capelle MA, Gurny R, Drake AF, Arvinte T 2011. Stability of Human Growth Hormone: Influence of Methionine Oxidation on Thermal Folding. J Pharm Sci 100:451-463.

25. Osborn BL, Sekut L, Corcoran M, Poortman C, Sturm B, Chen G, Mather D, Lin HL, Parry TJ 2002. Albutropin: a growth hormone-ablumin fusion with imroved pharmacokinetics and pharmacodymanics in rats and monkeys. Eur J Pharmacol 456:149-158.

26. Yu Z, Fu Y. 2007. Recombinant human albumin fusion proteins with long lasting biological effects. Patent 7,244,833.

27. Aki H, Yamamoto M 1993. Biothermodynamic characterization of monocarboxylic and dicarboxylic aliphatic acids binding to human serum albumin: A flow microcalorimetric study. Biophys Chem 46:91-99.

28. Kragh-Hansen U, Watanabe H, Nakajou K, Iwao Y, Otagiri M 2006. Chain Length-dependent Binding of Fatty Acid Anions to Human Serum Albumin Studied by Site-directed Mutagenesis. J Mol Biol 363:702-712.

29. Anraku M, Tsurusaki Y, Watanabe H, Maruyama T, Kragh-Hansen U, Otagiri M 2004. Stabilizing mechanisms in commercial albumin preparations: octanoate and N-acetyl-L-tryptophanate protect human serum albumin against heat and oxidative stress. Biochim Biophys Acta 1702:9-17.

30. Peters T. 1996. All About Albumin. San Diego: Academic Press Inc.

31. Honore B, Brodersen R 1988. Detection of carrier heterogeneity by rate of ligand dialysis: medium-chain fatty acid interaction with human serum albumin and competition wtih chloride. Anal Biochem 171:55-66.

32. Bagatolli LA, Kivatinitz SC, Fidelio GD 1996. Interactions of small ligands with human serum albumin subdomain IIIA. How to determine the affinity constant using an easy steady state fluorescent method. J Pharm Sci 85:1131-1132.

33. Tanford C 1969. Extension of the theory of linked functions to incorporate the effects of protein hydration. J Mol Biol 39:539-544.

34. Timasheff SN 2002. Protein-solvent preferential interactions, protein hydration, and the modulation of biochemical reactions by solvent components. PNAS 99:9721-9726.

35. Crisman RL, Randolph TW 2010. Crystallization of Recombinant Human Growth Hormone at Elevated Pressures: Pressure Effects on PEG-Induced Volume Exclusion Interactions. Biotechnol Bioeng 107:663-672.

36. Kratochvil P. 1987. Classical Light Scattering for Polymer Solutions. Amsterdam, The Netherlands: Elsevier.

37. Arakawa T, Wen J 2001. Determination of Carbohydrate Contents from Excess Light Scattering. Anal Biochem 299:158-161.

38. Pace CN 1986. Determination and Analysis of Urea and Guanidine Hydrochloride Denaturation Curves. Methods Enzymol 131:266-280.

39. Myers JK, Pace CN, Scholtz JM 1995. Denaturant m values and heat capacity changes: Relation to changes in accessible surface areas of protein unfolding. Protein Sci 4:2138-2148.

40. Chou DK, Krishnamurthy R, Randolph TW, Carpenter JF, Manning MC 2005. Effects of Tween 20 and Tween 80 on the stability of Albutropin during agitation. J Pharm Sci 94:1368-1381.

41. Sanchez-Ruiz JM 1992. Theoretical analysis of Lumry-Eyring models in differential scanning calorimetry. Biophys J 61: 921-935.

42. Alford JR, Kendrick BS, Carpenter JF, Randolph TW 2008. High Concentration Formulations of Recombinant Human Interleukin-1 Receptor Antagonist: II. Aggregation Kinetics. J Pharm Sci 97:3005-3021.

43. Bai S, Manning MC, Randolph TW, Carpenter JF 2011. Aggregatio of Recombinant Human Botulinum Protein Antigen Serotype C in Varying Solution Conditions: Implications of Conformational Stability for Aggregation Kinetics. J Pharm Sci 100:836-848.

44. Smith LA 1998. Development of Recombinant Vaccines for Botulinum Neurotoxin. Toxicon 36:1539-1548.

45. Neal BL, Asthagiri A, Lenhoff AM 1998. Molecular origins of osmotic second virial coefficients. Biophys J 75:2469-2477.

46. Yadav S, Sreedhara A, Kanai S, Liu J, Lien S, Lowman H, Kalonia DS, Shire SJ 2011. Establishing a Link Between Amino Acid Sequences and Self-Associating and Viscoelastic Behavior of Two Closely Related Monoclonal Antibodies. Pharm Res 28:1750-1764.

CHAPTER 5

SELECTIVE DOMAIN STABILIZATION AS A STRATEGY TO REDUCE HSA-GCSF AGGREGATION RATE

5.1 Introduction

The development of recombinant therapeutic proteins has provided new treatments for many serious conditions, including endogenous protein deficiencies, cancer and autoimmune disorders [1]. In order to be successful drug candidates, these complex molecules require stabilization by formulation excipients so that degradation rates are minimized from manufacturing through transportation to administration to patients [2,3]. Both chemical and physical instabilities of therapeutic proteins have the potential to negatively impact product quality [3]; this work focuses the aggregation, the most commonly observed physical instability. Much work has been done to investigate the stability and aggregation behaviors of protein therapeutics [3, 4, 5, 6]. Aggregation of protein products is a concern for several reasons. Aggregation can lead to loss of product during manufacture, storage and shipping [7, 8]. Moreover, if aggregates are administered to patients, they may trigger patient immune responses [9, 10, 11]. These potential adverse immune responses include anaphylactic shock and the production of anti-drug antibodies which can increase drug clearance and potentially cross react with endogenous protein [12, 13].

Aggregation rates can be modulated by both a protein's conformational stability and its colloidal stability in solution [8]. Conformational stability refers to the thermodynamic stability of the protein's proper three-dimensional folded structure, whereas colloidal stability refers to the energetics of protein-protein self interactions between molecules. Protein-protein interactions are repulsive in colloidally stable systems. For the purposes of this report we use the free energy of

unfolding, $\Delta G_{NU,}$ for HSA-GCSF as a measure of its conformational stability, and the osmotic second virial coefficient, B_{22}, for HSA-GCSF as a measure of its colloidal stability [8].

Granulocyte colony stimulating factor (GCSF) is an important therapeutic and is used as to increase the production of white blood cells in patients undergoing chemotherapy [14]. Its propensity to aggregate has been extensively studied and characterized. Previous studies [4] showed that rate of aggregation of 1.5 mg/mL GCSF in solution at near-physiological conditions (pH 6.9 in phosphate buffered saline, 37 °C) is rapid, with a reaction rate of 7.3 ± 0.6 μmol L^{-1} day^{-1} and an apparent reaction order that is second-order in protein concentration. However, an apparent first order dependency on protein concentration has also been observed at GCSF concentrations greater than 2.5 mg/mL (pH 7.0, 0.1 M MOPS), [15] with aggregation under these conditions involving a conformationally altered monomer state[14]. Both conformational and colloidal instabilities play a role in the aggregation of GCSF under varying solution conditions [16]. Addition of sucrose, a molecule that is preferentially excluded from the surface of proteins [17], increases the conformational stability of GCSF and reduces its rate of aggregation [4]. Furthermore, because of this stabilizing effect, sucrose partially counteracts the acceleration of GCSF aggregation caused by benzyl alcohol [18, 19]. Protein-protein interactions that impact the colloidal stability of proteins can be modified by the choice of solution pH. GCSF is more colloidally stable at pH 3.5 than at pH 7.0 (i.e. protein-protein interactions are more repulsive) and aggregates much less rapidly at pH 3.5 [4], even when protein tertiary structure is perturbed by benzyl alcohol [19]. Increasing the formulation ionic strength, which screens repulsive protein-protein electrostatic interactions at pH 3.5, results in an increased aggregation rate [16].

GSCF aggregation is of interest given a current trend for development of biopharmaceutical products with increased patient convenience and compliance. These efforts

include the development of strategies to increase the circulation half-life of the drug product and thus reduce the administration frequency [20, 21]. One method of increasing the circulation half-life is to create a fusion protein, co-expressing the drug molecule with another protein such as the Fc domain of an antibody [22] or human serum albumin (HSA) [21, 23,]. A fusion protein of GCSF and HSA has been developed to increase the circulation half-life of GCSF [24] and this fusion protein is the focus of the current research.

There are added stability challenges involved in the formulation of fusion proteins. Because the individual fusion domains did not co-evolve, they may lack built-in inter-domain interactions that contribute favorably to native-state stability. Also, solution conditions that stabilize one domain may not adequately stabilize the other domain(s) of the fusion protein. However, because aggregation of proteins in generally thought to result from their (partial) unfolding [8, 25], we hypothesized that the aggregation rate of fusion proteins can be reduced by increasing the conformational stability of the least-stable domain [26]. In the case of HSA fusion proteins, the addition of octanoic acid, an HSA ligand, is one potential strategy to selectively stabilize the HSA domain [8, 17, 27]. HSA was chosen as the target for selective domain stabilization because it has a lower free energy of unfolding value than GCSF (ΔG_{NU} for HSA is approximately 22.0 ± 0.5 kJ/mol, compared to 39.7 ± 2.1 kJ/mol for GCSF) [16, 28] and is thus presumed to be the least conformationally stable domain in HSA-GCSF. In addition, we hypothesized that the addition of the less thermodynamically stable HSA domain will increase aggregation rate for the resulting fusion protein compared to that for GCSF alone. To test these hypotheses, the aggregation rates, aggregation reaction orders and stability behavior of HSA-GCSF with and without selective domain stabilization were investigated and compared to the aggregation rates of both GCSF [4, 16] and another HSA fusion, HSA-hGH [29]. Conformational

stability was investigated using chaotrope- and thermally-induced denaturation, whereas colloidal stability was determined by static light scattering and zeta potential measurements. Octanoic acid was used as a small molecule ligand for the stabilization of HSA [30, 31].

5.2 Materials and Methods

5.2.1 Stock protein preparation

HSA-GCSF was donated by Teva Biopharmaceuticals (Rockville, MD) and stored frozen at -80 °C. For experimentation, HSA-GCSF was thawed and dialyzed into 10 mM sodium phosphate buffer (pH 7.0). For experiments where sodium chloride was added, HSA-GCSF was dialyzed into 10 mM phosphate, 150 mM NaCl buffer (pH 7.0) (PBS). The concentration of HSA-GCSF after dialysis was determined by absorbance at 280 nm, using a theoretical extinction coefficient of 0.6 $cm^2 mg^{-1}$. For experiments wherein the stabilizing effect of a binding ligand was tested, octanoic acid was added to the protein sample in 10 mM sodium phosphate buffer, pH 7.0, to a final concentration of 0.5 mM octanoic acid.

5.2.2 Thermal stability monitored by circular dichroism spectroscopy

Far UV circular dichroism (CD) was used to monitor the loss of alpha helical structure upon heating and to determine the apparent temperature midpoint of the thermal transition (T_m). Protein at a concentration of 0.1 mg/mL in a 1 mm pathlength cuvette was heated from 40 °C to 90 °C in one degree increments with a one minute hold at each temperature. Spectra covering the 200-250 nm range were collected at each temperature using a Chirascan Plus CD spectrometer (Applied Photophysics, Surrey, UK) with Peltier temperature control. At the end of each spectral scan, the target cell temperature (i.e., the temperature setting of the Peltier control) was

overwritten with the actual cell temperature at the time of the each measurement. Cell temperature was measured by a thermocouple. Plots of circular dichroism signal at 222 nm versus actual cell temperature were used to estimate the apparent T_m with the Global Analysis software (Applied Photophysics, Surrey, UK). Each apparent T_m value represents the average of three separate thermal scans ± the standard deviation.

5.2.3 Chaotrope denaturation monitored by intrinsic fluorescence

The chaotrope perturbation method described previously [32] was used to determine the free energies of unfolding for HSA-GCSF under various solution conditions at 25 °C. To obtain the data for chaotrope-induced unfolding of the protein, HSA-GCSF at a concentration of 0.1 mg/mL was incubated overnight at 25 °C in urea (0-10 M). After incubation, intrinsic fluorescence spectra were obtained. The protein was excited at 293 nm, and the emission spectra from 300-400 nm were recorded using an Aminco Bowman Series 2 fluorescence spectrophotometer (SLM Aminco, Urbana, Illinois). The center of spectral mass (CSM) of each emission spectrum was calculated using Equation 1 and plotted versus urea concentration.

$$\text{(1)} \qquad \text{CSM} = \frac{\sum F_i V_i}{\sum F_i}$$

In Equation 1, F_i is the fluorescence intensity at a given wavelength, v_i. Plots of CSM values versus chaotrope concentration were then fit to a two-state unfolding model using a linear least-squares fit to Equation 2 to calculate the free energies of unfolding (ΔG_{NU}) [33]. Equation 3 represents the linear approximation for ΔG_{NU} for chaotrope-induced denaturation [33].

$$(2) \qquad Y_0 = \frac{(k_N[D] + b_N) + (k_U[D] + b_U)\exp\left(\frac{-\Delta G_{NU}}{RT}\right)}{1+\exp\left(\frac{-\Delta G_{NU}}{RT}\right)}$$

$$(3) \qquad \Delta G_{NU}(D) = \Delta G_{NU}(H_2O) + m[D]$$

In Equation 2, k_N and k_U are the slopes of the baselines of the native and unfolding states respectively, b_N and b_U are the intercepts of these baselines, Y_0 is the center of spectral mass value T is temperature, and R is the molar gas constant. In Equation 3, [D] is the concentration of the chaotrope and m represents $d\Delta G_{NU}/d[D]$ (i.e., the sensitivity of ΔG_{NU} to chaotrope concentration). $\Delta G_{NU}(D)$ is the free energy of the unfolding with chaotrope present and $\Delta G_{NU}(H_20)$ is the free energy of unfolding at a zero chaotrope concentration.

5.2.4 Osmotic second virial coefficients determined by static light scattering

Static light scattering intensities of HSA-GCSF, either in buffer alone or with 0.5 mM octanoic acid or 150 mM NaCl, were measured at 25 °C using a Brookhaven light scattering system (Holtsville, NY) and an aperture set to 1.0 mm. For each solution condition, the scattering intensity at 90° from 633 nm incident light was measured for five samples ranging in protein concentration from 0.5-3 mg/mL. Prior to measurement, samples containing protein were filtered with a 0.1 μm inorganic filter (Whatman Anotop, Kent, UK), and the buffer was filtered with a 0.02 μm filter. The concentration of each sample was calculated from the A_{280} value measured post-filtration. The second osmotic virial coefficient (B_{22}) was calculated from the scattering intensity at 90° using the virial expansion of the ideal osmotic pressure equation [34] represented by Equation 4:

$$(4)\ \frac{Kc}{R_{90}} = \frac{1}{M_W} + 2(B_{22})c$$

In equation 4, K is the optical constant, R_{90} is the excess Raleigh scatter at 90°, M_W is the molecular weight and c is the protein concentration of the sample.

The optical constant K is represented by equation 5:

$$(5)\ K = \frac{4\pi^2 n_0^2 (dn/dc)^2}{N_A \lambda^4}$$

where n_o is the solvent refractive index, dn/dc is the refractive index increment, N_A is Avogadro's number and λ is incident wavelength (633 nm). For these calculations, a dn/dc value of 0.185 was used [35].

5.2.5 Zeta potential measurements

Electrophoretic mobilities were measured using the Malvern Zetasizer Nano ZS (Worcestershire, United Kingdom) and converted to zeta potentials using the Smoluchoski approximation to Henry's equation (Equation 6) [36].

$$(6)\ \mu_e = \frac{2\varepsilon k_s \zeta}{3\eta}$$

In Equation 6, μ_e is the electrophoretic mobility, η is the solution viscosity, ε is the dielectric constant, ζ is the zeta potential and k_s equals 1.5 in the Smoluchoski approximation [36]. Protein samples at 25 °C and a concentration of 1 mg/mL were placed in disposable folded capillary cells (Malvern Instruments Ltd, Worcestershire, United Kingdom). Zeta potentials were measured

after a 20 second equilibration in the instrument and the values reported represent the average for three samples ± the standard deviation.

The effective charge on the protein was calculated using the Debye-Hückel approximation (Equation 7) [37]:

$$(7) \qquad z = \frac{4\pi\varepsilon_r\varepsilon_0 r_p(1+kr_p)\zeta}{e}$$

where z is the effective charge, ε_r is the dielectric constant of the solution, ε_0 is the vacuum permittivity, r_p is the effective sphere radius of the protein, k is the inverse Debye length and e is the elementary charge. The effective charge, z, can then be used to calculate the electrostatic contribution to B22, or the Donnan term, using Equation 8 [38]:

$$(8) \qquad B_{22\ electrostatic} = \frac{z^2}{4M_w^2\rho_s m_{ions}}$$

where M_w is the molecular weight of the protein, ρ_s is the solvent density and m_{ions} is the molal concentration of ions.

5.2.6 Aggregation studies

HSA-GCSF was incubated at 40 °C so that comparison could be made with GCSF aggregation data in the literature [4]. 100 μL aliquots of 5 mg/mL protein were placed into polypropylene microcentrifuge tubes (Fisher Scientific, Pittsburgh, PA) that were sealed with Parafilm to prevent sample evaporation. Following incubation, samples were centrifuged for five minutes at 15400*g* to remove large particles and then analyzed by size exclusion chromatography (SEC). For the SEC analysis, a 3000Swxl gel sizing column (Tosoh Bioscience LLC, Montgomeryville, PA) was used in conjunction with a Beckman System Gold HPLC (Beckman Coulter, Brea, CA) and a Waters 717plus autosampler (Waters Technologies Corporation, Milford, MA). Peak areas were determined by integration using Bomem/Grams software version

7.00. Monomer concentrations were calculated from integrated peak area, and reaction rates were calculated from the slope of plots of monomer concentration versus time. The reported reaction rates represent the average of rate constants from three incubation experiments. Errors represent the standard deviation. To calculate the apparent reaction order, reaction rates were obtained for samples incubated at different initial protein concentrations. The reaction rates at the different initial concentrations were then used to calculate the reaction order by performing a natural log transformation on the rate equation:

$$r = k[c]^x \quad (7)$$

where r is the reaction rate, k is the rate constant and x is the apparent reaction order. The apparent reaction order is the slope of the plot of the natural log of the rate versus the natural log of the protein concentration and the reported error is ± the 95% confidence interval on the fit.

5.3 Results

5.3.1 Conformational stability

Chaotrope-induced denaturation resulted in an unfolding profile for HSA-GCSF that appeared to be two-state, apparently with overlapping and cooperative unfolding of the HSA and GCSF domains (Figure 5-1). The free energy of unfolding (ΔG_{NU}) values for HSA-GCSF in phosphate buffer alone, PBS or phosphate buffer with 0.5 mM octanoic acid at 25 °C are listed in Table 1. In 10 mM phosphate buffer and PBS, the free energy of unfolding values for the HSA-GCSF fusion protein were very similar to the value of ΔG_{NU} determined by earlier researchers for GCSF itself [16], and substantially higher than the previously determined value for HSA alone [28]. Also, the presence of 0.5 mM octanoic acid increased the ΔG_{NU} of HSA-GCSF by approximately10 kJ/mol.

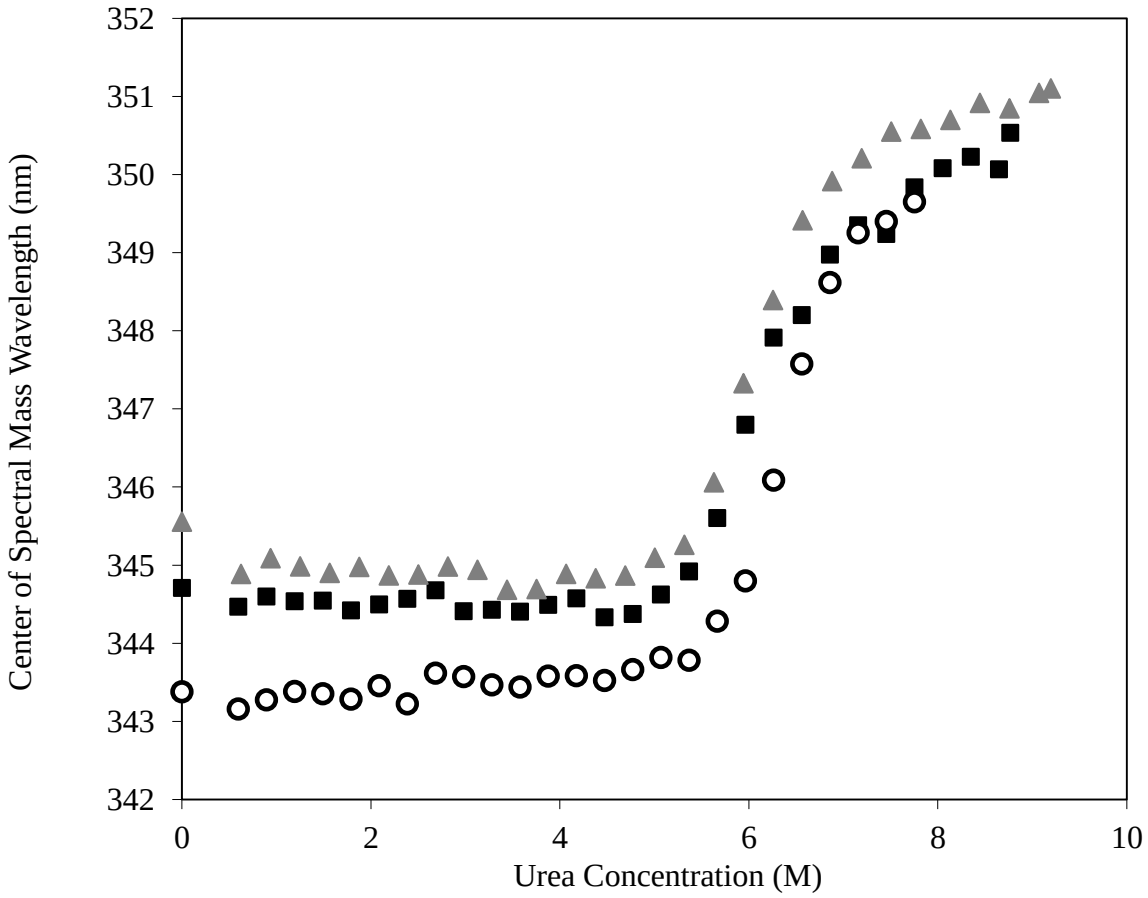

Figure 5-1: Representative urea-induced denaturation curves showing the center of spectral mass (CSM) versus urea concentration for HSA-GCSF alone (■), with 150 mM NaCl (▲) or with 0.5 mM octanoic acid (○). Free energies of unfolding were calculated from the combined unfolding curves of three separate experiments.

During heating in 10 mM sodium phosphate at pH 7.0, only one unfolding transition was observed for HSA-GCSF (Figure 5-2). Addition of 0.5 mM octanoic acid increased the apparent T_m of this transition by approximately 8 °C, whereas addition of 150 mM NaCl increased the apparent T_m only slightly (Table 5-1).

5.3.2 Colloidal stability

In 10 mM sodium phosphate buffer at pH 7.0, the net protein-protein self interactions for HSA-GCSF were attractive, as indicated by the negative B_{22} value (Table 5-2). When 0.5 mM octanoic acid was added, there was no detectable change in the net self-interaction. However, addition of 150 mM sodium chloride decreased the attractive self-interaction. No changes in zeta potential were detected with the addition of 0.5 mM octanoic acid. In contrast, the addition of 150 mM NaCl appeared to colloidally destabilize the system, as reflected in zeta potential values that were closer to zero than those for HSA-GCSF in phosphate buffer or phosphate buffer with 0.5 mM octanoic acid (Table 5-2). The electrostatic contributions to the zeta potential are similar in phosphate buffer and phosphate buffer with octanoic acid. In PBS, the electrostatic contributions to the zeta potential are decreased (Table 5-2).

5.3.3 Aggregation studies

Incubation of 5 mg/mL HSA-GCSF in 10 mM sodium phosphate at pH 7.0 and 40 °C resulted in an aggregation rate of 1.0 ± 0.1 μmol L^{-1} day^{-1}. The presence of 0.5 mM octanoic acid did not affect the aggregation rate significantly (Table 5-3). When incubated with 150 mM sodium chloride, there was a large increase in HSA-GCSF aggregation rate as compared to that in phosphate buffer alone. However, the aggregation rate of HSA-GCSF in PBS was still lower

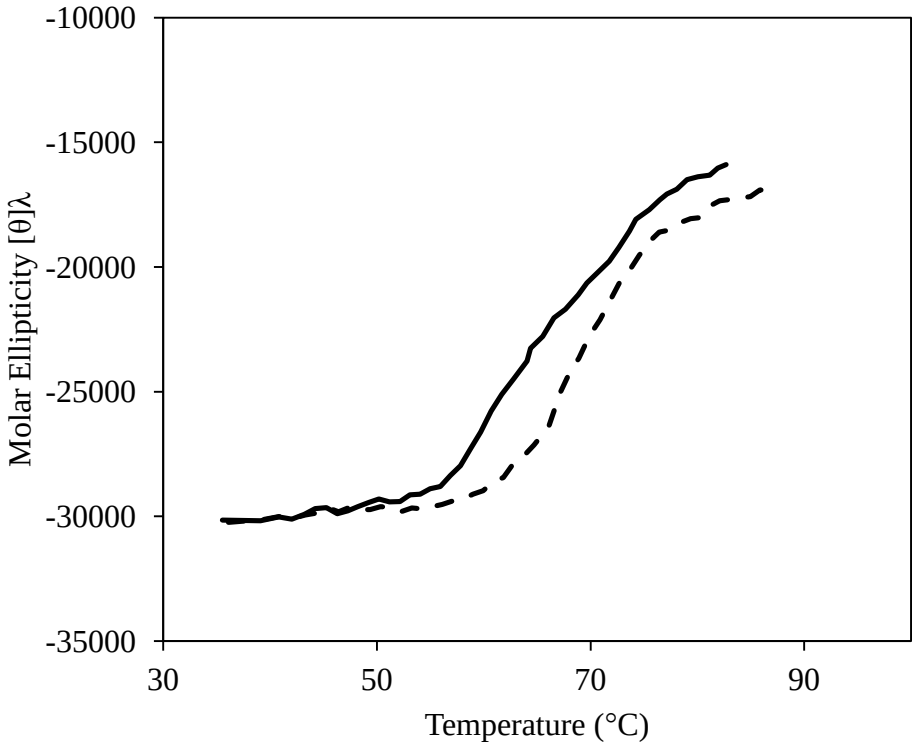

Figure 5-2: Far UV CD signal at 222 nm as a function of temperature for HSA-GCSF (solid line) and HSA-GCSF in the presence of 0.5 mM octanoic acid (dashed line) in 10 mM sodium phosphate (pH 7.0). Addition of octanoic acid increases the onset temperature of unfolding and the T_m.

Protein	**Solution conditions (pH 7.0)**	**Apparent T_m (°C)**	**ΔG_{NU} (kJ/mol)**
HSA-GCSF	10 mM sodium phosphate	60.1 ± 1.5	44.3 ± 6
HSA-GCSF	10 mM sodium phosphate, 150 mM NaCl	63.2 ± 1.5	43.4 ± 3.0
HSA-GCSF	10 mM sodium phosphate, 0.5 mM octanoic acid	68.6 ± 1.6	56.8 ± 6.9
GCSF	10 mM sodium phosphate, 150 mM NaCl	60.95 ± 2[#]	39.7 ± 2.1*, 41.9 [+]
HSA	67 mM sodium phosphate, pH 7.4	59.65 ± 0.05[^]	17.2 ± 4.2[^]

Table 5-1: Free energy of unfolding and T_m values for HSA-GCSF and GCSF in varying solution conditions. Values represent the average of three experiments ± the standard deviation. GCSF values at 25 °C are from [#]Krishnan et al. (2002), *Chi et al. (2003) [16], and [+]Raso, et al., 2005. HSA values are from [^]Kosa et al. (1998) [28].

Protein	**Solution Conditions**	**B_{22} x 10^3 (mL mol g^{-2})**	**Zeta potential (mV)**	**$B_{22electrostatic}$ x 10^5 (mL mol g^{-2}) (% of B22)**
HSA-GCSF	10 mM sodium phosphate, pH 7.0	-0.35 ± 0.22	-12.5 ± 2.3	6.8 (19.6%)
HSA-GCSF	10 mM sodium phosphate, 0.5 mM octanoic acid, pH 7.0	-0.33 ± 0.41	-10.3 ± 2.0	4.5 (13.5%)
HSA-GCSF	10 mM sodium phosphate, 150 mM NaCl, pH 7.0	-0.03 ± 0.03	-6.1 ± 1.1	0.1 (3.4 %)
GCSF	10 mM sodium phosphate, pH 7.0	-0.72 ± 0.45*	N/D	N/D
GCSF	10 mM sodium phosphate, 0.5 mM octanoic acid, pH 7.0	2.34 ± 1.9*	N/D	N/D

Table 5-2: B_{22} and zeta potential values for HSA-GCSF at pH 7.0 measured under different solution conditions, as well as the electrostatic contribution to the B_{22}. B_{22} and zeta potential values represent the average of three experimental determinations ± the standard deviation. B_{22} electrostatic values were calculated from the average B_{22} and zeta potential values. GCSF values are from Chi et al. (2003) [16]. N/D signifies not determined.

Protein	**Solution conditions (pH 7.0)**	**Reaction rates (μmol L^{-1} day^{-1})**	**Apparent reaction order**
HSA-GCSF	10 mM sodium phosphate	1.0 ± 0.1	0.80 ± 0.3
HSA-GCSF	10 mM sodium phosphate, 150 mM NaCl	3.7 ± 1.0	1.95 ± 0.4
HSA-GCSF	10 mM sodium phosphate, 0.5 mM octanoic acid	1.2 ± 0.1	1.71 ± 0.1
GCSF	10 mM sodium phosphate, 150 mM NaCl	7.3 ± 0.6*	2.17 ± 0.09*
HSA	10 mM sodium phosphate	0[#]	N/D[#]

Table 5-3: Aggregation behavior of HSA-GCSF at 5 mg/mL and GCSF, including reaction rates and apparent reaction orders for the given solution conditions. HSA-GCSF aggregation was measured at 40 °C. Reaction order values are the best fit to three combined experiments ± the 95% confidence interval on the fit. *GCSF values are from Krishnan et al. (2002) and were measured at a concentration of 1 mg/mL and 37 °C. [#]The reaction rate for HSA was zero, within error and thus the apparent reaction order was not determined.

than aggregation rate of GCSF which was determined by Krishnan et al. [39] under the same conditions. The apparent reaction order (Table 5-3) for HSA-GCSF aggregation was close to first order in phosphate buffer alone. Addition of octanoic acid resulted in an aggregation reaction order closer to second order. In PBS at pH 7.0, the aggregation of HSA-GCSF was second order in protein concentration, which matches the previous findings for GCSF [4] (Table 5-3).

5.4 Discussion

Fusion protein domains, which are chosen for particular therapeutic reasons (e.g., increased circulation half-life, added functionality), may have very different individual conformational and colloidal stability properties compared to those of the overall fusion protein. Thus, finding solution conditions that adequately stabilize the entire protein may be difficult. Similar issues can be seen with large multi-domain proteins such as antibodies. The Fab and Fc antibody domains may respond differently to the same stress condition due to differences in their surface properties [39, 40]. The Fab and Fc domains also exhibit differences in conformational stability, and the Fc domain may even exhibit two transitions due to the separate unfolding C_H2 and C_H3 regions [41, 42]. Aggregation and/or association of the intact antibody can thus be driven by the instability of a single domain [40, 43], with the overall stability behavior of the antibody corresponding more closely to the behavior of either the isolated Fab or Fc domains. There are several recent examples of this. In one case, the Fab region was responsible for the observed antibody self association [43]. In another study, the aglycosylated Fc domain was shown to aggregate more rapidly than the glycosylated Fc domain. The aggregation of the aglycosylated antibody also increased in a similar manner to that of the aglycosylated Fc domain [40]. Even within the IgG subclass, either the Fc or the Fab domain can drive aggregation for different IgG

molecules [39, 44], illustrating both the complexity of larger multi-domain proteins as well as the difficulties in making generalizations or predictions about the aggregation behavior.

In the current study, the HSA-GCSF fusion protein aggregated more slowly than has previously been found for the therapeutic GCSF alone [4] in PBS at pH 7.0. This is likely due to the presence of the HSA domain in the fusion protein, as the aggregation of HSA alone was previously found to be so slow as to be undetectable at pH 7.0 and 50 °C during one month of incubation [29], in spite of its lower conformational stability. Even though HSA is less conformationally stable than GCSF (Table 1), it appears to confer some of its resistance to aggregation to the fusion protein, as GCSF aggregation has previously been detected at pH 7.0 and 40 °C [16]. Previous studies in multi-domain proteins support the observation that the least conformationally stable domain is not necessarily the most aggregation prone [45]. The findings here are similar, with slower aggregation rates for the less conformationally stable HSA (ΔG_{NU} = 17.2 ± 4.2 kJ/mol) [28] compared to GCSF and HSA-GCSF which had higher free energies of unfolding of 39.7 ± 2.1 kJ/mol [16] and 44.3 ± 6 kJ/mol, respectively.

The aggregation rate of HSA-GCSF in 10 mM phosphate buffer, pH 7.0 increased approximately three-fold with the addition of 150 mM sodium chloride. No large changes in HSA-GCSF conformational stability were detected in solutions containing 150 mM NaCl compared to 10 mM sodium phosphate buffer alone. In contrast, zeta potential measurements indicate that HSA-GCSF is colloidally destabilized in the presence of salt. Although B_{22} measurements seem to indicate that the addition of salt shields attractive HSA-GCSF protein-protein interactions (Table 2), the error associated with B_{22} measurements is much larger than that of the zeta potential measurements and is not statistically significant. Furthermore, while zeta potential measurements reflect the role of electrostatic interactions, B_{22} values include the

contributions from all of the interaction forces (e.g., hard sphere, Van der Waals, electrostatic) [46]. The electrostatic component of the B_{22} is decreased with the addition of NaCl, from 19.6% of the total B_{22} to only 3.4% (Table 2). Taken together, the observations from the conformational stability studies and zeta potential measurements indicate that colloidal instability is the driving force for the aggregation observed in PBS. Further supporting this conclusion is previous work that showed the addition of NaCl increased GCSF net attractive protein-protein interactions as measured by static light scattering and also increased the rate of aggregation [4, 16]. As apparent second order reactions were measured for both HSA-GCSF and GCSF [4] in PBS, and because the reaction rates were similar, we speculate that the aggregation of HSA-GCSF is driven by the GCSF domain under these conditions.

The addition of octanoic acid, an HSA binding ligand [31, 47, 48], resulted in no change in the aggregation rate of 5 mg/mL HSA-GCSF, even though the conformational stability of the protein was increased under these conditions. No changes in HSA-GCSF colloidal stability were observed with the addition of octanoic acid (Table 2). This is in contrast to what was seen previously with HSA-hGH, where the addition of octanoic acid increased both conformational and colloidal stability of the fusion protein in addition to reducing aggregation rates [29]. Addition of octanoic acid presumably increases the conformational stability of the HSA domain in the HSA-GCSF fusion protein. Since this increase occurs without a concomitant decrease in aggregation rate, it appears that the aggregation behavior of the fusion protein is dominated by the behavior of the GCSF domain, supporting the conclusions from the experiments in PBS.

Although GCSF and hGH are fairly similar in structure (both are predominately alpha-helical, and there is only approximately 3 kDa difference in molecular weight) [15, 49], HSA-GCSF exhibits different stability behavior compared to that seen previously for HSA-hGH in almost

every aspect, including intrinsic conformational stability, colloidal stability and propensity to aggregate [29]. Only one unfolding transition is observed during HSA-GCSF denaturation by chaotropes, whereas two transitions are apparent for HSA-hGH [29, 50]. The colloidal stabilities of the two proteins are different as well. At pH 7.0, HSA-hGH self interactions are repulsive [29] but HSA-GCSF self interactions are attractive. Although B_{22} values are not necessarily expected to be additive, one possible explanation for this observation could be the pI values of the individual domains. The pI of hGH is pH 5.0 [51], whereas the pI values for both HSA (pH 5.8) [52] and GCSF (pH 6.1) [16] are approximately one pH unit closer to the solution condition pH 7.0. This could lead to HSA-GCSF having decreased intermolecular charge-charge repulsive interactions compared to HSA-hGH. Furthermore, HSA-GCSF aggregates more rapidly than HSA-hGH in phosphate buffer at pH 7.0 (1.0 ± 0.1 μmol L^{-1} day^{-1} for GCSF versus 0.6 ± 0.1 μmol L^{-1} day^{-1} for HSA-hGH) and the measured HSA-GCSF aggregation was detected at 40 °C in the current study, whereas HSA-hGH aggregation was not detected until incubation at 50 °C [29]. Whereas the HSA fusion protein aggregation behavior may be dominated by the non-HSA domain, clearly the behavior is different enough that each HSA fusion protein will likely require individually tailored conditions and the potential for a platform formulation approach is limited.

5.5 Conclusions

The fusion of HSA to GCSF reduces the rate of aggregation of the therapeutic HSA-GCSF compared to the rate of aggregation of GCSF itself. However, under the solution conditions tested, the overall aggregation rate and aggregation reaction order of the HSA-GCSF fusion protein are still more similar to those of GCSF than HSA. Because HSA-GCSF aggregation appears to be driven by the GCSF domain, the strategy of stabilizing HSA-GCSF via ligand binding to HSA does not reduce the rates of HSA-GCSF aggregation. This is in contrast

to previously reported results for another HSA fusion protein, HSA-hGH, where stabilizing the HSA domain via small molecule ligand binding reduced fusion protein aggregation rates. Thus, each HSA fusion protein may require individually tailored solution conditions to reduce aggregation.

5.6 Acknowledgements

Funding for this work was provided by NIH grant R01 EB006006. HSA-GCSF was generously donated by Teva Biopharmaceuticals.

5.7 References

1. Leader, B. Protein therapeutics: a summary and pharmacological classification. *Nature Reviews Drug Discovery* **2008,** *7* (1), 21-39.

2. Frokjaer, S. Protein Drug Stability: A Formulation Challenge. *Nature Reviews Drug Discovery* **2005,** *4*, 298-306.

3. Manning, M. C.; Patel, K.; Borchardt, R. T. Stability of Protein Pharmaceuticals. *Pharmaceutical Research* **1989,** *6* (11), 903-918.

4. Krishnan, S.; Chi, E. Y.; Webb, J. N.; Chang, B. S.; Shan, D.; Goldenberg, M.; Manning, M. C.; Randolph, T. W.; Carpenter, J. F. Aggregation of Granulocyte Colony Stimulating Factor under Physiological Conditions: Characterization and Thermodynamic Inhibtion. *Biochemistry* **2002,** *41* (20), 6422-6431.

5. Tsai, P. Formulation Design of Acidic Fibroblast Growth Factor. *Pharmaceutical Research* **1993,** *10* (5), 649-659.

6. Roberts, C. Non-Native Protein Aggregation Kinetics. *Biotechnology and Bioengineering* **2007,** *98* (5), 927-937.

7. Shire, S. Formulation and manufacturability of biologics. *Current Opinion in Biotechnology* **2009,** *20* (6), 708-714.

8. Chi, E. Y.; Krishnan, S.; Randolph, T. W.; Carpenter, J. F. Physical Stability of Proteins in Aqueous Solution: Mechanism and Driving Forces in Nonnative Protein aggregation. *Pharmaceutical Research* **2003,** *20* (9), 1325-1336.

9. Rosenberg, A. Effects of Protein Aggregates: An Immunologic Perspective. *The AAPS Journal* **2006,** *8* (3), 501-507.

10. Ring, J.; Seifert, J.; Jesch, F.; Brendel, W. Anaphylactoid reactions due to non-immune complex serum protein aggregates. *Monogr Allergy* **1977,** *12*, 27-35.

11. Barandun, S.; Kistler, P.; Jeunet, F.; Isliker, H. Intravenous Administration of Human gamma-Globulin. *Vox Sanguinis* **1962,** *7* (2), 157-174.

12. Stravitz, R.; Chung, H.; Sterling, R.; Luketic, V.; Sanyal, A.; Price, A.; Purrington, A.; Shiffman, M. Antibody-Mediated Pure Red Cell Aplasia Due to Epoetin Alfa During Antiviral Therapy of Chronic Hepatitis C. *The American Journal of Gastroenterology* **2005,** *100* (6), 1415-1419.

13. Bunn, H. Drug-Induced Autoimmune Red-Cell Aplasia. *New England Journal of Medicine* **2002,** *346* (7), 522-523.

14. Renwick, W.; Pettengell, R.; Green, M. Use of filgrastim and pegfilgrastim to support delivery of chemotherapy: twenty years of clinical experience. *BioDrugs* **2009,** *23* (3), 175-186.

15. Raso, S. W.; Abel, J.; Barnes, J. M.; Maloney, K. M.; Pipes, G.; Treuheit, M. J.; King, J.; Brems, D. N. Aggregation of granulocyte-colony stimulating factor in vitro involves a conformationally altered monomeric state. *Protein Science* **2005,** *14,* 2246-2257.

16. Chi, E. Y.; Krishman, S.; Kendrick, B.; Chang, B.; Carpenter, J.; Randolph, T. Roles of Conformational Stability and Colloidal Stability in the Aggregation of Recombinant Human Granulocyte Colony Stimulating Factor. *Protein Science* **2003,** *12,* 903-913.

17. Timasheff, S. N. Protein-solvent preferential interactions, protein hydration, and the modulation of biochemical reactions by solvent components. *PNAS* **2002,** *99* (15), 9721-9726.

18. Singh, S. K. Impact of Product-Related Factors on Immunogenicity of Biotherapeutics. *Journal of Pharmaceutical Sciences* **2011,** *100* (2), 354-387.

19. Thirumangalathu, R.; Krishnan, S.; Brems, D. N.; Randolph, T. W.; Carpenter, J. F. Effects of pH, temperature, and sucrose on benzyl alcohol-induced aggregation of recombinant human granulocyte colony stimulating factor. *Journal of Pharmaceutical Sciences* **2006,** *95* (7), 1480-1497.

20. Reginster, J.; Rabenda, V.; Neuprez, A. Adherence, patient preference and dosing frequency: understanding the relationship. *Bone* **2006,** *38* (4), S2-S6.

21. Muller, N.; Schneider, B.; Pfizenmajer, K.; Wajant, H. Superior serum half life of albumin tagged TNF ligands. *Biochem Biophys Res Commun* **2010,** *396* (4), 793-799.

22. In *Antibody Fusion Proteins*, 1st ed.; Chamow, S., Ashkenazi, A., Eds.; Wiley-Liss Inc: New York, 1999.

23. Syed, S.; Schuyler, P.; Kulczycky, M.; Scheffield, W. Potent antithrombin activity and delayed clearance from the circulation characterize recombinant hirudin genetically fused to albumin. *Blood* **1997,** *89* (9), 3243-3252.

24. Teva Biopharmaceuticals USA. http://www.tevapharm-na.com/Our-Business/Teva-Biopharmaceuticals-USA.aspx (accessed Nov 1, 2011).

25. Lumry, R.; Eyring, H. Conformation changes of proteins. *J Phys Chem* **1954,** *58,* 110-120.

26. Fast, J.; Cordes, A. A.; Carpenter, J. F.; Randolph, T. W. Physical Instability of a Therapeutic Fc Fusion Protein: Domain Contributions to Conformational and Colloidal Stability. *Biochemistry* **2009,** *48,* 11724-11736.

27. Tanford, C. Extension of the theory of linked functions to incorporate the effects of protein hydration. *Journal of Molecular Biology* **1969,** *39* (3), 539-544.

28. Kosa, T.; Maruyama, T.; Otagiri, M. Species Differences of Serum Albumins: II. Chemical and Thermal Stability. *Pharmaceutical Research* **1998,** *15* (3), 449-454.

29. Cordes, A. A.; Carpenter, J. F.; Randolph, T. W. Selective domain stabilization as a strategy to reduce fusion protein aggregation. **Submitted**.

30. Anraku, M.; Tsurusaki, Y.; Watanabe, H.; Maruyama, T.; Kragh-Hansen, U.; Otagiri, M. Stabilizing mechanisms in commercial albumin preparations: octanoate and N-acetyl-L-tryptophanate protect human serum albumin against heat and oxidative stress. *Biochimica et Biophysica Acta* **2004,** 9-17.

31. Peters, T. *All About Albumin;* Academic Press Inc: San Diego, 1996.

32. Pace, C. Determination and Analysis of Urea and Guanidine Hydrochloride Denaturation Curves. *Methods in Enzymology* **1986,** *131,* 266-280.

33. Myers, J. K.; Pace, C. N.; Scholtz, J. M. Denaturant m values and heat capacity changes: Relation to changes in accessible surface areas of protein unfolding. *Protein Science* **1995,** 2138-2148.

34. Kratochvil, P. *Classical Light Scattering for Polymer Solutions;* Elsevier: Amsterdam, 1987.

35. Arakawa, T.; Wen, J. Determination of Carbohydrate Contents from Excess Light Scattering. *Analytical Biochemistry* **2001,** 158-161.

36. Faude, A.; Zacher, D.; Muller, E.; Bottinger, H. Fast determination of conditions for maximum dynamic capacity in cation-exchange chromatography of human monoclonal antibodies. *Journal of Chromatography A* **2007,** *1161,* 29-35.

37. Chun, M.-S.; Lee, I. Rigorous estimation of effective protein charge from experimental electrophoretic mobilities for proteomics analysis using microchip electrophoresis. *Colloids Surf., A* **2008,** *318,* 191-198.

38. Asthagiri, D.; Paliwal, A.; Abras, D.; Lenhoff, A. M.; Paulaitis, M. E. A consistent experimental and modeling approach to light-scattering studies of protein-protein interactions

in solution. *Biophys. J.* **2005,** *88,* 3300-3309.

39. Chen, S.; Lau, H.; Brodsky, Y.; Kleemann, G. R.; Latypov, R. F. The use of native cation-exchange chromatography to study aggregation and phase separation of monoclonal antibodies. *Protein Science* **2010,** *19,* 1191-1204.

40. Hari, S. B.; Lau, H.; Razinkov, V. I.; Chen, S.; Latypov, R. F. Acid-Incuded Aggregation of Human Monoclonal IgG1 and IgG2: Molecular Mechanism and the Effect of Solution Composition. *Biochemistry* **2010,** *49,* 9328-9338.

41. Liu, H.; Bulseco, G.-G.; Sun, J. Effect of posttranslational modifications on the thermal stability of a recombinant monoclonal antibody. *Immunology Letters* **2006,** *106* (2), 133-153.

42. Ghirlando, R.; Lund, J.; Goodall, M.; Jefferis, R. Glycosylation of human IgG-Fc: Influences on structure revealed by differential scanning micro-calorimetry. *Immunology Letters* **1999,** *68* (1), 47-52.

43. Yadav, S.; Sreedhara, A.; Kanai, S.; Liu, J.; Lien, S.; Lowman, H.; Kalonia, D. S.; Shire, S. J. Establishing a Link Between Amino Acid Sequences and Self-Associating and Viscoelastic Behavior of Two Closely Related Monoclonal Antibodies. *Pharm Res* **2011,** *28,* 1750-1764.

44. Kameoka, D.; Masuzaki, E.; Ueda, T.; Imoto, T. Effect of Buffer Species on the Unfolding and the Aggregation of Humanized IgG. *J. Biochem* **2007,** *142,* 383-391.

45. Brummitt, R. K.; Nesta, D. P.; Chang, L.; Chase, S. F.; Laue, T. M.; Roberts, C. J. Nonnative Aggregation of an IgG1 Antibody in Acidic Conditions: Part 1. Unfolding, Colloidal Interactions, and Formulation of High-Molecular-Weight Aggregates. *Journal of Pharmaceutical Sciences* **2011,** *100* (6), 2087-2103.

46. Neal, B.; Asthagiri, A.; Lenhoff, A. M. Molecular origins of osmotic second virial coefficients. *Biophysical Journal* **1998,** *75,* 2469-2477.

47. Aki, H.; Yamamoto, M. Biothermodynamic characterization of monocarboxylic and dicarboxylic aliphatic acids binding to human serum albumin: A flow microcalorimetric study. *Biophysical Chemistry* **1993,** *46,* 91-99.

48. Kragh-Hansen, U.; Watanabe, H.; Nakajou, K.; Iwao, Y.; Otagiri, M. Chain Length-dependent Binding of Fatty Acid Anions to Human Serum Albumin Studied by Site-directed Mutagenesis. *Journal of Molecular Biology* **2006,** *363,* 702-712.

49. Ultsch, M. H.; Somers, W.; Kossiakoff, A. A.; de Vos, A. M. The Crystal Structure of Affinity-matured Human Growth Hormone at 2 A Resolution. *J. Mol. Biol.* **1994,** *236,* 286-299.

50. Chou, D. K.; Krishnamurthy, R.; Randolph, T. W.; Carpenter, J. F.; Manning, M. C. Effects of Tween 20 and Tween 80 on the stability of Albutropin during agitation. *Journal of Pharmaceutical Sciences* **2005,** 1368-1381.

51. Gellerfors, P.; Eketorp, G.; Fholenhag, K.; Pavlu, B.; Johansson, S.; Fryklund, L. Characterisation of a secreted form of recombinant derived human growth hormone, expressed in Escherichia coli cells. *J Pharm Biomed Anal* **1989,** *7* (2), 183-183.

52. Dockal, M.; Carter, D. C.; Ruker, F. The Three Recombinant Domains of Human Serum Albumin. *The Journal of Biological Chemistry* **1999,** *274* (41), 29303-29310.

53. Wertheimer, A.; Santella, T. M.; Finestone, A.; Levy, R. Drug delivery systems improve pharmaceutical profile and facilitate medication adherence. *Advances in Therapy* **2005,** *22* (6), 559-577.

CHAPTER 6

CONCLUSIONS

6.1 Fusion protein observations

Fusion proteins can offer many benefits as a platform, including extended serum half-life or creation of a bi-functional molecule [1, 2, 3]. These benefits, among others, make fusion proteins attractive drug candidates. However, these are complex molecules that may present formulation challenges. This thesis outlined some of the issues with fusion protein stability and potential methods to address those concerns and reduce overall protein aggregation.

One of the reasons for concern about the identification of stable fusion protein formulations is that these complex molecules combine two or more individual proteins/protein domains which did not co-evolve. Because the fusion domains did not co-evolve, the domains lack native stabilizing intra-domain interactions, making identification of solution conditions which adequately stabilize each domain potentially difficult.

Fusion domains may have very different conformational and colloidal stabilities. Although the colloidal stability of the domains is not expected to be predictive, differences in domain pI and domain net charge can still impact the overall stability of the fusion construct. Conformational stability of the individual domains in the fusion protein may more closely match the conformational stability of the individual domains, increasing the likelihood that formulation strategies to increase the conformational stability of the domain will work in the fusion as well.

This similarity in domain conformational stability between the original proteins and their stability as part of the fusion construct was seen in the case of the Fc-CTLA4 fusion protein. CTLA4 alone has a lower conformational stability than what has previously been reported for the

antibody Fc domain [4] and was one of the least conformationally stable domains in the protein, along with the C_H2 domain which had been mutated in this particular protein. Conditions which destabilized the CTLA4 and C_H2 domains resulted in a decreased activation energy for aggregation and an increased aggregation rate. Modifying protein-protein interactions to make them more repulsive did not reduce aggregation under solution conditions where the CTLA4 and C_H2 domains were still destabilized. This indicates that conformational instabilities of the CTLA4 and CH2 domains are the driving force for aggregation of this protein during accelerated stability studies at elevated temperature.

Domain conformational instabilities, which contributed heavily to the aggregation of Fc-CTLA4 during elevated temperature incubation studies, also drove the aggregation under different stress conditions. During freeze/thaw and agitation studies in buffer at pH 6.0 and at pH 7.5, greater amounts of aggregation were observed at pH 6.0. Stress conditions ranged from fairly mild (i.e., 5 freeze thaw cycles, no monomer loss observed by SEC) to harsh (i.e., 6 hours agitation, approximately 20% initial monomer lost observed by SEC) with the same observation of greater aggregation in solution conditions at pH 6.0. This was true whether one was following aggregation by monitoring increase in particle count (in the case of freeze/thaw cycling) or by monitoring monomer loss as detected by SEC. Differences in the two pH conditions were observed was after 24 hours of storage. For samples that had undergone 5 freeze/thaw cycles, particle counts at pH 7.5 decreased while those at pH 6.0 did not, indicating that particles formed at pH 7.5 due to freeze/thaw stress are more reversible than those formed at pH 6.0. For the Fc-CTLA4 fusion protein, increasing domain conformational stability results in the most stable formulation.

In the case of the HSA fusion proteins studied here (HSA-hGH and HSA-GCSF), the HSA domain was the least conformationally stable. However, unlike what was previously seen with the Fc-CLTA4, increasing the conformational stability of the least stable domain did not reduce aggregation. Binding octanoic acid, a small molecule ligand for HSA, to the fusion proteins increased the conformational stability of both proteins but the increased conformational stability did not seem to reduce aggregation. Although HSA-hGH aggregation was reduced with octanoic acid, the binding of the small molecule also increased repulsive protein-protein interactions and aggregation was reduced by shifting from pH 5 to pH 7. This shift from pH 5 to pH 7 increased HSA-hGH repulsive protein-protein interactions but did not seem to significantly increase the conformational stability. Binding of octanoic acid to HSA-GCSF did not cause any changes to protein-protein interactions and did not reduce aggregation. Thus it seems that HSA fusion protein aggregation is driven more by colloidal instabilities.

Interestingly, HSA fusions are aggregating much faster than the HSA domain alone, even though HSA is the least conformationally stable domain in each fusion protein. The aggregation of each fusion seems to be more close to that of the active molecule alone, either hGH or GCSF. Even though HSA alone is resistant to aggregation, this does not result in HSA fusion constructs that also are resistant to aggregation.

Overall, the two HSA fusion proteins studied here are fairly similar. The molecular weight values are close: approximately 86 kDa for HSA-GCSF [5, 6, 7] and approximately 89 kDa for HSA-hGH [3],. Both combine a smaller alpha helical protein with HSA to produce to fusion product and the pI values for the fusion partners aren't wildly different (approximately 6.1 for GCSF [5] and 5.1 for hGH [8]). However, the resulting fusion products have very different stability and aggregation profiles, as outlined above and in previous chapters. Given that such different

aggregation profiles were obtained for these two products, it is unlikely that HSA fusions with even more dissimilar fusion partners would behave similarly to either of the proteins previously studied here.

This faster aggregation of the HSA fusion proteins does not necessarily indicate that HSA fusions are not a viable strategy to pursue for the extension of circulation half-life. Since the aggregation studies are conducted under elevated stress conditions, the overall HSA fusion protein aggregation under real time storage conditions may still be acceptable and meet the storage criteria. However, a therapeutic protein which is unstable and has difficulty meeting the aggregation criteria during real time storage is likely not a good candidate for a HSA fusion protein. In cases like those, if there is a need for extended serum half-life, other strategies should be explored.

That being said, there are currently no FDA approved HSA fusion protein products on the market. Human Genome Sciences submitted a BLA for the treatment of hepatitis using an HSA-Interferon alpha (IFNα) fusion, but the application was withdrawn prior to a decision by the FDA, according to their corporate website. The reasons cited for the withdrawal of the application were safety concerns related to the dosing schedule and the company indicated they may refile at a future date. However, HSA-IFNα is not currently listed as a product or pipeline candidate on the HGS corporate website, www.hgsi.com, as of July 10th, 2011.

6.2 Future of the ligand binding approach for domain stabilization

Although the addition of a small molecule ligand was shown to reduce the aggregation in some instances (e.g. HSA-hGH aggregation), there remain some challenges for future work. If this approach is to be further pursued as a stabilizing strategy, there is a need to move beyond

exploring the ligand binding approach as a proof-of-concept and to start addressing the concerns involved as well. Protein formulation does not happen in a vacuum. Regardless of how stable of a formulation one is able to design, if the formulation components are not safe for the patient, the formulation is useless. Thus one would need to identify safe, FDA approved small molecules for use as stabilizing ligands.

In the case of dialysis procedures that involve the use of HSA, it has been shown that patients are also exposed to octanoic acid [9]. Octanoic acid is used to stabilize HSA during the heat treatment step in production and is often present in commercial formulations at an octanoic acid: HSA molar ratio of 5.4:1. Increases in the concentration of octanoic acid in the patients' bloodstreams were observed during treatment. This is a concern because octanoic acid has been shown to have a direct involvement in the pathogenesis of liver failure [9]. Even though octanoic acid is present in the commercial HSA formulations, one might want to investigate safer ligands and reduce octanoic acid exposure when possible. This could be especially important in the case of the HSA-interferon alpha fusion protein which was investigated for the treatment of hepatitis C. In that case, avoiding excipients which may contribute to liver failure would be of utmost importance and octanoic acid is not likely to be a good choice, regardless of its ability to reduce aggregation of some HSA fusion proteins.

There are further questions involved depending on which domain of the fusion protein is targeted for selective stabilization. If one is binding a molecule to the active domain of the fusion, what might the impact be in the body? This is not likely to be a concern for selective stabilization of HSA, since the HSA domain is not designed to be an active part of the therapeutic molecule but rather just a way to extend serum half life. However, this may be different in the case of the Fc fusion protein constructs. The Fc domain has a relatively high

conformational stability [4] making it likely that the active domain would be the less conformationally stable domain, as is the case with the Fc-CTLA4 fusion. Additionally, in some cases the biological activity of the Fc domain is desirable, such as the ability to induce antibody dependent cell mediated cytotoxicity or trigger the release of inflammatory cytokines. The choice of a small molecule ligand must reflect these concerns and care must be taken to identify a ligand which is not bound too strongly such that the activity and efficacy of the therapeutic protein is affected.

6.3 Final recommendations

The results of the studies contained herein indicate that fusion proteins are very complex molecules and that understanding individual domain behavior or the behavior of a similar fusion protein is unlikely to allow one to make predictions about formulating a new fusion protein. Each fusion protein requires individual study and we have yet to identify any potential shortcuts in the development of fusion protein formulations.

In the case of the Fc-CTLA4 fusion, the domain which was driving the aggregation behavior is unlikely to be the conserved domain in any future fusion proteins. Thus strategies aimed at stabilizing this protein may have limited utility in other cases. Furthermore, Fc domains in other fusions may require the Fc biological activity and lack the mutations that may have reduced C_H2 stability and contributed to the aggregation. One could also imagine a scenario where a Fc domain with mutations in the C_H2 region is partnered with a more conformationally stable protein in the fusion construct and that having the more stable fusion partner and the C_H3 domain on either side of the mutated C_H2 domain could lead to increases in C_H2 conformational stability.

Even with the conserved HSA domain, the two HSA fusions aggregated very differently, as mentioned above. Ligand binding did not appear to reduce aggregation in the manner hypothesized initially, and did not work as a method to reduce aggregation across the HSA fusion protein class. As mentioned in the case of the Fc fusions, it is likely that each HSA fusion protein must be investigated independently in order to develop the most stable formulation.

6.4 References

1. In *Antibody Fusion Proteins,* 1st ed.; Chamow, S., Ashkenazi, A., Eds.; Wiley-Liss Inc: New York, 1999.

2. Jazayeri, J.; Carroll, G. Fc-based cytokines: prospects for engineering superior therapeutics. *BioDrugs* **2008,** *22* (1), 11-26.

3. Osborn, B.; Sekut, L.; Corcoran, M.; Poortman, C.; Sturm, B.; Chen, G.; Mather, D.; Lin, H.; Parry, T. J. Albutropin: a growth hormone-ablumin fusion with imroved pharmacokinetics and pharmacodymanics in rats and monkeys. *Eur J Pharmacol* **2002,** *456* (1-3), 149-158.

4. Ionescu, R.; Vlasakk, J.; Price, C.; Kirchmeier, M. Contribution of variable domains to the stability of humanized IgG1 monoclonal antibodies. *J Pharm Sci* **2008,** *97* (4), 1414-1426.

5. Chi, E. Y.; Krishman, S.; Kendrick, B.; Chang, B.; Carpenter, J.; Randolph, T. Roles of Conformational Stability and Colloidal Stability in the Aggregation of Recombinant Human Granulocyte Colony Stimulating Factor. *Protein Science* **2003,** *12,* 903-913.

6. Krishnan, S. Aggregation of Granulocyte Colony Stimulating Factor under Physiological Conditions: Characterization and Thermodynamic Inhibtion. *Biochemistry* **2002,** *41* (20), 6422-6431.

7. Peters, T. *All About Albumin;* Academic Press Inc: San Diego, 1996.

8. Ettori, C.; Righetti, P. G.; Chiesa, C.; Frigerio, F.; Galli, G.; Grandi, G. Purification of recombinant human growth hormone by isoelectric focusing in a multicomponent electrolyzer with Immobiline membranes. *Journal of Biotechnology* **1992,** *25* (3), 307-318.

9. Klammt, S.; Koball, S.; Hickstein, H.; Gloger, M.; Henschel, J.; Mitzner, S.; Stange, J.; Reisinger, E. C. Increase of octanoate concentrations during extracorporeal albumin dialysis treatments. *Ther Apher Dial* **2009,** *13* (5), 437-443.

BIBLIOGRAPHY

Aki, H.; Yamamoto, M. Biothermodynamic characterization of monocarboxylic and dicarboxylic aliphatic acids binding to human serum albumin: A flow microcalorimetric study. *Biophysical Chemistry* **1993,** *46,* 91-99.

Alford, J. R.; Kendrick, B. S.; Carpenter, J. F.; Randolph, T. W. High Concentration Formulations of Recombinant Human Interleukin-1 Receptor Antagonist: II. Aggregation Kinetics. *Journal of Pharmaceutical Sciences* **2008,** *97* (8), 3005-3021.

Anraku, M.; Tsurusaki, Y.; Watanabe, H.; Maruyama, T.; Kragh-Hansen, U.; Otagiri, M. Stabilizing mechanisms in commercial albumin preparations: octanoate and N-acetyl-L-tryptophanate protect human serum albumin against heat and oxidative stress. *Biochimica et Biophysica Acta* **2004,** 9-17.

Arakawa, T.; Wen, J. Determination of Carbohydrate Contents from Excess Light Scattering. *Analytical Biochemistry* **2001,** 158-161.

Aruffo, e. a. Inhibiting B cell activation with soluble CD40 or fusion proteins thereof. 6,376,459, April 23, 2002.

Asthagiri, D.; Paliwal, A.; Abras, D.; Lenhoff, A.; Paulaitis, M. A consistent experimental and modeling appraoch to light-scattering studies of protein-protein interactions in solution. *Biophysical Journal* **2005,** *88* (5), 3300-3309.

Azuaga, A.; Dobson, C.; Mateo, P.; Conejero-Lara, F. Unfolding and aggregation during the thermal denaturation of streptokinase. *European Journal of Biochemistry* **2002,** *269* (16), 4121-4133.

Bagatolli, L. A.; Kivatinitz, S. C.; Fidelio, G. D. Interactions of small ligands with human serum albumin subdomain IIIA. How to determine the affinity constant using an easy steady state fluorescent method. *Journal of Pharmaceutical Sciences* **1996,** *85* (10), 1131-1132.

Bai, S.; Manning, M. C.; Randolph, T. W.; Carpenter, J. F. Aggregatio of Recombinant Human Botulinum Protein Antigen Serotype C in Varying Solution Conditions: Implications of Conformational Stability for Aggregation Kinetics. *Journal of Pharmaceutical Sciences* **2011,** *100* (3), 836-848.

Bam, N. B.; Cleland, J. L.; Yang, J.; Manning, M. C.; Carpenter, J. F.; Kelley, R. F.; Randolph, T. W. Tween protects recombinant human growth hormone against agitation-induced damage via hydrophobic interactions. *J Pharm Sci* **1998,** *87* (12), 1554-1559.

Barandun, S.; Kistler, P.; Jeunet, F.; Isliker, H. Intravenous Administration of Human gamma-Globulin. *Vox Sanguinis* **1962,** *7* (2), 157-174.

Barnard, J. G.; Singh, S.; Randolph, T. W.; Carpenter, J. F. Subvisible Particle Counting Provides a Sensitive Method of Detecting and Quantifying Aggregation of Monoclonal Antibody Caused by Freeze-Thawing: Insigns Into the Roles of Particles in the Protein Aggregation Pathway. *Journal of Pharmaceutical Scinces* **2011,** *100* (2), 492-503.

Bee, J. S.; Stevenson, J. L.; Mehta, B.; Svitel, J.; Pollastrini, J.; Platz, R.; Freund, E.; Carpenter, J. F.; Randolph, T. W. Response of a Concentrated Monoclonal Antibody Formulation to High Shear. *Biotechnol Bioeng* **2009,** *103* (5), 936-943.

Bee, J.; Randolph, T. W.; Carpenter, J.; Bishop, S.; Dimitrova, M. Effects of Surfaces and Leachables on the Stability of Biopharmaceuticals. *J Pharm Sci* **2011**.

Berg, J. M.; Tymoczko, J. L.; Stryer, L. Protein Structure and Function. In *Biochemistry,* 5th ed.; W.H. Freeman and Company: New York, 2002; pp 41-73.

Bhatnagar, B. S.; Bogner, R. H.; Pikal, M. J. Protein Stability During Freezing: Separation of Stresses and Mechanisms of Protein Stabilization. *Pharmaceutical Development and Technology* **2007,** *12,* 505-523.

Brems, D. N.; Brown, P. L.; Becker, G. W. Equilibrium Denaturation of Human Growth Hormone and Its Cysteine-modified Forms. *The Journal of Biological Chemistry* **1990,** *265* (10), 5504-5511.

Brummitt, R. K.; Nesta, D. P.; Chang, L.; Chase, S. F.; Laue, T. M.; Roberts, C. J. Nonnative Aggregation of an IgG1 Antibody in Acidic Conditions: Part 1. Unfolding, Colloidal Interactions, and Formulation of High-Molecular-Weight Aggregates. *Journal of Pharmaceutical Sciences* **2011,** *100* (6), 2087-2103.

Brummitt, R. K.; Nesta, D. P.; Roberts, C. J. Predicting Accelerated Aggregation Rates for Monoclonal Antibody Formulations, and Challenges for Low-Temperature Predictions. *Journal of Pharmaceutical Sciences* **2011,** *DOI 10.1002/jps.22633*.

Bunn, H. Drug-Induced Autoimmune Red-Cell Aplasia. *New England Journal of Medicine* **2002,** *346* (7), 522-523.

Buttel, I.; Chamberlain, P.; Chowers, Y.; Ehmann, F.; Greinacher, A.; Jefferis, R.; Kramer, D.; Kropshofer, H.; Lloyd, P.; Lubiniecki, A.; Krause, R.; Mire-Sluis, A.; Platts-Mills, T.; Ragheb, J.; Reipert, B.; Schellekens, H.; Seitz, R.; Stas, P.; Subramanyam, M.; Thorpe, R.; Trouvin, J.; Weise, M.; Windisch, J.; Schneider, C. Taking Immunogenicity Assessment of Therapeutic Proteins to the Next Level. *Biologicals* **2011,** *39,* 100-109.

Carpenter, J. F.; Randolph, T. W.; Jiskoot, W.; Crommelin, D. J.; Middaugh, C. R.; Winter, G.; Fan, Y.-X.; Kirshner, S.; Verthelyi, D.; Kozlowski, S.; Clouse, K. A.; Swann, P. G.; Rosenberg, A.; Cherny, B. Overlooking Subvisible Particles in Therapeutic Protein Products: Gaps That

May Compromise Product Quality. *Journal of Pharmaceutical Sciences* **2009,** *98* (4), 1201-1205.

In *Antibody Fusion Proteins,* 1st ed.; Chamow, S., Ashkenazi, A., Eds.; Wiley-Liss Inc: New York, 1999.

Chen, S.; Lau, H.; Brodsky, Y.; Kleemann, G. R.; Latypov, R. F. The use of native cation-exchange chromatography to study aggregation and phase separation of monoclonal antibodies. *Protein Science* **2010,** *19,* 1191-1204.

Chi, E. Y.; Krishnan, S.; Randolph, T.; Carpenter, J. Physical Stability of Proteins in Aqueous Solution: Mechanism and Driving Forces in Nonnative Protein aggregation. *Pharmaceutical Research* **2003,** *20* (9), 1325-1336.

Chi, E. Y.; Krishman, S.; Kendrick, B.; Chang, B.; Carpenter, J.; Randolph, T. Roles of Conformational Stability and Colloidal Stability in the Aggregation of Recombinant Human Granulocyte Colony Stimulating Factor. *Protein Science* **2003,** *12,* 903-913.

Chou, D. K.; Krishnamurthy, R.; Randolph, T. W.; Carpenter, J. F.; Manning, M. C. Effects of Tween 20 and Tween 80 on the stability of Albutropin during agitation. *Journal of Pharmaceutical Sciences* **2005,** 1368-1381.

Chuang, V. Pharmaceutical Strategies Utilizing Recombinant Human Serum Albumin. *Pharmacuetical Research* **2002,** *19* (5), 569-577.

Crisman, R.; Randolph, T. W. Crystallization of Recombinant Human Growth Hormone at Elevated Pressures: Pressure Effects on PEG-Induced Volume Exclusion Interactions. *Biotechnology and Bioengineering* **2010,** 663-672.

Cromwell, M.; Hilario, E.; Jacobson, F. Protein Aggregation and Bioprocessing. *The AAPS Journal* **2006,** *8* (3), 572-579.

Davis, P.; Abraham, R.; Xu, L.; Nadler, S. G.; Suchard, S. J. Abatacept binds to the Fc receptor CD64 but does not mendiate complement-dependent cytotoxicity or antibody-dependent cellular cytotoxicity. *J Rheumatol* **2007,** *34,* 2204-2210.

Dumetz, A.; Chockla, A.; Kaler, E. W.; Lenhoff, A. M. Effects of pH on protein-protein interactions and implications for protein phase behavior. *Biochimica et Biophysica Acta* **2008,** *1784,* 600-610.

Ettori, C.; Righetti, P. G.; Chiesa, C.; Frigerio, F.; Galli, G.; Grandi, G. Purification of recombinant human growth hormone by isoelectric focusing in a multicomponent electrolyzer with Immobiline membranes. *Journal of Biotechnology* **1992,** *25* (3), 307-318.

Eugene, J.; McNally, C. The imporance of a thorough preformulation study.. In *Protein Formulation and Delivery,* 1st ed.; McNally, E., Ed.; Marcel Dekker: New York, 1999; pp 111-138.

Farruggia, B.; Pico, G. A. Thermodynamic Features of the Chemical and Thermal Denaturations of Human Serum Albumin. *International Journal of Biological Macromolecules* **1999,** *26,* 317-323.

Fast, J.; Cordes, A. A.; Carpenter, J. F.; Randolph, T. W. Physical Instability of a Therapeutic Fc Fusion Protein: Domain Contributions to Conformational and Colloidal Stability. *Biochemistry* **2009,** *48,* 11724-11736.

Fradkin, A.; Carpenter, J. F.; Randolph, T. W. Glass particles as an adjuvant: A model for adverse immunoenicity of therapeutic proteins. *Journal of Pharmaceutical Sciences* **2011,** doi: 10.1002/jps.22683.

Gellerfors, P.; Eketorp, G.; Fholenhag, K.; Pavlu, B.; Johansson, S.; Fryklund, L. Characterisation of a secreted form of recombinant derived human growth hormone, expressed in Escherichia coli cells. *J Pharm Biomed Anal* **1989,** *7* (2), 183-183.

George, A.; Wilson, W. Predicting protein crystallization from a dilute solution property. *Acta Crystallogr D Biol Crystallogr* **1994,** *50* (4), 361-365.

Hari, S. B.; Lau, H.; Razinkov, V. I.; Chen, S.; Latypov, R. F. Acid-Incuded Aggregation of Human Monoclonal IgG1 and IgG2: Molecular Mechanism and the Effect of Solution Composition. *Biochemistry* **2010,** *49,* 9328-9338.

Hawe, A.; Kasper, J. C.; Friess, W.; Jiskoot, W. Structural properties of monoclonal antibody aggregates induced by freeze-thawing and thermal stress. *European Journal of Pharmaceutical Sciences* **2009,** *38,* 79-87.

Honore, B.; Brodersen, R. Detection of carrier heterogeneity by rate of ligand dialysis: medium-chain fatty acid interaction with human serum albumin and competition wtih chloride. *Anal Biochem* **1988,** 55-66.

Ingersoll, K. The impact of medication regiment factors on adherence to chronic treatment: a review of literature. *J Behav Med* **2008,** *31* (3), 213-224.

Ionescu, R.; Vlasakk, J.; Price, C.; Kirchmeier, M. Contribution of variable domains to the stability of humanized IgG1 monoclonal antibodies. *J Pharm Sci* **2008,** *97* (4), 1414-1426.

Kendrick, B. S.; Carpenter, J. F.; Cleland, J. L.; Randolph, T. W. A transient expansion of the native state precedes aggregation of recombinant human interferon-gamma. *Proc. Natl. Acad.*

Sci. USA **1998,** *95,* 14142-14146.

Kern, N.; Frenkel, D. Fluid-fluid coexistence in colloidal systems with short-ranged strongly directional attraction. *Journal of Chemical Physics* **2003,** *118* (21), 9882-9889.

Ishikawa, T.; Kobayashi, N.; Osawa, C.; Sawa, E.; Wakamatsu, K. Prevention of Stirring-Induced Microparticle Formation in Monoclonal Antibody Solutions. *Biol. Pharm. Bull.* **2010,** *33* (6), 1043-1046.

Jazayeri, J.; Carroll, G. Fc-based cytokines: prospects for engineering superior therapeutics. *BioDrugs* **2008,** *22* (1), 11-26.

Joubert, M. K.; Luo, Q.; Nashed-Samuel, Y.; Wypych, J.; Narhi, L. O. Classification and Characterization of Therapeutic Antibody Aggregates. *Journal of Biological Chemistry* **2011,** *286* (28), 25118-25133.

Kameoka, D.; Masuzaki, E.; Ueda, T.; Imoto, T. Effect of Buffer Species on the Unfolding and the Aggregation of Humanized IgG. *J. Biochem* **2007,** *142*, 383-391.

Katakam, M.; Bell, L. N.; Banga, A. K. Effect of surfactants on the physical stability of recombinant human growth hormone. *J Pharm Sci* **1995,** *84* (6), 713-716.

Kiese, S.; Pappenberger, A.; Friess, W.; Mahler, H.-C. Shaken, Not Stirred: Mechanical Stress Testing of An IgG1 Antibody. *Journal of Pharmaceutical Sciences* **2008,** *97* (10), 4347-4366.

Kim, Y.; Berry, A.; Spencer, D.; Stites, W. Comparing the effect on protein stability of methionine oxidation versus mutagenesis: steps toward engineering oxidative resistance in proteins. *Protein Engineering* **2001,** *14* (5), 343-347.

Klammt, S.; Koball, S.; Hickstein, H.; Gloger, M.; Henschel, J.; Mitzner, S.; Stange, J.; Reisinger, E. C. Increase of octanoate concentrations during extracorporeal albumin dialysis treatments. *Ther Apher Dial* **2009,** *13* (5), 437-443.

Kosa, T.; Maruyama, T.; Otagiri, M. Species Differences of Serum Albumins: II. Chemical and Thermal Stability. *Pharmaceutical Research* **1998,** *15* (3), 449-454.

Kragh-Hansen, U.; Watanabe, H.; Nakajou, K.; Iwao, Y.; Otagiri, M. Chain Length-dependent Binding of Fatty Acid Anions to Human Serum Albumin Studied by Site-directed Mutagenesis. *Journal of Molecular Biology* **2006,** *363,* 702-712.

Kratochvil, P. *Classical Light Scattering for Polymer Solutions;* Elsevier: Amsterdam, 1987.

Krishnan, S. Aggregation of Granulocyte Colony Stimulating Factor under Physiological Conditions: Characterization and Thermodynamic Inhibtion. *Biochemistry* **2002,** *41* (20), 6422-6431.

Laptenok, S.; Visser, N.; Engel, R.; Wstphal, A.; van Hoek, A.; van Mierlo, C.; van Stokkum, I.; van Amerongen, H.; Visser, A. A general approach for detecting folding intermediates from steady-state and time-resolved fluorescence of single-tryptophan containing proteins. *Biochemistry* **2011,** *50* (17), 3441-3450.

Leader, B. Protein therapeutics: a summary and pharmacological classification. *Nature Reviews Drug Discovery* **2008,** *7* (1), 21-39.

Lee, A.; Clark, R.; Youn, H.; Ponter, S.; Burstyn, J. Guanidine hydrochloride-induced unfolding of the three heme coordination states of the CO-sensing transcription factor, CooA. *Biochemistry* **2009,** *48* (28), 6585-6597.

Linsley, P. Binding Stoichiometry of the Cytotoxic T Lymphocyte-associated Molecule-4 (CLTA-4). *The Journal of Biological Chemistry* **1995,** *270* (25), 15417-15424.

Liu, W.; Swift, R.; Torraca, G.; Nashed-Samuel, Y.; Wen, Z. Q.; Jiang, Y.; Vance, A.; Mire-Sluis, A.; Freund, E.; Davis, J.; Narhi, L. Root Cause Analysis of Tungsten-Induced Protein Aggregation in Pre-filled Syringes. *PDA Journal of Pharmaceutical Science and Technology* **2010,** *64* (1), 11-19.

Ludwig, D.; Carpenter, J. F.; Hamel, J. B.; Randolph, T. W. Protein adsorption and excipient effects on kinetic stability of silicone oil emulsions. *J Pharm Sci* **2010,** *99* (4), 1721-1733.

Lumry, R.; Eyring, H. Conformation changes of proteins. *J Phys Chem* **1954,** *58*, 110-120.

Maa, Y.-F.; Hsu, C. C. Investigation on foulding mechanisms for recombinant human growth hormone sterile filtration. *Journal of Pharmaceutical Sciences* **1998,** *87* (7), 808-812.

Maa, Y.-F.; Hsu, C. C. Protein Denaturation by Combined Effect of Shear and Air-Liquid Interface. *Biotechnology and Bioengineering* **1997,** *54* (6), 503-512.

Majumdar, S.; Ford, B. M.; Mar, K. D.; Sullivan, V. J.; Ulrich, R. G.; D'Souza, A. J. M. Evaluations of the Effect of Syringe Surfaces on Protein Formulations. *Journal of Pharmaceutical Sciences* **2011,** *100* (7), 2563-2573.

Manning, M.; Patel, K.; Borchardt, R. Stability of Protein Pharmaceuticals. *Pharmaceutical Research* **1989,** *6* (11), 903-918.

McQuarrie, D. *Statisticam mechanics, p. 641;* Harper & Row: New York, 1976.

Mulinacci, F.; Capelle, M. A.; Gurny, R.; Drake, A. F.; Arvinte, T. Stability of Human Growth Hormone: Influence of Methionine Oxidation on Thermal Folding. *Journal of Pharmaceutical Sciences* **2011,** *100* (2), 451-463.

Muller, N.; Schneider, B.; Pfizenmajer, K.; Wajant, H. Superior serum half life of albumin tagged TNF ligands. *Biochem Biophys Res Commun* **2010,** *396* (4), 793-799.

Myers, J. K.; Pace, C. N.; Scholtz, J. M. Denaturant m values and heat capacity changes: Relation to changes in accessible surface areas of protein unfolding. *Protein Science* **1995,** 2138-2148.

Narhi, L. O.; Jiang, Y.; Cao, S.; Benedek, K.; Shnek, D. A Critical Review of Analytical Methods for Subvisible and Visible Particles. *Current Pharmaceutical Biotechnology* **2009,** *10,* 373-381.

Neal, B.; Asthagiri, A.; Lenhoff, A. M. Molecular origins of osmotic second virial coefficients. *Biophysical Journal* **1998,** *75,* 2469-2477.

Orencia Product Information Sheet; Bristol-Myers Squibb, 2007.

Orencia Product Monograph; Bristol-Myers Squibb Canada, 2006.

Osborn, B.; Sekut, L.; Corcoran, M.; Poortman, C.; Sturm, B.; Chen, G.; Mather, D.; Lin, H.; Parry, T. J. Albutropin: a growth hormone-ablumin fusion with imroved pharmacokinetics and pharmacodymanics in rats and monkeys. *Eur J Pharmacol* **2002,** *456* (1-3), 149-158.

Pace, C. Determination and Analysis of Urea and Guanidine Hydrochloride Denaturation Curves. *Methods in Enzymology* **1986,** *131,* 266-280.

Peters, T. *All About Albumin;* Academic Press Inc: San Diego, 1996.

Philo, J. S. A Critical Review of Methods for Size Characterizatio of Non-Particulate Protein Aggregates. *Current Pharmaceutical Biotechnology* **2009,** *10,* 359-372.

Randolph, T. W.; Carpenter, J. F. Engineering Challenges of Protein Formulations. *AIChE Journal* **2007,** *53* (8), 1902-1907.

Raso, S. W.; Abel, J.; Barnes, J. M.; Maloney, K. M.; Pipes, G.; Treuheit, M. J.; King, J.; Brems, D. N. Aggregation of granulocyte-colony stimulating factor in vitro involves a conformationally altered monomeric state. *Protein Science* **2005,** *14,* 2246-2257.

Rathore, N.; Rajan, R. S. Current Perspectives on Stability of Protein Drug Products during Formulation, Fill and Finish Operations. *Biotechnol. Prob.* **2008,** *24* (3), 504-514.

Reginster, J.; Rabenda, V.; Neuprez, A. Adherence, patient preference and dosing frequency: understanding the relationship. *Bone* **2006,** *38* (4), S2-S6.

Reichert, J. Antibody-based therapeutics to watch in 2011. *MAbs* **2010 [Epub],** *3* (1).

Remmele, R. L.; Zhank-van Enk, J.; Dharmavaram, V.; Balaban, D.; Durst, M.; Shoshitaishvili, A.; Rand, H. Scan-Rate Dependent Melting Transitions of Interleukin-1 Receptor (Type II): Elucidation of Meaningful Thermodynamic and Kinetic Parameters of Aggregation Acquired from DSC Simulations. *J. Am. Chem. Soc.* **2005,** *127*, 8328-8339.

Renwick, W.; Pettengell, R.; Green, M. Use of filgrastim and pegfilgrastim to support delivery of chemotherapy: twenty years of clinical experience. *BioDrugs* **2009,** *23* (3), 175-186.

Ring, J.; Seifert, J.; Jesch, F.; Brendel, W. Anaphylactoid reactions due to non-immune complex serum protein aggregates. *Monogr Allergy* **1977,** *12*, 27-35.

Roberts, C.; Das, T. K.; Sahin, E. Predicting solution aggregation rates for therapeutic proteins: Approaches and challenges. *Int J Pharm* **2011,** *doi: 10.1016/j.ijpharm.2011.03.064*.

Roberts, C.; Das, T. K.; Sahin, E. Predicting solutoin aggregation rates for therapeutic proteins: Approaches and challenges. *International Journal of Pharmaceutics* **2011,** *doi:10.1016/j.ijpharm.2011.03.064*.

Roberts, C. Non-Native Protein Aggregation Kinetics. *Biotechnology and Bioengineering* **2007,** *98* (5), 927-937.

Rosenberg, A. Effects of Protein Aggregates: An Immunologic Perspective. *The AAPS Journal* **2006,** *8* (3), 501-507.

Sanchez-Ruiz, J. M. Theoretical analysis of Lumry-Eyring models in differential scanning calorimetry. *Biophys J.* **1992,** *61* (4), 921-935.

Schmidt, S. R. Current Status of Fusion Protein Applications Including the Use of the Zera Peptide. *AAPS National Biotechnology Conference*, San Francisco, 2011.

Shire, S. Formulation and manufacturability of biologics. *Current Opinion in Biotechnology* **2009,** *20* (6), 708-714.

Smith, L. A. Development of Recombinant Vaccines for Botulinum Neurotoxin. *Toxicon* **1998,** *36* (11), 1539-1548.

Steadman, B. L.; Thompson, K. C.; Middaugh, C. R.; Matsuno, K.; Vrona, S.; Lawson, E. Q.; Lewis, R. V. The effects of surface adsorption on the thermal stability of proteins. *Biotechnology and Bioengineering* **1991,** *40* (1), 8-15.

Stravitz, R.; Chung, H.; Sterling, R.; Luketic, V.; Sanyal, A.; Price, A.; Purrington, A.; Shiffman, M. Antibody-Mediated Pure Red Cell Aplasia Due to Epoetin Alfa During Antiviral Therapy of Chronic Hepatitis C. *The American Journal of Gastroenterology* **2005,** *100* (6), 1415-1419.

Syed, S.; Schuyler, P.; Kulczycky, M.; Scheffield, W. Potent antithrombin activity and delayed clearance from the circulation characterize recombinant hirudin genetically fused to albumin. *Blood* **1997,** *89* (9), 3243-3252.

Tanford, C. Extension of the theory of linked functions to incorporate the effects of protein hydration. *Journal of Molecular Biology* **1969,** *39* (3), 539-544.

Thirumangalathu, R.; Krishnan, S.; Brems, D. N.; Randolph, T. W.; Carpenter, J. F. Effects of pH, temperature, and sucrose on benzyl alcohol-induced aggregation of recombinant human granulocyte colony stimulating factor. *Journal of Pharmaceutical Sciences* **2006,** *95* (7), 1480-1497.

Timasheff, S. N. Protein-solvent preferential interactions, protein hydration, and the modulation of biochemical reactions by solvent components. *PNAS* **2002,** *99* (15), 9721-9726.

Tooze, B. C. Introductio to protein structure. Garland Scicne: New York, 1998; p 410.

Wertheimer, A.; Santella, T. M.; Finestone, A.; Levy, R. Drug delivery systems improve pharmaceutical profile and facilitate medication adherence. *Advances in Therapy* **2005,** *22* (6), 559-577.

Yadav, S.; Sreedhara, A.; Kanai, S.; Liu, J.; Lien, S.; Lowman, H.; Kalonia, D. S.; Shire, S. J. Establishing a Link Between Amino Acid Sequences and Self-Associating and Viscoelastic Behavior of Two Closely Related Monoclonal Antibodies. *Pharm Res* **2011,** *28,* 1750-1764.

Yu, Z.; Fu, Y. Recombinant human albumin fusion proteins with long lasting biological effects. 7,244,833, July 17, **2007**.